A STUDY OF THE VORTEX SHEET BEHIND A LIFTING WING

DAVID PRIOR WILLIAMS M.A.

DEPARTMENT OF APPLIED MATHEMATICS

UNIVERSITY OF ADELAIDE

Awarded March 1977

JANUARY 1976

CONTENTS

SUMMARY

This thesis is the result of a study of the behaviour of the vortex sheet which forms behind a wing producing lift in its passage through the air, usually assumed to be an ideal fluid. Various mathematical models have been constructed to account for the experimentally observed roll-up which is the dominant feature of the motion of such a sheet. The significant theories here reviewed are those of Sprieter and Sacks, which postulates a ~~uniform-~~ core of uniform vorticity ~~ly viscous core~~ in each of the two vortices formed in the rolled up state; Betz, where the pair of vortices in the ultimate configuration have vorticity dependent on distance from the centre and governed by the wing loading profile; Williams, which modifies the Betz model to allow for viscosity; and Moore and Saffman which allows for an axial flow neglected in the other models.

The computer simulation of the motion of an array of point vortices used to approximate a vortex sheet trace in a Trefftz plane is described together with Moore's technique to suppress the chaotic behaviour of such an array. A description and results of the present computer study are given in which the motion of point vortices corresponding to a variety of wing loadings is examined. Moore's method of chaos suppression is used with varying success. The relative merits of more and less accurate

numerical integration methods are discussed and the conclusion is drawn that the most accurate is not necessarily the most useful for some purposes.

To the best of my knowledge and belief except where due acknowledgement has been made none of the material which follows has been previously written or published by another person and has not been used previously by me for the award of a diploma or degree in any university.

My grateful thanks are due to Dr. P. M. Gill who supervised this work, Mr. M. D. Teubner with whom I had many valuable discussions, Mrs. R. G. Schilling who painstakingly produced the typescript and my family who did not mind sleeping on the floor.

CHAPTER 1

THE VORTEX SHEET

Introduction.

Apart from being of interest to students of fluid mechanics the behaviour of the air within the first few hundred wingspans downstream of an aircraft in flight has assumed increasing importance with the advent of larger and heavier aircraft. That within the wake there is disturbed air with very large velocity gradients is well known to pilots of light aircraft who have inadvertently found themselves behind larger ones but the exact nature of the airflow which produces these hazards to aviation especially near airports is still the subject of investigation. The present object is to review the literature to date and to display some of the theories which have evolved so far.

Elementary View.

In its motion through the air a lifting wing, because of its shape produces a downwash in its wake. This is a consequence of a pressure difference between the top and bottom surfaces of the wing. Because the free stream of air moving along the chord at right angles to the leading and trailing edges inhibits the flow around either edge from lower to upper surface a secondary flow parallel to the wing span is set up which is caused by the higher

pressure below the wing and the lower pressure above it. The secondary flow moves towards the wing tip on the lower surface but away from the wing tip on the upper surface (Fig. 1). As these two different flows meet at the trailing edge they form a series of vortices with clockwise rotation when the left wing is viewed from the rear and anticlockwise when the right wing is viewed from the rear. The vortices are shed into the wake and form, at least immediately behind the trailing edge, a vortex sheet. This can be thought of as a sheet generated by discrete vortex filaments passing through and at right angles to the trailing edge such that the distance between them approaches zero and the total strength per unit spanwise distance is bounded, i.e. a vorticity distribution just aft of the trailing edge. If the vortex sheet remained so then the wake would consist of a vortex sheet (in reality of small vertical dimension) which dissipates with time, embedded in a downwash. However a significant part of the difficulty of investigating a wing wake is due to the fact that the vortex sheet rolls up (Fig. 2) in a very short distance behind the wing (a few wingspans) into a spiral vortex sheet which then diffuses into a single vortex. The single vortex has a centre line which when produced back meets the wing at a point typically about 3/4 of the semispan out from the wing centre although the figure depends on the wing loading profile. Among the first to recognise the wake roll up phenomenon was F.W. Lanchester in his

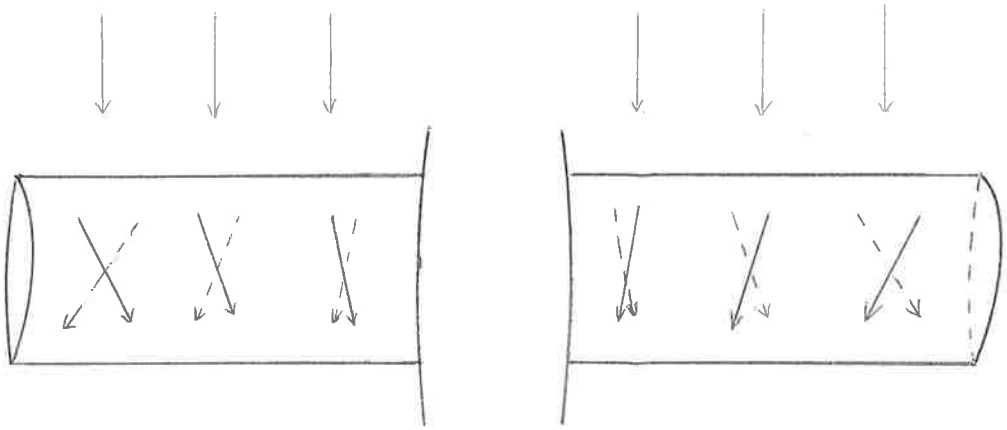

Figure 1

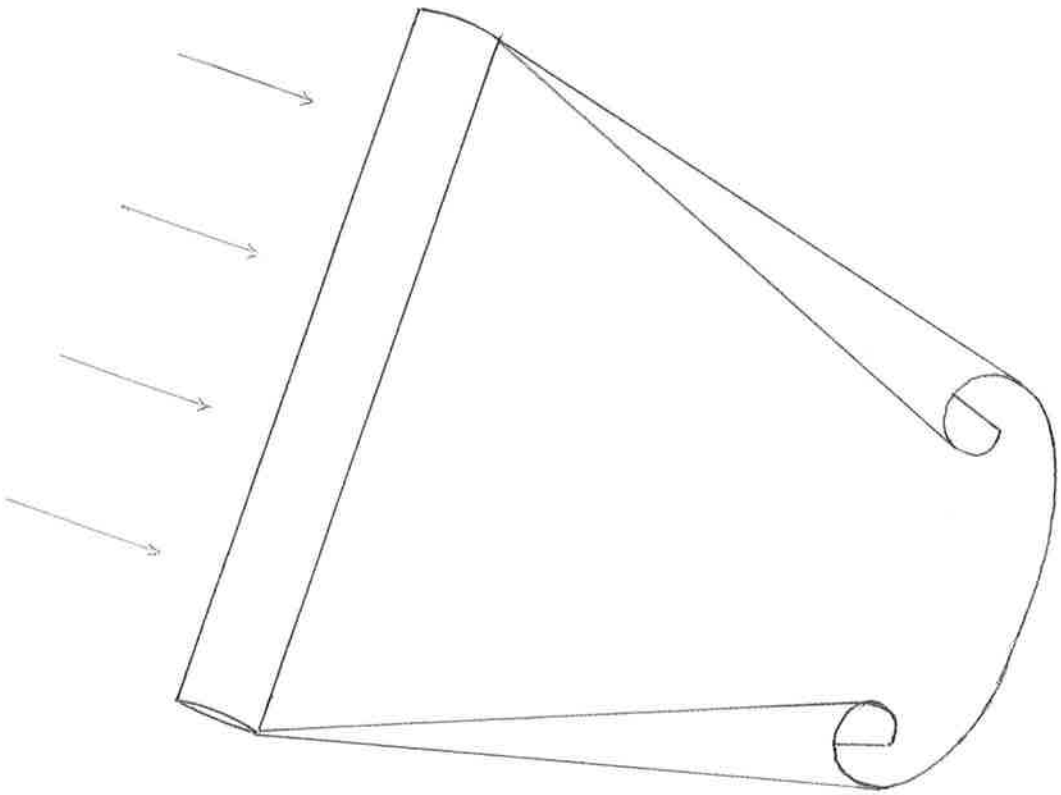

Figure 2

"Aerodynamics" published in 1907.

In classical fluid dynamics a vortex sheet is regarded mathematically as a surface of discontinuity with zero thickness and the physically impossible property of having different velocity vectors at adjacent points on opposite sides of the sheet. This means that if P is a point in a vortex sheet and $\underset{\sim}{q}$ is the velocity at a point Q not in the sheet, and if $\lim_{Q\to P} \underset{\sim}{q} = \underset{\sim}{q}_1$ when Q is on one side of the sheet while $\lim_{Q\to P} \underset{\sim}{q} = \underset{\sim}{q}_2$ when Q is on the other side of the sheet then in general $\underset{\sim}{q}_1 \neq \underset{\sim}{q}_2$

In fact the physical vortex "sheet" has finite thickness through which the velocity gradients are large compared with those elsewhere in the flow. The vortex sheet is an abstraction to which the real physical flow approximates but it has the advantage of lending itself to mathematical analysis.

CHAPTER II

THE SPRIETER AND SACKS MODEL

Perhaps an obvious starting point in the investigation of the far-field structure of trailing vortices was to assume that each vortex approximates to a potential vortex at least in part. Since such a vortex has indefinitely large velocities near its centre one of the first modifications to this assumption was to rule out the very high velocities by postulating a central core within which the air rotated very much as a solid body, so that the velocity was proportional to the distance from the centre. Outside the core the speed was permitted to decrease according to the potential vortex law of inverse variation with distance from the centre. Thus all of the vorticity was assumed to be uniformly distributed within the core (Fig. 3). Presumably it was hoped that such a model would adequately account for viscosity. This flow is known as a Rankine vortex.

It was this type of model which was used by Sprieter and Sacks (1951) on whose work were based many early discussions of trailing vortices in the 1950's and 60's.

A wing with loading which varies along its span must have variable circulation to account for the variable lift produced since $L=\rho V\Gamma$ where the symbols represent lift per unit length, density, velocity and circulation

per unit length. At a distance x from the midspan position $L_x = \rho V^2 c_l c$ where c_l is the coefficient of lift at that position (section lift coefficient) and c is the chord. In general both c_l and c are functions of x.

At the midspan position

$$L_0 = \rho V \Gamma_0 = \tfrac{1}{2}\rho V^2 c_{l_0} c_0$$

i.e. $$\Gamma_0 = \tfrac{1}{2} V c_{l_0} c_0$$

The total lift is $\int_{-s}^{s} L_x dx$

for a wing of semispan s.

As the loading L_x, and hence the circulation Γ_x, decreases towards the wing tip, vorticity is shed into the wake.

Sprieter and Sacks attacked the problem of finding the spacing between the fully rolled up vortices by considering two wings of equal total lift, one with the required variable loading and the other uniformly loaded. The assumption was then made that far down stream the pairs of vortices produced by each wing have equal strengths and are equally spaced.

The uniformly loaded wing will shed all its vorticity at the wing tips so that the vortices formed are separated by a distance $2s^1$ between their centres, where s^1 is the uniformly loaded wing semispan.

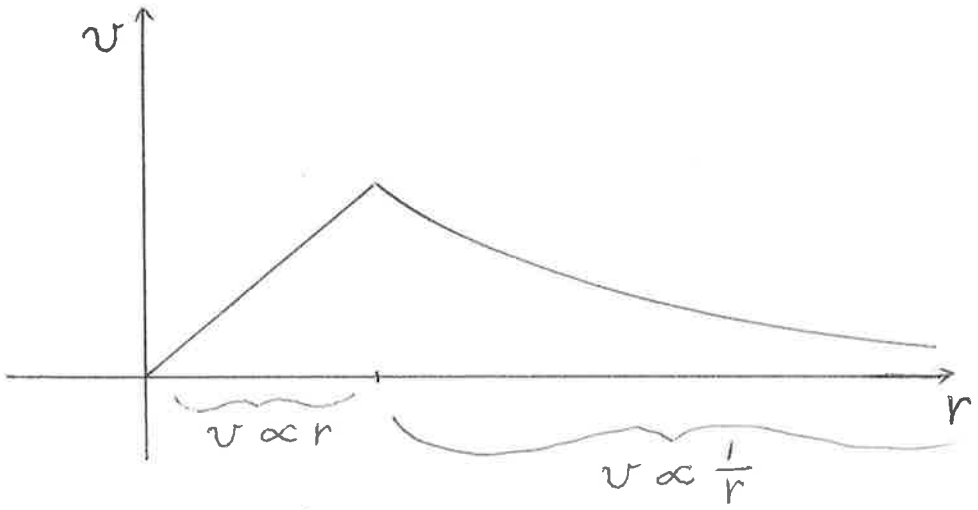

Figure 3

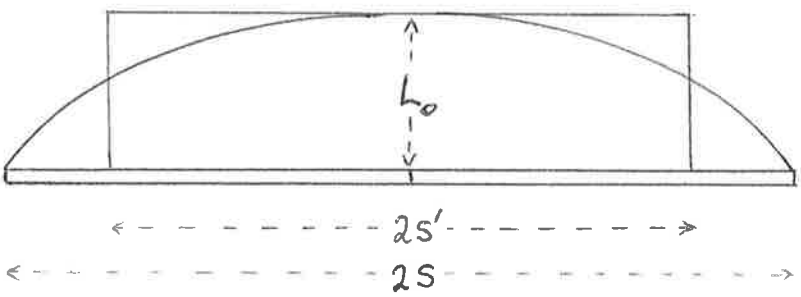

Figure 4

The total lift of either wing is then (Fig. 4)

$$L=2s^1L_0$$

$$\tfrac{1}{2}\rho V^2 C_L S = 2s^1 \rho V \Gamma_0$$

$$= 2s^1 \rho V (\tfrac{1}{2} V c_{l_0} c_0)$$

$$\therefore s^1 = \frac{C_L S}{2c_{l_0} c_0}$$ where C_L is the mean value of c_l along the wing (coefficient of lift) and S is wing area.

For a wing with rectangular plan form

$$s^1=\frac{C_L S}{c_{l_0}}$$

Clearly the distance $2s^1$ is the length of the rectangle with the same height and the same area as the wing loading profile.

For an elliptically loaded wing $s^1=\frac{\pi s}{4}$

Since each vortex is in the induced velocity field of the other (given by $\frac{\Gamma_0}{2\pi r}$ at a distance r from the centre) they both move downwards at a speed

$$u = \frac{\Gamma_0}{4\pi s^1} = \frac{\Gamma_0}{\pi^2 s}$$ for a rectangular wing

The vortices under consideration here are assumed to be of the Rankine type i.e. those which have a "solid" core. Outside the cores we have potential flow such that the velocity potential ϕ is

$$\phi = \frac{\Gamma_0}{2\pi} \left[\operatorname{artan} \frac{y}{x-s^1} - \operatorname{artan} \frac{y}{x+s^1} \right]$$

since the velocity potential of a potential vortex at the origin of strength Γ_0 is

$$\frac{\Gamma_0}{2\pi} \operatorname{artan} \frac{y}{x}.$$

The streamlines are given by ψ = const where

$$\frac{\partial\phi}{\partial x} = \frac{\partial\psi}{\partial y} \text{ and } \frac{\partial\phi}{\partial y} = \frac{\partial\psi}{\partial x}$$

hence $(x+s^1)^2+y^2=R(x-s^1)^2+Ry^2$ give the stream lines for different values of R.

The streamlines can also be written

$\left(x\pm\sqrt{b^2+s^{1\,2}}\right)^2 + y^2=b^2$ where b is a parameter, which are two families of circles with centres at $x=\pm\sqrt{b^2+s^{1\,2}}$ and radii b.

To determine the size of the core a, of each vortex the authors equate the total kinetic energy (per unit length in the stream direction) to the induced drag.

The kinetic energy inside the two cores is given by $I\omega^2$ where I is the moment of inertia of the cylinder of air and ω is its angular velocity

$$\text{i.e. } \tfrac{1}{2}\rho a^4\pi\left(\frac{\Gamma_0}{2\pi a^2}\right)^2=\frac{\rho\Gamma_0^{\,2}}{8\pi}$$

The kinetic energy outside the two cores is obtained by evaluating the integral

$\tfrac{1}{2}\rho\int_S(\nabla\phi)^2dS$ where S is the entire plane but excluding the two cores.

Now $(\nabla\phi)^2=\nabla.(\phi\nabla\phi)-\phi\nabla^2\phi$

$= \nabla.(\phi\nabla\phi)$ since ϕ is a potential function which satisfies $\nabla^2\phi=0$.

$$\therefore \text{ Kinetic energy } = \tfrac{1}{2}\rho \int_S \nabla.(\phi \underset{\sim}{\nabla}\phi)\,dS$$

$$= \tfrac{1}{2}\rho \int_c \phi \underset{\sim}{\nabla}\phi . d\underset{\sim}{s} \qquad \text{(s here is arc length)}$$

where c is the collection of the three contours c_1, c_2 c_3 and the cross cuts joining them, and $d\underset{\sim}{s}=\underset{\sim}{n}ds$ where $\underset{\sim}{n}$ is the outward drawn normal to c (Fig. 5), c_1 and c_2 are circles (enclosing the two cores) centred at $x=\pm\sqrt{a^2+s^{1\,2}}$ and radii a. c_3 is a large circle, radius R centred on the origin.

$$\text{Now } \phi = \operatorname{artan} \frac{y}{x-s^1} - \frac{y}{x+s^1}$$

$$= \operatorname{artan} \left(\frac{\frac{y}{x-s^1} - \frac{y}{x+s^1}}{1 + \frac{y^2}{x^2-s^{1\,2}}} \right)$$

$$= \operatorname{artan} \left(\frac{2s^1 y}{R^2-s^{1\,2}} \right) \qquad = O\left(\frac{1}{R}\right) \text{ for large R.}$$

$$\nabla\phi = \left(\frac{-y}{(x-s^1)^2+y^2} \right)\underset{\sim}{i} + \left(\frac{y}{(x+s^1)^2+y^2} \right)\underset{\sim}{i} + \left(\frac{(x-s^1)}{(x-s^1)^2+y^2} \right)\underset{\sim}{j} - \left(\frac{(x+s^1)}{(x+s^1)^2+y^2} \right)\underset{\sim}{j}$$

$$= \left(\frac{-y}{R^2-2s^1x} + \frac{y}{R^2+2s^1x} \right)\underset{\sim}{i} + \left(\frac{x-s^1}{R^2-2s^1x} - \frac{x+s^1}{R^2+2s^1x} \right)\underset{\sim}{j}$$

$$= \frac{-4s^1xy\underset{\sim}{i}}{R^4-4s^{1\,2}x^2} + \frac{-2s^1R^2+4s^1x^2}{R^4-4a^{1\,2}x^2}\,\underset{\sim}{j}$$

$$\therefore |\nabla\phi| = O\left(\frac{1}{R^2}\right)$$

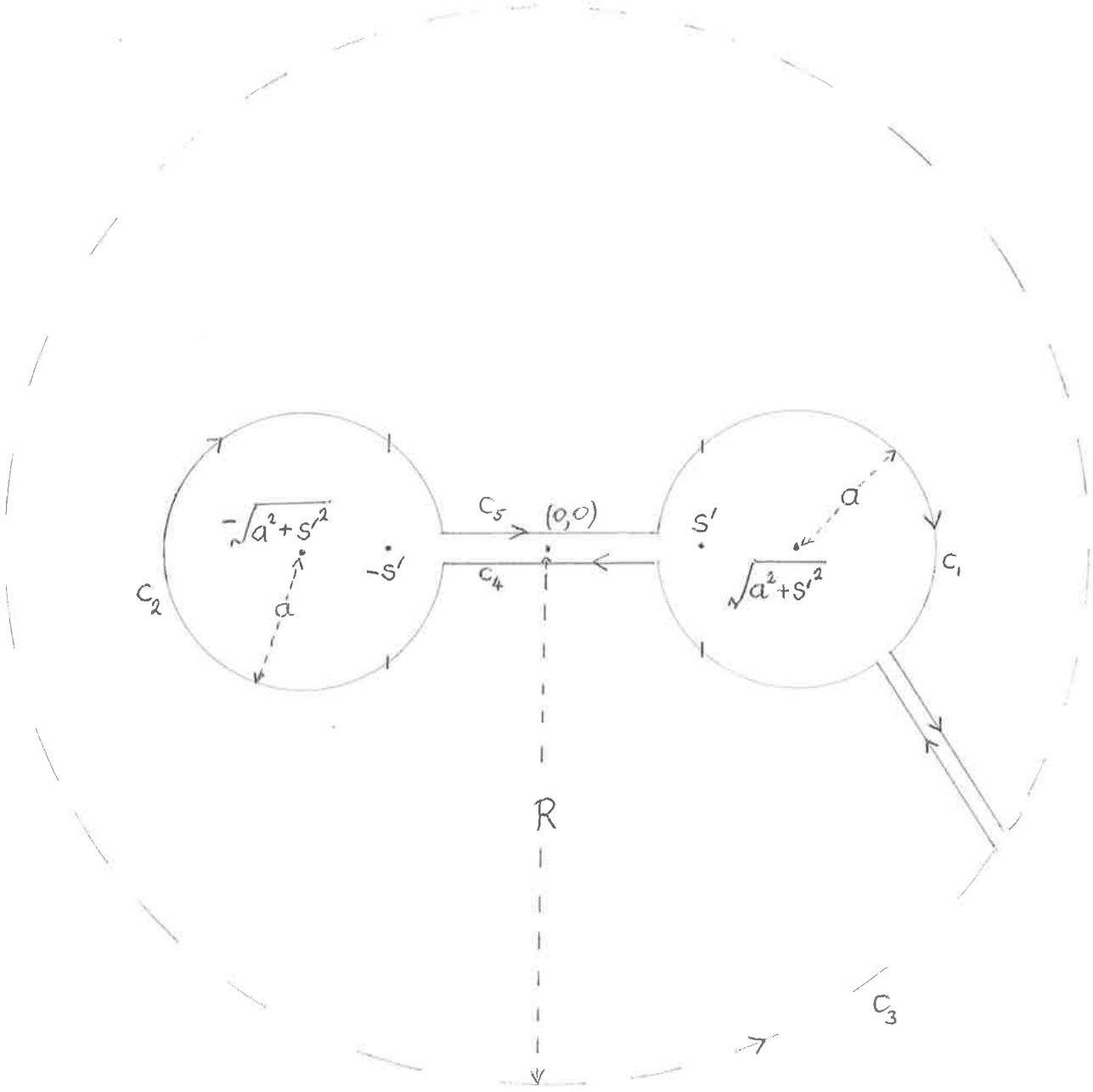

Figure 5

$$\therefore |\phi\nabla\phi| = O\left(\frac{1}{R^3}\right), \qquad s = 2\pi R \text{ on } c_3$$

$$\therefore \int_{c^3} \phi\underset{\sim}{\nabla}\phi.d\underset{\sim}{s} = O\left(\frac{1}{R^2}\right) \to 0 \text{ as } R\to\infty$$

The contours c_1 and c_2 are streamlines and so along these contours $\underset{\sim}{\nabla}\phi$ is tangent to the curve and hence

$$\underset{\sim}{\nabla}\phi.\underset{\sim}{n} = 0$$

$$\therefore \int_{c_1,c_2} \phi\nabla\underset{\sim}{\phi}.d\underset{\sim}{s} = 0$$

The two cross cuts joining the circle, radius R, to c_1 make equal but opposite contributions.

Along c_4 since y=0 we can take

$$\text{artan } \frac{y}{x-s_1} = 0 = \text{artan } \frac{y}{x+s_1}$$

However as we move from c_4 to c_5 via c_2 $\frac{y}{x+s_1}$ takes values described in order as

$$0, -, -\infty, +\infty, +, 0, -, -\infty, +\infty, +, 0$$

$\therefore$ artan $\frac{y}{x+s_1}$ changes its value from 0 to -2π as c_2 is traversed.

$\frac{y}{x-s_1}$ does not become infinite at any stage so on c_5 artan $\frac{y}{x-s_1}$ is still zero.

$\therefore$ The kinetic energy per unit length in the streamwise direction over the whole plane outside the core is

$$\frac{\rho\Gamma^2}{8\pi^2}\int_{c_1+c_2+c_3+c_4+c_5}\phi\nabla\phi.\underset{\sim}{n}ds$$

$$=\frac{\rho\Gamma^2}{4\pi}\int_{C_5}\left[\frac{-y\underset{\sim}{i}}{(x-s^1)^2+y^2}+\frac{(x-s^1)\underset{\sim}{j}}{(x-s^1)^2+y^2}+\frac{y\underset{\sim}{i}}{(x+s^1)^2+y^2}-\frac{(x+s^1)\underset{\sim}{j}}{(x+s^1)^2+y^2}\right].(-\underset{\sim}{j})dx$$

$$=\frac{\rho\Gamma^2}{4\pi}\int\left(\frac{1}{x+s^1}-\frac{1}{x-s^1}\right)dx$$

since $\arctan\frac{y}{x-s^1}-\arctan\frac{y}{x+s^1}=2\pi$ and $y=0$

Now $$\int_{-\sqrt{a^2+s^{1\,2}}+a}^{\sqrt{a^2+s^{1\,2}}-a}\left(\frac{1}{x+s^1}-\frac{1}{s^1-x}\right)dx=2\ln\left(\frac{s^1+\sqrt{a^2+s^{1\,2}}-a}{s^1-\sqrt{a^2+s^{1\,2}}+a}\right)$$

The total energy, including the two cores, is

$$\frac{\rho\Gamma_0^{\,2}}{8\pi}\left(1+4\ln\left[\frac{s^1+\sqrt{a^2+s^{1\,2}}-a}{s^1-\sqrt{a^2+s^{1\,2}}+a}\right]\right)$$

The authors then equate this to the induced drag and hence find the value of a for the case of an elliptically loaded wing. Their argument depends on the simplifying assumption that a is small compared to s^1 and hence $\sqrt{a^2+s^{1\,2}}$ is replaced by s^1. In this case the value

obtained for the core radius is a = 0.155s which is much greater than experimental evidence suggests. McCormick, Tangler and Sherrieb (1968) describe experiments made with light aircraft which, among other results, give a value for a/s somewhat less than 0.04.

It was also observed that not all of the vorticity was in the core but was some function of the radial distance from the centre of the vortex.

CHAPTER III

THEOREMS ON DISCRETE VORTICES MOVING IN A PLANE.

An early and recently much quoted attempt to describe vortex behaviour in two dimensional inviscid flow was made by Betz in 1932. He relies for his analysis on a number of theorems which we shall now discuss.

Imagine a number of small cylinders placed in the fluid with their axes normal to the plane of motion and which rotate about their axes. The velocity of the fluid induced by the rotation of each cylinder in the limit as its radius tends to zero is that associated with a vortex filament along the axis of the cylinder. The strength of such a vortex is Γ such that in the absence of any other fluid motion the only velocity is transverse and, at a distance r from the filament, is $\frac{\Gamma}{2\pi r}$ in the anti-clockwise direction.

The Kutta-Joukowski theorem states that when such a rotating cylinder is placed in a uniform stream $\underset{\sim}{v}$ and restrained from moving with the stream while allowing its rotational motion to continue, then there is a force on the cylinder at right angles to $\underset{\sim}{v}$ in the plane of flow given by

$$\underset{\sim}{P}=\rho\Gamma\underset{\sim}{v}\times\underset{\sim}{k}$$

where $\underset{\sim}{P}$ is the Kutta-Joukowski force, ρ is the fluid density and $\underset{\sim}{k}$ is the dimensionless unit vector normal to the plane of flow (Fig. 6).

When the cylinder is unrestrained then it moves with the fluid.

Analogous to the centre of mass of mass particles let us define the centre of vorticity or vortical centroid at $\bar{\underset{\sim}{r}}$ given by

$$\bar{\underset{\sim}{r}}\Sigma\Gamma_i = \sum_i \Gamma_i \underset{\sim}{r}_i$$

where Γ_i is the strength of the vortex at $\underset{\sim}{r}_i$

$\bar{\underset{\sim}{r}}$ is undefined when $\sum_i \Gamma_i = 0$

Assuming that the Γ_i are constants we have by differentiation

$$\bar{\underset{\sim}{v}}\Sigma\Gamma_i = \sum_i \Gamma_i \underset{\sim}{v}_i$$

$$\therefore \rho(\bar{\underset{\sim}{v}} \times \underset{\sim}{\kappa})\Sigma\Gamma_i = \rho\Sigma\Gamma_i \underset{\sim}{v}_i \times \underset{\sim}{\kappa}$$

$$= \Sigma\underset{\sim}{P}_i$$

$$\therefore (\bar{\underset{\sim}{v}} \times \underset{\sim}{\kappa})\Gamma = \underset{\sim}{P}$$ where $\bar{\underset{\sim}{v}}$ is the

velocity of the vortical centroid, $\Gamma = \Sigma\Gamma_i$ and $\underset{\sim}{P}$ is the resultant Kutta-Joukowski force. This means that if $\underset{\sim}{P} = \underset{\sim}{0}$ then $\bar{\underset{\sim}{v}} = \underset{\sim}{0}$

Now in the restrained vortex situation the equal and opposite reaction force to $\underset{\sim}{P}$ is provided by the fluid boundary which is stationary. Suppose the boundary (imagine it circular) is distant d from the vortex at $\underset{\sim}{r}_i$. Then the velocity u at the boundary induced by Γ_i

is proportional to $\frac{1}{d}$ and the pressure difference there from the fluid at infinity is $p-p_0$ which is proportional to u^2 by Bernoulli's therem. Also the boundary area A is proportional to d.

i.e. $P = A(p-p_0) \propto du^2 \propto d^{-1}$

$\therefore P \to 0$ as $d \to \infty$

Hence in an infinite unbounded fluid, P=0. So we can state that in an unbounded two dimensional fluid where the velocity field depends only on the presence of vortices then the position of the vortical centroid is constant.

The equation

$\rho(\underset{\sim}{\bar{v}} x \underset{\sim}{K})\Gamma = \underset{\sim}{P}$ implies that $\underset{\sim}{P}$ is the force equal and opposite to that required to restrain a single vortex of strength (circulation) Γ in a flow of velocity $\underset{\sim}{\bar{v}}$. If the vortices are in the proximity of a single plane boundary normal to the plane of motion the equation also implies that since $\underset{\sim}{P}$ is normal to the boundary, $\underset{\sim}{\bar{v}}$ is parallel to it and hence the position $\underset{\sim}{\bar{r}}$ is a constant distance from it.

Now let the vortical centroid be the origin of polar coordinates and consider the vortex of strength Γ_i at the polar point (r_i, θ_i). The fluid velocity at this point in the absence of the vortex there, would be $\underset{\sim i}{u}$ and $\underset{\sim i}{w}$ in the radial and transverse directions

respectively. The Kutta-Joukowski force $\underset{\sim}{P}_{w_i}$ due to the component $\underset{\sim}{w}_i$ is along the radius from the pole and so has no moment about the vortical centroid. But the force $\underset{\sim}{P}_{u_i} = \rho\Gamma_i \underset{\sim}{u}_i \times \underset{\sim}{\kappa}$ has a moment

$$\underset{\sim}{r}_i \times \underset{\sim}{P}_{u_i} = \underset{\sim}{r}_i \times \left[\rho\Gamma_i \underset{\sim}{u}_i \times \underset{\sim}{\kappa}\right] \quad \text{about the vortical centroid (Fig. 7).}$$

The sum of all such moments is

$$\begin{aligned}
\Sigma \underset{\sim}{r}_i \times \underset{\sim}{P}_{u_i} &= \Sigma \underset{\sim}{r}_i \times \left[\rho\Gamma_i \underset{\sim}{u}_i \times \underset{\sim}{\kappa}\right] \\
&= \rho\Sigma\Gamma_i \left[(\underset{\sim}{r}_i \cdot \underset{\sim}{\kappa})\underset{\sim}{u}_i - (\underset{\sim}{r}_i \cdot \underset{\sim}{u}_i)\underset{\sim}{\kappa}\right] \\
&= -\rho\Sigma\Gamma_i (\underset{\sim}{r}_i \cdot \underset{\sim}{u}_i)\underset{\sim}{\kappa} \\
&= -\tfrac{1}{2}\rho\Sigma\Gamma_i \frac{d}{dt}(\underset{\sim}{r}_i^2)\underset{\sim}{\kappa} \\
&= \frac{d}{dt}(-\tfrac{1}{2}\rho\Sigma\Gamma_i \underset{\sim}{r}_i^2)\underset{\sim}{\kappa}
\end{aligned}$$

∴ When the sum of the external moments is zero then $\Sigma\Gamma_i r_i^2$ is constant. The term $\Sigma\Gamma_i r_i^2$ is the circulation analogue of moment of inertia about an axis normal to the plane of flow through the vortical centroid. Note that we cannot argue that the moments of external forces due to the presence of a fluid boundary tend to zero as the boundary recedes to infinity since although the forces themselves tend to zero their moments are proportional to dd^{-1} which may not tend to zero as $d \to \infty$. The quantity $\Sigma\Gamma_i r_i^2$ is a measure of the spread or scatter of the vortices and is called the vortical dispersion.

The result can thus be stated: The rate of change of vortical dispersion about the vortical centroid is proportional to the sum of the moments of the external forces about that point. For the present discussion an important special case is when the sum of the moments of the external forces about the vortical centroid is zero i.e. when the vortical dispersion is constant.

Vortex induced energy.

The energy due to the vortex induced velocity in the annulus between the concentric circles of radii r and r+δr, centre the vortex with strength Γ is

$$\tfrac{1}{2}\rho\left(\frac{\Gamma}{2\pi r}\right)^2 2\pi r\,dr = \frac{\rho\Gamma^2}{4\pi r}dr$$

∴ The energy contained within an annulus between circles of radii $\frac{1}{R}$ and R is

$$\frac{\rho\Gamma^2}{4\pi}\left(\ln R - \ln\frac{1}{R}\right) = \frac{\rho\Gamma^2}{2\pi}\ln R$$

As $R\to\infty$ we find that the energy $\to\infty$ both at the vortex itself and at infinity. If we consider the vortical motion to be induced by a rotating cylinder of small radius ϵ with peripheral velocity $\frac{\Gamma}{2\pi\epsilon}$ then the singularity at the vortex itself is eliminated. We are still left with the fact that the energy of the fluid in a circle with

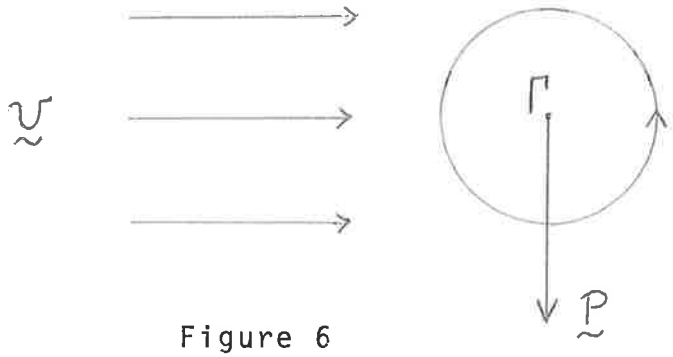

Figure 6

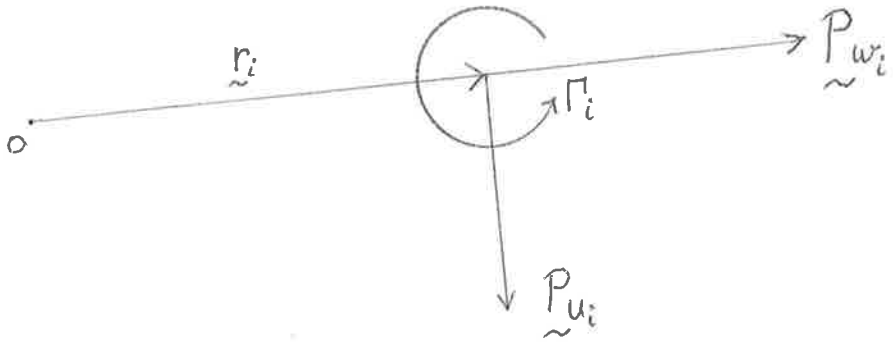

Figure 7

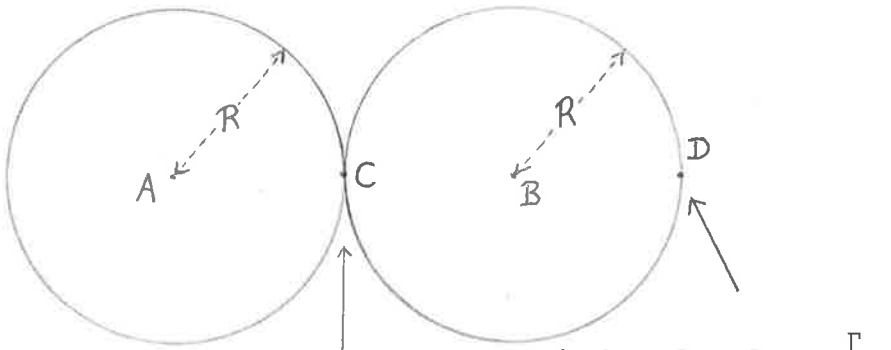

Figure 8

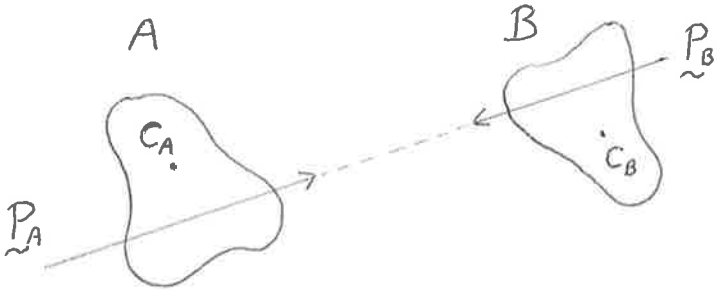

Figure 9

an isolated vortex at its centre tends to infinity with the logarithm of its radius. The same can be said of any group of vortices whose total circulation is not zero. The conclusion is that in a fluid at rest at infinity vortices can only exist in groups whose total strength is zero. In fact the parts of such groups cannot even be very far apart since the energy induced increases with their distance apart. We can show this by considering a pair of equal and opposite vortices with distance 2R between them and strengths Γ and $-\Gamma$ (Fig. 8).

Within the circle centred on B, radius R the maximum A-induced velocity is at C with a value $\frac{\Gamma}{2\pi R}$ while the minimum A-induced velocity is at D with a value $\frac{\Gamma}{4\pi R}$. Thus the energy within the circle centre B induced by the vortex at A is E satisfying

$$\frac{\rho\Gamma^2}{8\pi} > E > \frac{\rho\Gamma^2}{32\pi}$$

i.e. E is bounded as $R\to\infty$. But as we have seen, the B-induced energy within the circle about B tends to infinity with logR. A similar argument holds for the energy within the circle about A.

The equal and opposite vortices are far apart only in the presence of high energy. We can argue in a similar kind of way for numbers of vortices in two groups.

Hence any isolated set of vortices must be such that their total circulation is zero and no subset is very far

removed from the others unless the total circulation of the subset is also zero.

When all the vortices in two groups are restrained (the groups having equal and opposite circulation) then in the absence of fluid boundaries the resultant restraining force for one group must be equal and opposite to that for the other group and in the same line of action for vortices whose total vortical dispersion about the centroid is zero. By the equation $\rho(\bar{\underset{\sim}{v}} \times \underset{\sim}{\kappa})\Gamma = \underset{\sim}{P}$ the velocities of the vortical centroids of the two groups must be equal, i.e. the vortical centroids remain the same distance apart when allowed to move with the fluid. They move at right angles to the common line of action of the equal and opposite forces (Fig. 9). In general the common line of action of $\underset{\sim}{P}_A$ and $\underset{\sim}{P}_B$ will not be parallel to the line joining the vortical centroids but if it is then the moment of $\underset{\sim}{P}_A$ about the centroid C_B is the same as the moment of $\underset{\sim}{P}_B$ about C_A but in the opposite sense. Thus by the equation

$$\Sigma \underset{\sim}{r}_i \times \underset{\sim}{P}_{u_i} = \frac{d}{dt}\left(-\tfrac{1}{2}\Gamma_i r_i^2\right)\underset{\sim}{\kappa}$$

the rate of increase in vortical dispersion of one group about its own vortical centroid is equal to the rate of decrease of vortical dispersion of the other.

The important results about vortices can be summarised as follows:

(1) The vortical centroid of a set of vortices is defined as

$$\underset{\sim}{\bar{r}} = \frac{\Sigma \Gamma_i \underset{\sim}{r_i}}{\Sigma \Gamma_i}, \quad \Sigma \Gamma_i \neq 0$$

Its velocity $\underset{\sim}{\bar{v}}$ is linked with the sum of the external forces $\Sigma \underset{\sim}{P_i}$ according to

$$\rho (\underset{\sim}{\bar{v}} \times \underset{\sim}{\kappa}) \Sigma \Gamma_i = \Sigma \underset{\sim}{P_i}$$

(2) The vortical dispersion of a set of vortices about its centroid is the scalar $\Sigma \Gamma_i (\underset{\sim}{r_i} - \underset{\sim}{\bar{r}})^2$. Its rate of change is proportional to the sum of the moments of the external forces about the centroid.

(3) Sets of vortices whose total circulation is not zero cannot exist in isolation in an unbounded fluid.

(4) When a set of vortices whose total circulation is zero is divided into two subsets whose separate total circulations are not zero, then the vortical centroids of the two sets move at the same speed in the same direction, i.e. the position of each relative to the other is constant.

These are the theorems on which the following analysis of the behaviour of a vertex sheet depends. The application of them to the vortex sheet, which is

considered as a continuous vortex distribution rather than as a set of discrete vortices, is made on the assumption that the Σ can be replaced by $\int$ whenever necessary. See also Appendix A.

CHAPTER IV

THE BETZ MODEL

In the case of a lifting wing we are discussing flow in three dimensions. The lift per unit span is directly proportional to the chordwise circulation at that point and changes in the circulation as we move along the span can only be effected by more or fewer vortex filaments being included within the chordwise contour containing the wing. The classical explanation for this is depicted in the figure 10. The "virtual" vortex filaments within the wing turn through 90^{o} and trail into the stream from the trailing edge. Since vortex filaments can only occur in closed loops, or terminate on a fluid boundary, classical theory has each pair of vortices, trailing from points symmetrical about midwing point, joined at the position relative to the fluid occupied by the wing at the time motion began.

The two dimensional flow to which our foregoing results apply is in a plane at right angles to the flow at infinity and stationary relative to it. The trailing vortices are then point vortices in this plane. Fluid velocities normal to this plane are small compared with those in the plane and are neglected in the application of the above theorems.

Vortex sheet behaviour behind a lifting wing.

Consider an elliptically loaded lifting wing of semispan s. This implies, since circulation is proportional to lift, that the circulation outboard of a point distant x from the midwing is

$$\Gamma_x = \Gamma_o\left(1-\frac{x^2}{s^2}\right)^{\frac{1}{2}}$$ where Γ_o is the midspan circulation (total semispan circulation) (Fig. 10).

The vorticity per unit spanwise distance at x is

$$\gamma_x = -\frac{d\Gamma_x}{dx} = \frac{x\Gamma_o}{s^2}\left(1-\frac{x^2}{s^2}\right)^{-\frac{1}{2}}$$

The vortical centroid between the point x and the wing tip is at c_x where

$$c_x\Gamma_x = \int_x^s \xi\gamma_\xi\, d\xi$$

$$= \frac{\Gamma_o}{s}\int_x^s \frac{\xi^2 d\xi}{\sqrt{s^2-\xi^2}}$$

$$= s\Gamma_o\int_\theta^{\frac{\pi}{2}} \sin^2\phi\, d\phi \quad \text{where } \xi = s\sin\phi, \quad x = s\sin\theta$$

$$= \frac{s\Gamma_o}{2}\left(\frac{\pi}{2} - \theta + \cos\theta\ \sin\theta\right)$$

$$= \frac{s\Gamma_o}{2}\left(\frac{\pi}{2} - \sin^{-1}\frac{x}{s} + \frac{x}{s}\sqrt{1-\frac{x^2}{s^2}}\right)$$

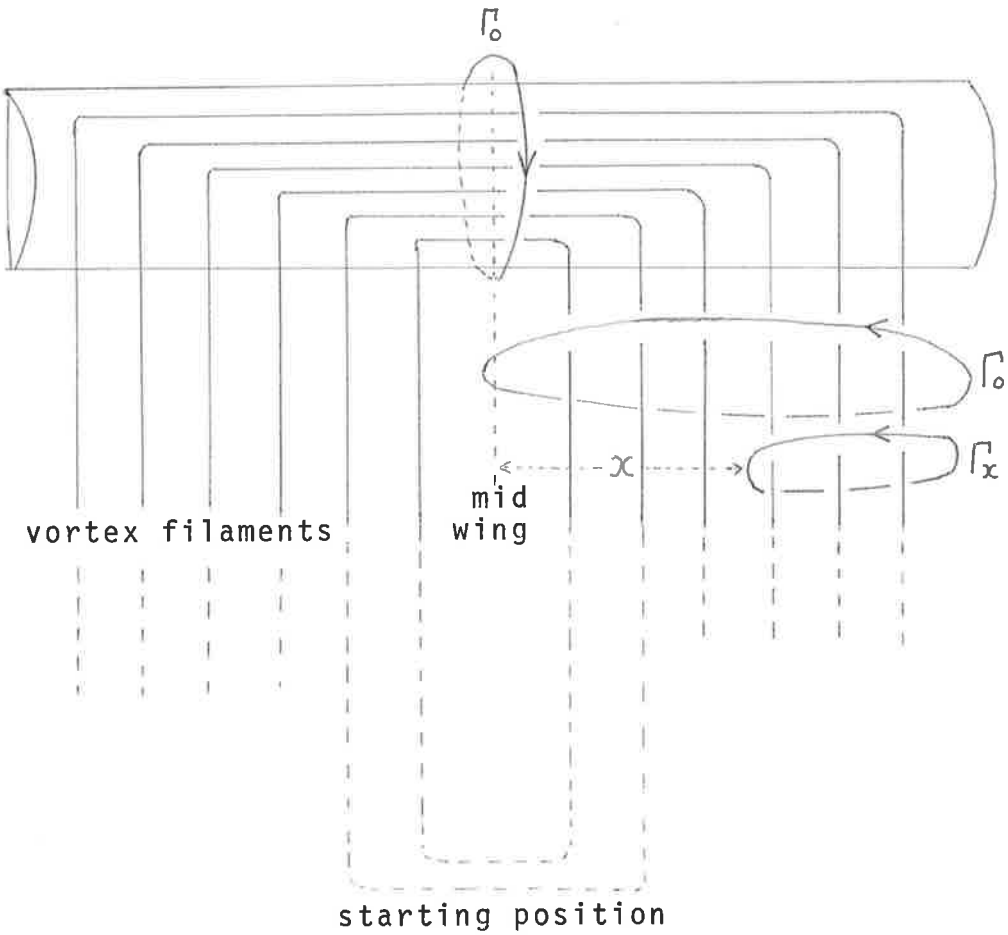
Γ_o
Γ_o
Γ_x
x
mid
wing
vortex filaments
starting position

Figure 10

Now the vortical dispersion about the midwing position of the vorticity between the point x and the wing tip is

$$J_o = \int_x^s \xi^2 \gamma_\xi d\xi$$

$$= s^2 \Gamma_o \int_\theta^{\frac{\pi}{2}} \sin^3\phi d\phi$$

$$= s^2 \Gamma_o (\cos\theta - \tfrac{1}{3}\cos^3\theta)$$

∴ The vortical dispersion of this vorticity about the vortical centroid is

$$J_x = \int_x^s (c_x - \xi)^2 \gamma_\xi d\xi$$

$$= \int_x^s c_x^2 \gamma_\xi d\xi - 2c_x \int_x^s \xi\gamma_\xi d\xi + \int_x^s \xi^2 \gamma_\xi d\xi$$

$$= c_x^2 \Gamma_x - 2c_x^2 \Gamma_x + J_o$$

$$= J_o - c_x^2 \Gamma_x$$

The assumption of the Betz wing wake model is that the vortex sheet rolls up from the wing tips into a circle containing all the vortex filaments outboard of the point x (Fig. 11).

Let the radius of the circle be r, then by the theorems on vortex behaviour its centre is at c_x and its vortical

dispersion about c_x is $J_r = J_x$. We have also assumed that the vortex concentration within the circle is dependent only on the distance from c_x and not on the angular distance from, say, the outboard direction of the wing

$$\therefore \frac{dJ_r}{d\theta} = \frac{dJ_x}{d\theta}$$

$$\therefore \frac{dJ_r}{dr}\frac{dr}{d\theta} = \frac{dJ_x}{dx}\frac{dx}{d\theta}$$

$$= -(c_x - x)^2 \gamma_x s \cos\theta$$

$$= -\left[\frac{\Gamma_o s}{2}\left(\frac{\frac{\pi}{2}-\theta}{\Gamma_o \cos\theta} + \frac{\sin\theta}{\Gamma_o}\right) - s\sin\theta\right]^2 \frac{\Gamma_o \sin\theta}{s\cos\theta} s \sin\theta$$

$$= -\frac{s^2}{4}\left(\frac{\frac{\pi}{2}-\theta}{\cos\theta} - \sin\theta\right)^2 \Gamma_o \sin\theta$$

But $$\frac{dJ_r}{dr} = \frac{d\Gamma_r}{dr} r^2$$

$$= \frac{d\Gamma_\theta}{d\theta}\frac{d\theta}{dr} r^2$$

$$= -\Gamma_o \sin\theta \frac{d\theta}{dr} r^2$$

i.e. $$\frac{dJ_r}{dr}\frac{dr}{d\theta} = -\Gamma_o r^2 \sin\theta$$

$$\therefore -\Gamma_o r^2 \sin\theta = -\frac{s^2}{4}\left(\frac{\frac{\pi}{2}-\theta}{\cos\theta} - \sin\theta\right)^2 \Gamma_o \sin\theta$$

$$\therefore r = \frac{s}{r}\left(\frac{\frac{\pi}{2}-\theta}{\cos\theta} - \sin\theta\right)$$

As $\theta \to \frac{\pi}{2}$ the ratio of r to the (small) width of the vortex sheet that has rolled up tends to:

$$\lim_{\theta \to \frac{\pi}{2}} \frac{r}{s-x} = \lim \frac{\frac{\pi}{2} - \theta - \cos\theta \sin\theta}{2\cos\theta\,(1-\sin\theta)}$$

$$= \lim_{\alpha \to 0} \left(\frac{\alpha - \sin\alpha\cos\alpha}{2\sin\alpha(1-\cos\alpha)} \right) \qquad \alpha = \frac{\pi}{2} - \theta$$

$$= \lim \left(\frac{1 - \cos 2\alpha}{2(\cos\alpha - \cos 2\alpha} \right) \qquad \text{L'Hopital's Rule}$$

$$= \lim \frac{\sin 2\alpha}{(2\sin 2\alpha - \sin\alpha} \qquad "$$

$$= \lim \frac{2\cos\alpha}{4\cos\alpha - 1}$$

$$= \frac{2}{3}$$

Thus a narrow outside strip of the vortex sheet rolls up into a circle whose radius is approximately $\frac{2}{3}$ of the width of the strip before rolling up occurred.

The whole vortex sheet semispan rolls into a circle whose radius is $\frac{s\pi}{4}$ with centre $c_o = \frac{s\pi}{4}$. This means that when roll up is complete behind both wing semispans the two circles of vorticity touch at the midspan and have a diameter $\frac{\pi}{2}$ times that of the wing semispan s. It is likely however that the circular shape of the rolled up vortex sheet (which was itself an assumption) would be modified for values of x which approach zero.

The point c_x on the semiwing becomes the centre of

the circle which forms after the development of the vortex sheet into a rolled up circle of vorticity. On the basis of the theorems on vortex behaviour we have assumed that this point is the vortical centroid for all future stages of development of the system. This point however is in the induced velocity field of the system of vorticity which has simultaneously developed behind the other semiwing and which complements its circulation to zero as must happen in isolated vortex systems. By symmetry and by the theorem (4) on vortex behaviour the two vortical centroids must move at equal constant speeds perpendicular to the line joining them. In the case of a "clean" lifting wing the direction is downwards.

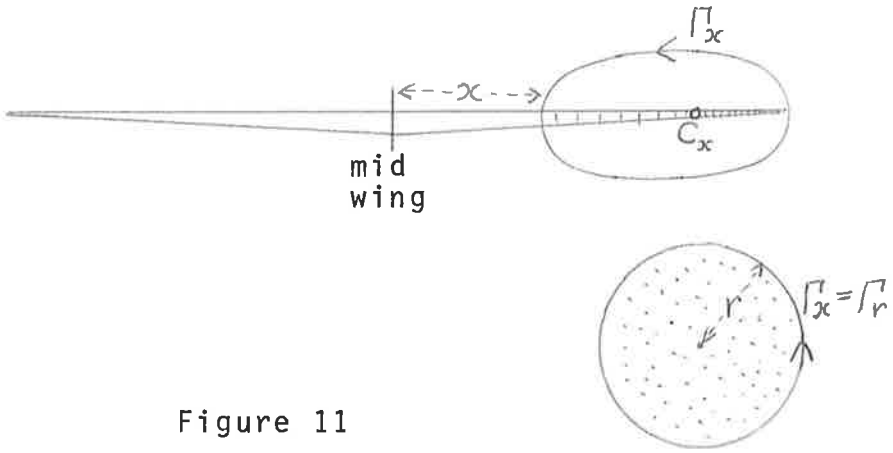

Figure 11

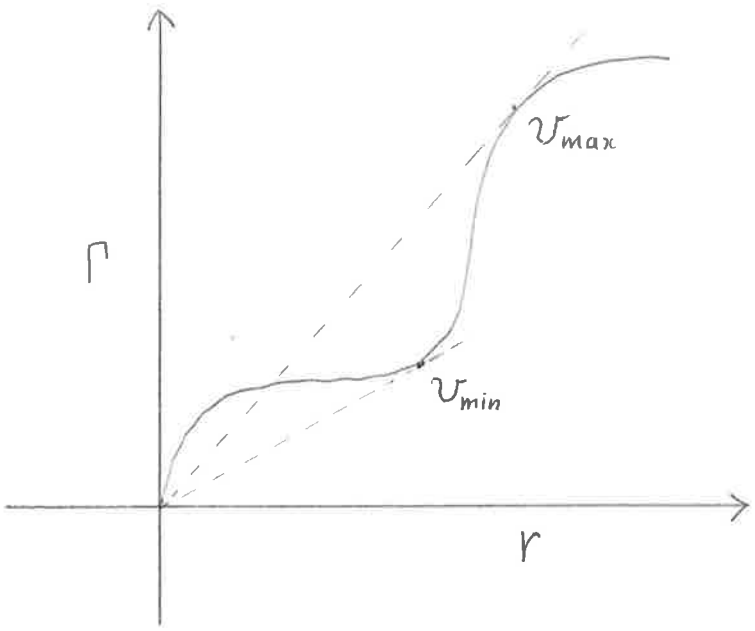

Figure 12

CHAPTER V

GENERALIZATION OF THE BETZ MODEL FOR ARBITRARY WING LOADING.

As before let Γ_x be the circulation around the trailing edge outboard of a point distant x from the midwing position and let r be the radius of the circle containing the vorticity along this part of the wing after development (Fig. 11). If J_x and J_r are the two vortical dispersions about the centroids before and after rollup respectively then by the theorem (2) on vortex behaviour $J_r = J_x$

Now $\frac{d}{dr}(J_r) = \frac{d\Gamma_r}{dr} r^2$

$$= \frac{d\Gamma_x}{dx} \frac{dx}{dr} r^2$$

and $\frac{d}{dr}(J_x) = \frac{d}{dx}(J_x) \frac{dx}{dr}$

$$= (c_x - x)^2 \frac{d\Gamma_x}{dx} \frac{dx}{dr}$$

$$\therefore r = c_x - x$$

But $c_x = -\frac{1}{\Gamma_x}\int_x^s \xi \frac{d\Gamma_\xi}{d\xi} d\xi$ since $\gamma_\xi = -\frac{d\Gamma_\xi}{d\xi}$

$$= -\frac{1}{\Gamma_x}\int \xi d\Gamma_\xi$$

$$= -\frac{1}{\Gamma_x}\left[\xi\Gamma_\xi\Big|_x^s - \int_x^s \Gamma_\xi d\xi\right]$$

$$= -\frac{1}{\Gamma_x}\left(-x\Gamma_x\right) + \frac{1}{\Gamma_x}\int_x^s \Gamma_\xi d\xi \quad \text{since } \Gamma_s = 0$$

$$= x + \frac{1}{\Gamma_x}\int_x^s \Gamma_\xi d\xi$$

$$\therefore \quad r = \frac{1}{\Gamma_x}\int_x^s \Gamma_\xi d\xi \qquad 0 < x < s$$

$$\text{or } r_x\Gamma_x = \int_x^s \Gamma_\xi d\xi \qquad \text{(see Jordan 1973).}$$

The subscripted r will be needed later.

Also we have

$$J_x = \int_x^s (c_x-\xi)^2 \gamma_\xi d\xi$$

$$= J_o - c_x^2\Gamma_x \qquad \text{shown earlier}$$

$$= \int_x^s \gamma_\xi \xi^2 d\xi - c_x^2\Gamma_x$$

$$= -\int_x^s \xi^2 d\Gamma_\xi - c_x^2\Gamma_x \qquad \text{since } \frac{d\Gamma_\xi}{d\xi} = -\gamma_\xi$$

$$= -\left[\xi^2\Gamma_\xi\Big|_x^s - 2\int \xi\Gamma_\xi d\xi\right] \quad c_x^2\Gamma_x$$

$$= x^2\Gamma_x - 2\int \xi d(r_\xi\Gamma_\xi) - c_x^2\Gamma_x$$

$$\text{since } r_x\Gamma_x = \int_x^s \Gamma_\xi d\xi \text{ and } \Gamma_s = 0$$

$$= (x^2-c_x^2)\Gamma_x - 2\left[\xi r_\xi\Gamma_\xi\Big|_x^s - \int r_\xi\Gamma_\xi d\xi\right]$$

$$= (x^2-c_x^2)\Gamma_x + 2xr_x\Gamma_x + 2\int_x^s r_\xi\Gamma_\xi d\xi$$

$$= 2\int_x^s r_\xi\Gamma_\xi d\xi - r_x^2\Gamma_x \qquad \text{using } r_x = c_x - x.$$

Substituting for r_ξ and r_x by using

$$r_x = \frac{1}{\Gamma_x}\int_x^s \Gamma_\xi d\xi$$

we have

$$J_x = 2\int_x^s \int_n^s \Gamma_n dn d\xi - \frac{1}{\Gamma_x}\left[\int_x^s \Gamma_\xi d\xi\right]^2$$

Thus for a given wing loading Γ we have c_x, r_x and J_x in terms of x. From the equation $r_x=c_x-x$ we can now establish generally that since $r_o=c_o$, the two circles which contain all of the rolled up vorticity behind each wing touch at the midwing position. This was shown to be true in the particular case of the elliptic loading:

$$\Gamma = \Gamma_o\left(1-\frac{x^2}{s^2}\right)^{\frac{1}{2}}$$

Consider, within a circle, some continuous vortex distribution which depends only on the distance r from the centre. Outside the circle the velocity field induced by the vorticity inside the circle is identical to that which would be produced if all the vorticity were concentrated at the centre i.e. a single vortex of equivalent strength. For the peripheral velocity v, at the circumference of a circle radius r, we have

$$v = v(r) = \frac{\Gamma_r}{2\pi r}$$

where $\Gamma_r=\Gamma_x$ is the circulation round the circumference and depends only on the vorticity inside the circle.

v has stationary values with respect to r when

$$\frac{dv}{dr} = 0 \quad \text{i.e. when } \frac{d\Gamma}{dr} = \frac{\Gamma}{r}$$

Since we are dealing with a continuous vortex distribution and not vortex singularities, when r=0, Γ=0 so that v always has a stationary value at r=0. There may be other values for r for which Γ=0.

Now $r\Gamma = \int_x^s \Gamma_\xi d\xi$ and by differentiating with respect to r and remembering that $\Gamma_x=\Gamma_r$ we have

$$r\frac{d\Gamma}{dr} + \Gamma = -\Gamma\frac{dx}{dr}$$

∴ For stationary values of v, i.e. when $\frac{d\Gamma}{dr} = \frac{\Gamma}{r}$ (Fig.12)

then $2\Gamma = -\Gamma\frac{dx}{dr}$

i.e. $\Gamma = 0$ or $\frac{dr}{dx} = -\frac{1}{2}$

The following table gives the functional properties of the rolled up vortex sheet behind one (starboard) wing for a variety of wing loadings. In all the cases tabulated $\frac{\Gamma}{\Gamma_o}$ is given as a function of p which is the distance out from the midwing position normalised with respect to s, the wing semispan. Γ is monotone

increasing from 0 to Γ_o as p decreases from 1 to 0.

The values of $\frac{r}{s}$ and $\frac{2\pi sv}{\Gamma_o}$ which are normalised radius and peripheral velocity at that radius respectively, are evaluated at p=1 and p=0. These are, of course, reciprocals when p=0. In most cases the value of v when p=1 was found by a limiting process. n is a positive integer.

$\frac{\Gamma}{\Gamma_o}$	$\frac{r}{s}$	$\frac{2\pi sv}{\Gamma_o}$	p	$\frac{r}{s}$	$\frac{2\pi sv}{\Gamma_o}$
$\sqrt{1-p^2}$	$\frac{1}{2}\left(\frac{\pi-2\theta}{2\cos\theta} - \sin\theta\right)$ where $x=s\sin\theta$	$\frac{2(1+\cos 2\theta)}{(\pi-2\theta)-\sin 2\theta}$	(1 ((0	0 $\frac{\pi}{4}$	∞ $\frac{4}{\pi}$
$1-p^2$	$\frac{(1-p)(2+p)}{3(1+p)}$	$\frac{3(1+p)^2}{2+p}$	(1 ((0	0 $\frac{2}{3}$	4 $\frac{3}{2}$
$1-p$	$\frac{1}{2}(1-p)$	2	(1 ((0	0 $\frac{1}{2}$	2 2
$\cos\frac{p\pi}{2}$	$\frac{2}{\pi}\left(\frac{1-\sin\frac{p\pi}{2}}{\cos\frac{p\pi}{2}}\right)$	$\frac{\pi}{2}\left(1+\sin\frac{p\pi}{2}\right)$	(1 ((0	0 $\frac{2}{\pi}$	π $\frac{\pi}{2}$

$\frac{\Gamma}{\Gamma_o}$	$\frac{r}{s}$	$\frac{2\pi sv}{\Gamma_o}$	p	$\frac{r}{s}$	$\frac{2\pi sv}{\Gamma_o}$
$1-\sin\frac{p\pi}{2}$	$\frac{1-p-\frac{2}{\pi}\cos\frac{p\pi}{2}}{1-\sin\frac{p\pi}{2}}$	$\frac{(1-\sin\frac{p\pi}{2})^2}{1-p-\frac{2}{\pi}\cos\frac{p\pi}{2}}$	$\begin{cases}1\\ \\ 0\end{cases}$	$\begin{cases}0\\ \\ \frac{\pi-2}{\pi}\end{cases}$	$\begin{cases}0\\ \\ \frac{\pi}{\pi-2}\end{cases}$
$1-p^n$	$\frac{1-\frac{1}{n+1}\sum_{i=o}^{n} p^i}{\sum_{i=o}^{n-1} p^i}$	$\frac{(1-p)\left[\sum_{i=o}^{n-1} p^i\right]^2}{1-\frac{1}{n+1}\sum_{i=o}^{n} p^i}$	$\begin{cases}1\\ \\ 0\end{cases}$	$\begin{cases}0\\ \\ \frac{n}{n+1}\end{cases}$	$\begin{cases}2n\\ \\ \frac{n+1}{n}\end{cases}$
$(1-p)^n$	$\frac{1-p}{n+1}$	$(n+1)(1-p)^{n-1}$	$\begin{cases}1\\ \\ \\ 0\end{cases}$	$\begin{cases}0\\ \\ \\ \frac{1}{n+1}\end{cases}$	$\begin{cases}0 \text{ if } n>1\\ 2 \text{ if } n=1\\ \\ n+1\end{cases}$
$\frac{e-e^p}{e-1}$	$\frac{e^{p-1}-p}{1-e^{p-1}}$	$\frac{e(1-e^{p-1})^2}{(e-1)(e^{p-1}-p)}$	$\begin{cases}1\\ \\ 0\end{cases}$	$\begin{cases}0\\ \\ \frac{1}{e-1}\end{cases}$	$\begin{cases}\frac{2e}{e-1}\\ \\ e-1\end{cases}$
e^p-ep	$\frac{1-2e^{p-1}+p^2}{2(e^{p-1}-p)}$	$\frac{2e(e^{p-1}-p)^2}{1-2e^{p-1}+p^2}$	$\begin{cases}1\\ \\ 0\end{cases}$	$\begin{cases}0\\ \\ \frac{1}{2}(e-2)\end{cases}$	$\begin{cases}0\\ \\ \frac{2}{e-2}\end{cases}$

CHAPTER VI

AXIAL FLOW IN VORTEX CORES.

All the preceeding discussion has assumed negligible the axial motion of a fluid in a vortex but the fact that axial flow does occur has been observed experimentally and was deduced by Batchelor (1964). The pressure in the core is lower than that upstream of the wing and thus if viscosity is ignored, fluid particles in a stream line are accelerated downstream. However, observations have shown that more often than not the axial flow is opposite to that predicted on the basis of neglecting viscosity.

Using an analysis by Kaden (1931. Aufwickling einer unstabilen unstetigkeitsflache. R.A. library translation no. 403), Moore and Saffman (1973) have constructed a laminar flow model allowing for viscous effects which produce the observed axial flow. Without viscosity the induced drag of the wing appears as kinetic energy of rotation. When viscosity is taken into account the rotational kinetic energy is depleted in favour of an axial flow in the direction of the retreating wing.

An elliptically loaded wing of span b has circulation $\frac{2\Gamma_0}{b}[x(b-x)]^{\frac{1}{2}}$ at distance x from the tip, where Γ_0 is the midwing circulation. For small x we can write

the circulation as $K(x)=2\gamma x^{\frac{1}{2}}$, $\gamma=\Gamma_0 b^{-\frac{1}{2}}$

Assuming that the vortex sheet rolls up tightly from the tip and that each turn is circular then near the centre the circulation will depend on the time t since roll up commenced and on the distance r from the centre. When viscous dissipation of velocity is neglected then there is no radial motion to change the vorticity inside turns of the sheet concentric with the centre. This means that after roll up, Γ is a function of r only. Since the dimensions of γ are $L^{\frac{3}{2}}T^{-1}$ it follows that

$\Gamma(r)=2\gamma(\lambda r)^{\frac{1}{2}}$ where λ is an undetermined dimensionless constant, and the transverse velocity is

$$v=\frac{\Gamma}{2\pi r}=\frac{\gamma\sqrt{\lambda}}{\pi\sqrt{r}}.$$

P is a point on one of the (nearly circular) turns around which the circulation is Γ_p, and the angular coordinate θ_p is given by

$$v_p t = r_p \theta_p \text{ at time } t$$

Substituting for v_p gives

$$r_p = \left(\frac{\gamma^2\lambda}{\pi^2}\right)^{\frac{1}{3}}\left(\frac{t}{\theta_p}\right)^{\frac{2}{3}}$$ as the polar equation

of the inner part of the rolled up sheet traced onto a cross-flow plane at distance Ut downstream from the wing; U being the fluid velocity at infinity.

The corresponding results using a near-tip loading of $K(x)=2\gamma x^{1-u}$ are $\Gamma(r)=2\gamma(\lambda r)^{1-n}$, $v\text{-}\beta r^{-n}$, $r=\left(\frac{\beta t}{\theta}\right)^{\frac{1}{1+n}}$

where $\beta=\frac{\gamma\lambda^{1-n}}{\pi}$ and γ is a constant with dimensions $T^{-1}L^{1+n}$. n is restricted to the range $0<n<1$. Whichever way the definition of the radius, $a_0(t)$, of this inner portion of the rolled up spiral is chosen it suffices to note that $a_0 \propto (\beta t)^{\frac{1}{n+1}}$

Still neglecting the effects of viscosity, suppose there is an axial velocity u in the inner part of the rolled up vortex, then by the Bernoulli equation

$$\frac{p}{\rho} + \frac{1}{2}(U+u)^2 + \frac{1}{2}v^2 = \frac{p_\infty}{\rho} + \frac{1}{2}U^2$$

where p_∞ is the upstream undisturbed pressure. Making the assumption $u<<U$ leads to

$$\frac{p-p_\infty}{\rho} + uU + \frac{1}{2}v = 0$$

Also the pressure gradient must produce the centripetal acceleration

$$\text{i.e.} \quad \frac{1}{\rho}\frac{\partial p}{\partial r} = \frac{v^2}{r}$$

$$= \frac{\beta^2}{r^{2u+1}}$$

$$\therefore \frac{p-p_\infty}{\rho} = -\frac{\beta^2}{2nr^{2n}} \qquad \text{for small r.}$$

From the Bernoulli equation

$$u = -\frac{1}{U}\frac{p-p_\infty}{\rho} + \frac{\beta^2}{2r^{2n}}$$

$$\therefore \quad u \sim \frac{\beta^2(1-n)}{2Unr^{2n}} \quad \text{as} \quad r \to 0$$

($\sim$ "approaches asymptotically")

Here u has the sign of U which confirms the theory of

Batchelor that for the inviscid case, axial flow is downstream. The singularities in u and v at r=0 must be removed by viscosity.

It is assumed that there is a viscous core with radius of the order of $(\nu t)^{\frac{1}{2}}$ which is small compared with the radius a_0 of the inner region of the rolled up spiral vortex.

i.e. $a_0 \propto (\beta t)^{\frac{1}{n+1}} >> (\nu t)^{\frac{1}{2}}$ which means

$$t >> \left(\frac{\nu^{1+n}}{\gamma^2}\right)^{\frac{1}{1-n}}$$

The equations of motion are

$$\frac{\partial v}{\partial t} = \nu\left(\frac{\partial^2 v}{\partial r^2} + \frac{1}{r}\frac{\partial v}{\partial r} - \frac{v}{r^2}\right)$$

$$\frac{v^2}{r} = \frac{1}{\rho}\frac{\partial p}{\partial r}$$

$$\frac{\partial u}{\partial t} = -\frac{1}{\rho U}\frac{\partial p}{\partial t} + \nu\left(\frac{\partial^2 u}{\partial r^2} + \frac{1}{r}\frac{\partial u}{\partial r}\right)$$

with boundary conditions

v=0, u finite at r=0.

Also, within the core we require the relations

$$p-p_\infty \sim -\frac{\beta^2}{2nr^{2n}},\quad v \sim \beta r^{-n},\quad w \sim \frac{\beta^2(1-n)}{2Unr^{2n}}$$

to hold for $r\to\infty$ where ∞ here means $O(a_0)$.

In imposing these conditions upon the flow the authors are careful to point out the implied assumption that the action of viscosity has smoothed out the discrete jumps

in the flow field. The radial distance between jumps given by

$$\left(\frac{\beta t}{\theta}\right)^{\frac{1}{1+n}} - \left(\frac{\beta t}{\theta+2\pi}\right)^{\frac{1}{1+n}} \qquad \text{for } \theta >> 2\pi$$

is $\left(\frac{\beta t}{\theta}\right)^{\frac{1}{1+n}} \left(\frac{2\pi}{\theta(1+n)}\right) + O\left(\frac{2\pi}{\theta}\right)^2$

i.e. approximately $\frac{2\pi r^{n+2}}{\beta t(1+n)}$ but since $\beta t >> (\nu t)^{\frac{n+1}{2}}$ and $r < (\nu t)^{\frac{1}{2}}$ then each jump is small and there are many of them for $O<r<O(\nu t)^{\frac{1}{2}}$. The assumption that v is a continuous function of r is valid.

These equations of motion together with the initial conditions

$$v=\beta r^{-n} \quad \text{and} \quad u=\frac{\beta^2(1-n)}{2Unr^{2n}} \quad \text{when } t=0 \text{ are solved}$$

giving v in terms of the Γ function and M, the confluent hypergeometric function of the first kind.

The radius at which v is maximum is thus found to agree substantially with the observed core radius. The pressure is found numerically from $\frac{1}{\rho}\frac{\partial p}{\partial r} = \frac{v^2}{r}$ using the now known expression for v.

The axial velocity u is found, again numerically, from the third of the equations of motion. The results show that for $n>.44$ the axial flow is towards the wing and for $n<.44$ it is away from the wing.

To study the effect of the boundary layer at the wing surfaces on the axial flow in a rolled up vortex the momentum thickness δ_2 is used. This is usually defined as

$$\delta_2 = \int_{-\infty}^{\infty} \frac{u^1}{U}\left[1-\frac{u^1}{U}\right] dz \qquad \text{where}$$

$u^1(z)$ is local velocity in the direction of U and z is the coordinate normal to the wing surface. δ_2 is a measure of momentum loss due to viscous retardation at the wing surface and will in general be a function of span position x.

The two equations $K(x)=2\gamma x^{1-n}$ for the circulation outboard of a span position x, and $\Gamma(r)=2\gamma(\lambda r)^{1-n}$ for the circulation about the circle of radius r, imply that the vorticity within a distance x from the tip at the wing trailing edge is enclosed by a circle of radius $r=x/\lambda$ in the rolled up vortex sheet (Fig. 13).

The flux deficit per unit area at the trailing edge brought about by stopping the flow past the wing is U, so that the flux deficit over a small rectangular area $\delta_2\delta x$ at distance x from the tip is $U\delta_2\delta x$ and this is entrained in the rolled up vortex in an annulus between r and $r+\delta r$. Therefore the flux deficit per unit area at r is such that

$$u.2\pi r\delta r = U\delta_2\delta x$$

$$\text{i.e. } u = \frac{\lambda U\delta_2}{2\pi r} \quad \text{since } \delta x=\lambda\delta r$$

from which, given values for δ_2, boundary and initial conditions are found for the core equation:

$$\frac{\partial u}{\partial t} = \nu\left(\frac{\partial^2 u}{\partial r^2} + \frac{1}{r}\frac{\partial u}{\partial r}\right)$$

The form for δ_2 used by Moore and Saffman is $1.33\left(\frac{\nu c(x)}{U}\right)^{\frac{1}{2}}$ where c is the chord. The solution is again given in terms of the Γ and M functions.

The theoretical core velocity profile is thus found for small r as the sum of the effects due to induced drag and those due to boundary layer retardation.

When compared with what experimental evidence is available the authors describe their results as quite reasonable. As far as application to the study of vortices behind real aircraft goes however, their work is severely limited to the light loading approximation $u<<U$ on which their theory is heavily dependent.

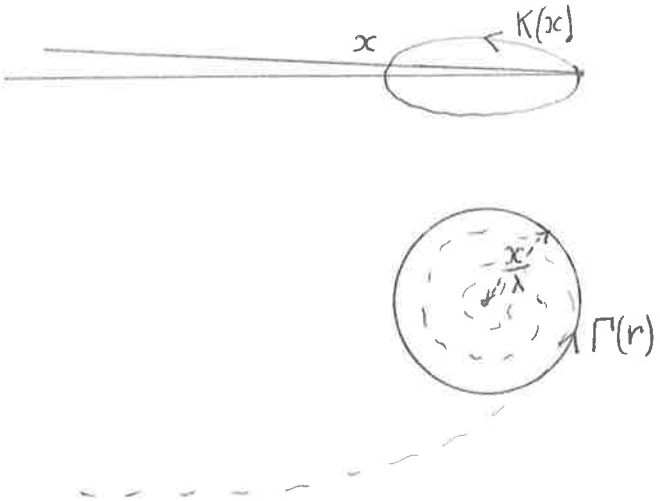

Figure 13

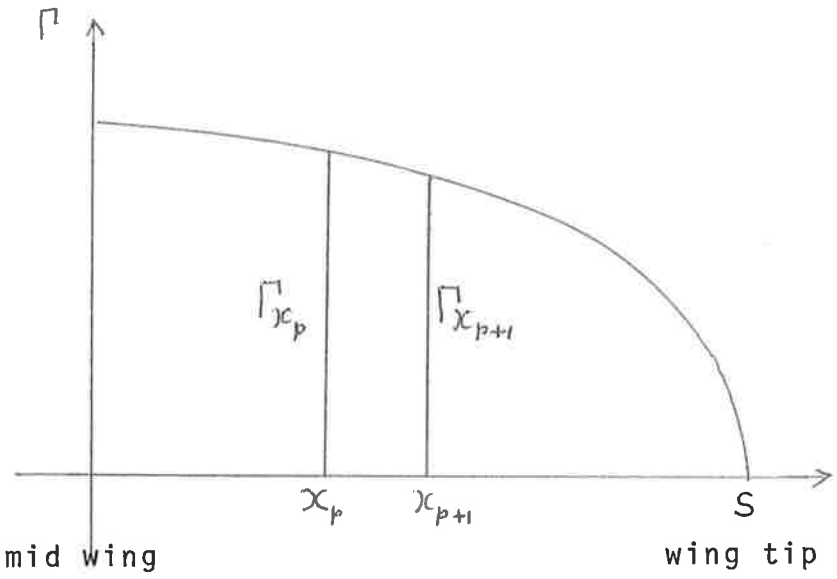

Figure 14

CHAPTER VII

MODIFICATION OF THE BETZ MODEL TO INCORPORATE VISCOSITY.

The Betz's model uses an inviscid fluid. As has been remarked earlier in discussion of the Sprieter and Sacks model, one of the effects of viscosity on a vortex is to change its character to the extent that instead of the velocity decreasing inversely with distance from the vortex centre, it increases from zero at the centre to some maximum after which its behaviour is close to that for inviscid flow. Viscosity produces a core within which the fluid rotates as if it were a solid cylinder. the maximum velocity being at the core perimeter. The action of viscosity is also to diffuse and hence weaken vorticity with time.

The equation governing vorticity, ζ, in axially symmetric flow is

$$\frac{\partial \zeta}{\partial t} = \nu\left(\frac{\partial^2 \zeta}{\partial r^2} + \frac{1}{r}\frac{\partial \zeta}{\partial r}\right)$$ in cylindrical coordinates.

This is the same equation as for radial heat flow in two dimensions.

Lamb (Hydrodynamics p 592) gives a solution of this as $\zeta = \frac{\Gamma_\infty}{4\pi\nu t} e^{-\frac{r}{4\nu t}}$

where Γ_∞ is the initial circulation about any circle radius r (i.e. the strength

of the initial point vortex) centred on r=0. For given r>0, ζ increases with t from zero to a maximum and then decreases to zero as t tends to infinity.

The circulation about a circle radius r is

$$\Gamma = \int \zeta(R).2\pi R dR \quad \text{at time t}$$

$$= \Gamma_\infty \left(1-e^{-\frac{r^2}{4\nu t}}\right) \quad \text{and the velocity at the same radius is}$$

$$q = \frac{\Gamma_\infty}{2\pi r}\left[1 - e^{-\frac{r^2}{4\nu t}}\right]$$

At time t the value of q(r,t) is maximum for r given by

$$\frac{\partial q}{\partial r} = 0 \qquad \text{i.e. by} \quad e^{\frac{r^2}{4\nu t}} = 1+\frac{r^2}{2\nu t}$$

which is very nearly $r^2 = 5\nu t$

For air at 0^oC, $\nu = 1.8 \times 10^{-2}$ cm^2/sec so that maximum q is at $r = .3\sqrt{t}$ cm.

The value of q at this radius is $\frac{0.38\Gamma_\infty}{\sqrt{t}}$ cm/sec if Γ_∞ is measured in cm^2/sec.

It will be noted that this solution depends on an initial point vortex Γ_∞ and takes no account of the vorticity distribution which the Betz inviscid model predicts as the state of affairs when the roll up process is completed. The Lamb solution of the vorticity diffusion equation is independent of the loading of the wing which has produced the vortex. Observations

indicate this not to be the case and a solution which allows for more variability in the initial conditions is required.

A more general solution of the equation

$$\frac{\partial \zeta}{\partial t} = \nu\left(\frac{\partial^2 \zeta}{\partial r^2} + \frac{1}{r}\frac{\partial \zeta}{\partial r}\right)$$ has been provided by Williams (1974). This takes the form

$$\zeta = \sum_{i=1}^{n} \frac{\Delta\Gamma_i}{\pi a_i^2} e^{-\frac{r^2}{a_i^2+4\nu t}}$$

each term of which is similar to the Lamb solution but with built in variability of $\Delta\Gamma_i$, the incremental circulation between radii of a_{i-1} and a_i. The Williams solution is an exact solution of the vorticity diffusion equation and can be regarded as the sum of n solutions of the Lamb type.

Initially, the vorticity, circulation and vortical dispersion are respectively:

$$\zeta = \sum_{i=1}^{n} \frac{\Delta\Gamma_i}{\pi a_i^2} e^{-\frac{r^2}{a_i^2}}$$

$$\Gamma = \int_0^r 2\pi R\zeta(R)\,dR$$

$$= \sum_{i=1}^{n} \Delta\Gamma_i\left(1-e^{-\frac{r^2}{a_i^2}}\right)$$

$$J_\infty = \sum_{i=1}^{n} \Delta\Gamma_i a_i^2 \quad \text{(Fig. 14)}.$$

These are then matched with the appropriate values of the vorticity distribution at the wing trailing edge after roll up has taken place. The assumption is that roll up occurs instantaneously at the trailing edge to become the vortex with the radial vorticity distribution predicted by the Betz inviscid model. By selecting values of $\Delta\Gamma_i$ corresponding to increments in Γ between a_{i-1} and a_i such that the more general solution of the vorticity equation agrees, at t=0, with the completely rolled up Betz vortex at a large (Williams chose 15) number of radial distances, a viscous model is achieved. The Betz model is used as an initial condition for the solution of the vorticity diffusion equation. It is also assumed that the far field vortex structure is the same whether the Betz vortex is instantaneously formed and then begins to decay or whether decay takes place throughout the roll up process. Roll up, of course, does not occur instantaneously at the trailing edge but the author's claim is that the model so constructed will show progressively better agreement with observation as time goes on and that in the case of a wing elliptically loaded with 1000kg of approximately 13 metres span the agreement is good after about 3 seconds.

CHAPTER VIII

COMPUTER SIMULATION

An exact solution of the motion of a vortex sheet, given its vorticity distribution and initial position, is not known. Indeed it is not even possible to solve the problem of N discrete vortices moving in a plane if N>3. However attempts have been made to follow their motion using numerical integration procedures which do throw some light on the behaviour of a continuous line with a given vorticity distribution. The large number of calculations required to give sufficiently accurate results make the use of an electronic computer almost a necessity, but an early attempt on the problem was made by Westwater (1935, Rolling up of the surface of discontinuity behind an aerofoil of finite span. Aero. Res. Council. no. 1962).

Westwater assumed an elliptically loaded wing and approximated the trace of the vortex on the Trefftz plane by a series of discrete, equal strength vortices spaced in such a way as to produce the required strength per unit length. After what must have been an enormous amount of tedious arithmetic Westwater reported a smooth spiral structure at the tips from which the rate of roll up could be estimated. Later work has not been able to confirm Westwater's results in spite of the fact that it had been shown analytically (Kaden 1931, Aufwicklung

einer unstabilen Unstetigkeitsfläche, Ing. Archiv 2, 140. English translation R.A.E. Library Trans no. 403.) that his results were to be expected. The fact that later workers agreed among themselves cast doubt upon the validity of his method.

Because of the number of calculations he would have had to perform it was obvious first to call in question Westwater's numerical accuracy. Also considering the method he used, Euler integration, and the fact that he would probably have chosen time steps large enough to be able to arrive at results in a reasonable time, the combination might well have doubtful validity. The difficulty remained that his results seemed more likely to be correct in the light of Kadens analysis than the later attempts which were able to achieve sixteen figure accuracy with better methods of numerical integration. The validity of the methods used by the later investigators had to be established.

Moore (1971, The discrete vortex approximation of a vortex sheet. California Inst. of Tech. Rep. AFOSR-1084-69) repeated Westwater's calculations using a Runge-Kutta 4th order numerical integration method and a time step much smaller than the orbital period of the closest pair of vortices. Moore claimed nine figure accuracy after forty complete revolutions of such a pair. His results agree significantly with those of Takami (1964,

A numerical experiment with discrete vortex approximation with reference to the rolling up of a vortex sheet. Dept. of Aero. & Astro., Stanford University SUDAER 202).

There is little doubt that these results are very close to the actual behaviour of such a system of point vortices. Both Moore and Takami reported apparent chaotic motion of the vortices close to the centre of the spiral which quickly spread to the outer turns and before long destroyed the spiral pattern entirely. An interesting feature of Moore's experiment was that after a large number of time steps he changed the sign of the circulation about each of the vortices. They retraced their steps and ultimately resumed their original positions. Had there been errors in the method due to round off or instability this would not have happened.

It now seems certain that the process of replacing a vortex sheet by a series of point vortices suitably spaced or with suitable variations in strength is not valid for the inner turns of the spiral which has analytically been shown to form. Since the number of turns in the spiral is indefinitely large there must be several of the inner turns which contain only one of the discrete vortices on its circumference. In fact all the turns of the spiral depend for their definition on the presence of vortices on their perimeters and those (almost circular) turns which have less than three are not even uniquely

determined. Also it is these irregularly placed vortices which, for most aircraft wing loadings, are the strongest. This asymmetry within an otherwise well behaved turn of the spiral then affects its outer neighbour and so the irregular motion is spread throughout the whole system.

A possible reason for the apparent respectability of the Westwater vortex points was suggested by Chorin and Bernard and mentioned before they published in a later paper of Moore's (1974). The Westwater combination of the Euler first order method of numerical integration with large time steps produced an increasing separation between adjacent vortex points and so spuriously slows the rate at which they orbit each other. This is borne out by one of the present computer programs described later which calculates the progressive value of the vortical dispersion about the vortical centroid. When the Euler integration method is used the vortical dispersion is shown to increase more rapidly than with other methods. The increased vortex point separation places a kind of increasing lower bound on the radius of the inner turns of the spiral and reduces the effect of the asymmetry on the outer turns.

In the same paper Moore (1974) describes an attempt by Chorin and Bernard artificially to slow the orbiting rate of close vortex pairs by introducing an arbitrarily

chosen cut off radius within which the induced velocity field does not increase indefinitely towards the vortex point but decreases steadily towards zero. This was claimed to produce an effect roughly equivalent to that of viscosity. That the results were not entirely satisfactory and led to the chaotic behaviour already encountered was probably due to the difficulty of deciding where the cut off point should occur for each vortex.

The primary object of Moore's (1974) paper was to describe a chaos suppressing technique and to discuss the results of its use in conjunction with the Runge-Kutta fourth order numerical integration method.

The asymmetry appears in the inner turns of a vortex spiral because there are too few vortices on its perimeter to approximate the circumferentially smooth induced velocity effects which would occur in a single turn of the line having the given continuous vorticity distribution. Moore's method consists in counting the number of vortex points on the inner most turn at each stage and if the number is below a certain minimum to replace them by a single vortex at their vortical centroid with strength equal to the sum of their strengths. Practically this was accomplished by finding the angle formed by the lines joining the second and third vortices from the tip, and the third and fourth. If this angle θ_c, exceeds some given value then the first vortex (at the tip) and the

second are combined and placed at their vortical centroid. This new vortex is considered to be at the tip position. It was found that when $\theta_c=90^o$ chaotic motion was suppressed. This corresponds to four vortices per turn. Increasing the tolerance to three vortices per turn was not adequate to prevent chaotic motion.

CHAPTER IX

THE CURRENT COMPUTER STUDY OF THE BEHAVIOUR OF A SYSTEM OF DISCRETE VORTICES. PART 1.

The time it takes for a point at a distance d from a vortex of strength Γ to make a complete orbit in the absence of any other velocity field is the same as the orbital period of a pair of vortices separated by a distance d, the sum of whose strengths is Γ. This period is $\frac{4\pi^2 d^2}{\Gamma}$. The time steps chosen for a numerical integration method must be very much smaller than the minimum value this takes for any pair of vortices in the system. What this minimum will be as the vortices move about is a matter for conjecture. The most that can be said is that for the outer turn of the spiral each vortex retains the immediate neighbours it had when in the initial flat sheet configuration and that in the absence of chaotic behaviour, their separation gradually increases.

The expression $\frac{4\pi^2 d^2}{\Gamma}$ is more sensitive to the distance between vortices than to their strengths. If chaos is unsuppressed in one experiment, doubling the number of vortices and halving their strengths will, as Moore discovered, only make matters worse. On the other hand increasing the distance between vortices gives a poorer approximation to the vortex sheet being studied.

The presence of the neighbours of a vortex pair does of course affect their orbital period. If B and C are an isolated pair of vortices with circulation strengths which do not sum to zero then they will perform revolutions about each other in a time given by the above expression. Each will move at right angles to the line joining them at any time and they will orbit their stationary vortical centroid which will be on the line. If their strengths have the same sign their centroid will be between them, otherwise it will be on the line joining them produced. Supposing that B and C have the same sign, then when two more vortices, A and D, are introduced whose circulations are both in the same sense as B and C, so that initially ABCD are in line in that order, then the tendency for B to move one way due to the presence of C is opposed by the effect of A. Similarly the motion of C is affected by the opposing velocity fields of B and D. The angular velocity of BC will thus be altered depending on the strength, sign and proximimity of A and D at any particular time.

It has been pointed out by Rossow (1975) that it is at least theoretically possible to prescribe the initial vertical speeds of a set of point vortices which are initially arranged along a horizontal line. The conditions under which this can be done are not mentioned by Rossow and deserve some consideration here.

The equations governing the speeds v_A, v_B of a pair of vortices A, B at right angles to the line joining them are

$$\frac{K_B}{2\pi d} = v_A \text{ and } \frac{-K_A}{2\pi d} = v_B \text{ or in matrix form:}$$

$$\begin{bmatrix} 0 & 1 \\ -1 & 0 \end{bmatrix} \begin{bmatrix} K_A \\ K_B \end{bmatrix} = 2\pi d \begin{bmatrix} v_A \\ v_B \end{bmatrix}$$

where K_A, K_B are the circulation strengths around A,B and d is their separation distance. Given d, v_A and v_B there is always a solution for K_A and K_B. Now consider three initially collinear, equally spaced vortices A, B, C. If AB=BC=d then in the previous notation:

$$\begin{bmatrix} 0 & \frac{1}{2} & 1 \\ -\frac{1}{2} & 0 & \frac{1}{2} \\ -1 & -\frac{1}{2} & 0 \end{bmatrix} \begin{bmatrix} K_A \\ K_B \\ K_C \end{bmatrix} = 2\pi d \begin{bmatrix} v_A \\ v_B \\ v_C \end{bmatrix}$$

Since the coefficient matrix is singular the general solution for K_A, K_B, K_C does not exist.

More generally, suppose initially collinear vortices A_0, A_1, A_2 ---, A_n with strengths K_0, K_1, K_2 ---, K_n are arranged such that $A_oA_i=a_i$, i=1, 2,---n. This implies $a_o=0$.

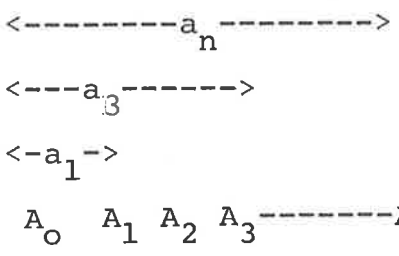

If the initial downward velocity of A_j is v_j then:

$$-\frac{K_0}{2\pi a_j} - \frac{K_1}{2\pi(a_j-a_1)} - \frac{K_2}{2\pi(a_j-a_2)} - \text{----} - \frac{K_{j-1}}{2\pi(a_j-a_{j-1})} + \frac{K_{j+1}}{2\pi(a_{j+1}-a_j)}$$

$$+ \frac{K_{j+2}}{2\pi(a_{j+2}-a_j)} + \text{-------} + \frac{K_n}{2\pi(a_n-a_j)} = v_j$$

or more compactly:-

$$\sum_{\substack{i=0 \\ i\neq j}}^{n} \frac{Ki}{a_i-a_j} = 2\pi v_j \qquad j=1,\ 2,\ \text{---}\ n.$$

The coefficient matrix

$$\begin{bmatrix} 0 & \frac{1}{a_1} & \frac{1}{a_2} & \frac{1}{a_3} & \text{------} & \frac{1}{a_n} \\ -\frac{1}{a_1} & 0 & \frac{1}{a_2-a_1} & \frac{1}{a_3-a_1} & \text{-----} & \frac{1}{a_n-a_1} \\ -\frac{1}{a_2} & \frac{1}{a_1-a_2} & 0 & \frac{1}{a_3-a_2} & \text{-----} & \frac{1}{a_n-a_2} \\ \vdots & \vdots & & \vdots & & \vdots \\ -\frac{1}{a_n} & \frac{1}{a_1-a_n} & \frac{1}{a_2-a_n} & \text{----------} & & 0 \end{bmatrix} = M$$

of the above system is skew symmetric and is singular if n is odd since

$$\det(M) = \det(M^T) = \det(-M) = (-1)^n \det(M)$$

i.e. $\det(M) = -\det(M) = 0$ if n is odd.

Thus for an even number of collinear vortices it is possible to prescribe their initial vertical motion by

suitably choosing their circulation strengths but for an odd number it is not. In the case discussed by Rossow an attempt was made to inhibit roll up of the vortex sheet being simulated. This meant giving the same initial vertical velocity to all the vortices so that they would retain their positions relative to each other, and merely translate instead of rolling up. This requires that adjacent vortices have roughly equal but opposite circulations. It is difficult to see how such an arrangement can be used to approximate a continuous vortex sheet.

For a first attempt in the present computer study of the behaviour of a vortex system a simple program was written using an unsophisticated numerical integration method which plotted the movements of ten point vortices of equal strengths equally spaced at 2cm intervals along a line. The QIKPLOT subroutine available with the computing system at this university was used. The strength of each vortex was 4π $cm^2 sec^{-1}$ so that the contribution of that vortex to the velocity of a point distant r from it was $\frac{2}{r}$ in the anticlockwise direction. The method (referred to in the following disucssion as the H method, see Appendix C) was to calculate the displacement each vortex would suffer in the given time step due to the combined induced velocity of all the others assuming they were stationary. The new positions were then stored and plotted and the procedure was repeated. As expected,

when a smooth curve was drawn through the points the effect was that of a straight line which rotated about its centre anticlockwise at the same time curling up its ends also in the anticlockwise direction (Fig. 15). The vortices were widely spaced, two units of length apart, and the time step $\Delta t=1$, was small enough to satisfy the criterion for accuracy at least in their initial positions. Although the method of integration was crude the pattern of curl up was well established and no chaotic behaviour was observed for the ten time steps computed.

The program was run again with the vortices initially in the same position but with their strengths proportional to their distances from the left hand end. The strengths ranged from 0 sq.units/sec at the left hand end to 4π at the right end increasing to the right in steps of $\frac{2\pi}{5}$. Roll up began at the right hand end and by the tenth step a loose spiral of about 1¼ turns had formed (Fig. 16). This was equivalent to treating a widely spaced discretization of the right hand half of a parabolically loaded wing, neglecting the influence of the symmetrically placed points on the left hand half of the wing which would have equal but opposite circulation.

To avoid the difficulty of the QIKPLOT subroutine which automatically adjusts the scale to allow the plotted points to extend to the limits of the page, it was

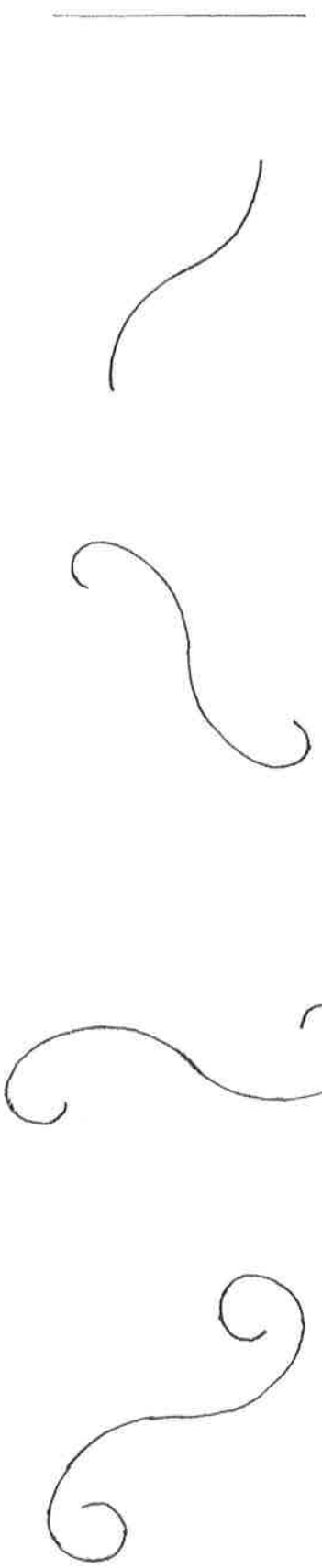

Figure 15

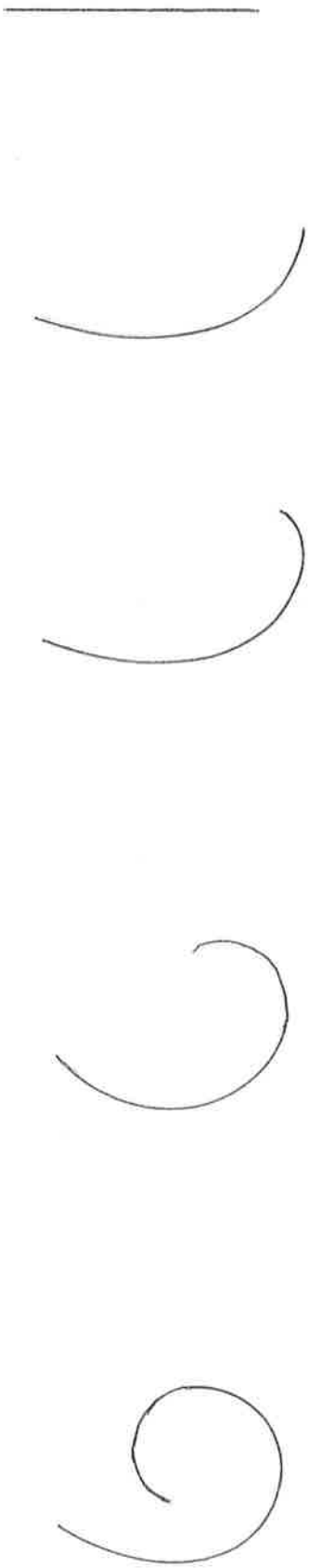

Figure 16

decided to use the more flexible LP plotting package. Although the positional accuracy of any line printer plotting package is limited to half the width or height of a character position on an output page, it was not felt necessary to employ a more accurate plotting output device. The slight inaccuracies of each plot are neither cumulative nor transmitted to subsequent plots. Also it was helpful to be able to identify the points by using a different plotting symbol for each vortex.

The next run included the formerly neglected, symmetrically placed left wing vortices corresponding to a parabolically loaded wing

$$\Gamma = 20\pi(1-\frac{x^2}{100})$$

$$\gamma = \frac{2\pi x}{5}$$

The 21 vortices were equally spaced at intervals of 1cm with values of x ranging from -10cm to 10cm. The trace which evolved was very similar to the five frames of Plot Set 1 shown in Appendix B except that 41 points were used in that case.

After ten time steps of $\Delta t=1$, all the vortices had descended to below their initial position. The lowest point (of zero circulation) had descended to more than seventeen units below its original level.

CHAPTER X

THE CURRENT STUDY PART 2.

At this stage it was considered necessary to use a more accurate numerical integration method than the H method employed hitherto. The new position of each vortex had been calculated assuming that all the others did not move for that time step, i.e. they remained at the positions they had taken up at the beginning of the time step. It was thought that a more correct result would be obtained by placing each vortex at the midpoint of its old and new positions as calculated by the method then recalculating the new position of each vortex for the same time step. The process was repeated until the sum of the squares of the differences between each corrected position and the previous corrected position for the same point was within a chosen tolerance. These positions were then taken to be the starting points for the next time step. However it was not clear what the tolerance should be and there was no certainty that there would be convergence to the correct values, or for that matter, to any values.

In the early stages at least, this iteration method seemed to be producing results which were comparable with the H method but it was so expensive of computer time that it was abandoned in favour of a generalised Runge-

Kutta fourth order method of numerical integration now described.

The pair of equations

$$\frac{dx}{dt} = g(t,x,y), \quad \frac{dy}{dt} = f(t,x,y)$$

can be integrated numerically by first finding the eight quantities k_{ij}, i=1,2,3,4 j=1,2 according to the scheme:-

$k_{11}= hg(t_r,x_r,y_r)$, $k_{12}=hf(t_r,x_r,y_r)$

$k_{21}= hg(t_r+\frac{1}{2}h,x_r+\frac{1}{2}k_{11},y_r+\frac{1}{2}k_{12})$ $k_{22}=hf(t_r+\frac{1}{2}h,x_r+\frac{1}{2}k_{11},y_r+\frac{1}{2}k_{12})$

$k_{31}= hg(t_r+\frac{1}{2}h,x_r+\frac{1}{2}k_{21},y_r+\frac{1}{2}k_{22})$ $k_{32}=hf(t_r+\frac{1}{2}h,x_r+\frac{1}{2}k_{21},y_r+\frac{1}{2}k_{22})$

$k_{41}= hg(t_r+h,x_r+k_{31},y_r+k_{32})$ $k_{42}=hf(t_r+h,x_r+k_{31},y_r+k_{32})$

then $x_{r+1}=x_r+\frac{1}{6}(k_{11}+2k_{21}+2k_{31}+k_{41})$

and $y_{r+1}=y_r+\frac{1}{6}(k_{12}+2k_{22}+2k_{32}+k_{42})$

where x_r, y_r are the values of x,y at $t=t_r$ and $h=t_{r+1}-t_r$ is the time step.

Extending this to the n points (x_i,y_i) i=1,2,----n we have to solve the system

$$\left.\begin{aligned}\frac{dx_i}{dt} &= g_i(t,x_1,x_2,\ldots x_n,y_1,y_2,\ldots y_n)\\ \frac{dy_i}{dt} &= f_i(t,x_1,x_2,\ldots x_n,y_1,y_2,\ldots y_n)\end{aligned}\right)$$

or more compactly

$$\frac{dx_i}{dt} = g_i(t,\underset{\sim}{x},\underset{\sim}{y}), \quad \frac{dy_i}{dt} = f_i(t,\underset{\sim}{x},\underset{\sim}{y})$$

$i=1,2,---n$; $\underset{\sim}{x}=x_1,x_2,---x_n$; $\underset{\sim}{y}=y_1,y_2,---y_n$

The numerical solution then follows the procedure:-

$$k_{11i} = kg_i(t_r, \underset{\sim}{x}_r, \underset{\sim}{y}_r) \qquad k_{12i} = hf_i(t_r, \underset{\sim}{x}_r, \underset{\sim}{y}_r)$$

$$k_{21i} = hg_i(t_r+\tfrac{1}{2}h, \underset{\sim}{x}_r+\tfrac{1}{2}\underset{\sim}{k}_{11}, \underset{\sim}{y}_r+\tfrac{1}{2}\underset{\sim}{k}_{12})$$

$$k_{22i} = hf_i(t_r+\tfrac{1}{2}h, \underset{\sim}{x}_r+\tfrac{1}{2}\underset{\sim}{k}_{11}, \underset{\sim}{y}_r+\tfrac{1}{2}\underset{\sim}{k}_{12})$$

$$k_{31i} = kg_i(t_r+\tfrac{1}{2}h, \underset{\sim}{x}_r+\tfrac{1}{2}\underset{\sim}{k}_{21}, \underset{\sim}{y}_r+\tfrac{1}{2}\underset{\sim}{k}_{22})$$

$$k_{32i} = hf_i(t_r+\tfrac{1}{2}h, \underset{\sim}{x}_r+\tfrac{1}{2}\underset{\sim}{k}_{21}, \underset{\sim}{y}_r+\tfrac{1}{2}\underset{\sim}{k}_{22})$$

$$k_{41i} = hg_i(t_r+h, \underset{\sim}{x}_r+\underset{\sim}{k}_{31}, \underset{\sim}{y}_r+\underset{\sim}{k}_{32})$$

$$k_{42i} = hf_i(t_r+h, \underset{\sim}{x}_r+\underset{\sim}{k}_{31}, \underset{\sim}{y}_r+\underset{\sim}{k}_{32})$$

where $\underset{\sim}{k}_{pq} = (k_{pq1}, k_{pq2}, \text{---} k_{pqn})$

Then $\underset{\sim}{x}_{r+1} = \underset{\sim}{x}_r+\frac{1}{6}(\underset{\sim}{k}_{11}+2\underset{\sim}{k}_{21}+2\underset{\sim}{k}_{31}+\underset{\sim}{k}_{41})$

$\underset{\sim}{y}_{r+1} = \underset{\sim}{y}_r+\frac{1}{6}(\underset{\sim}{k}_{12}+2\underset{\sim}{k}_{22}+2\underset{\sim}{k}_{32}+k_{42})$

The contribution to the velocity of the i th vortex point (x_i, y_i) by the j th vortex at (x_j, y_j) is of magnitude of $\frac{K_j}{2\pi d_{ij}}$ in a direction normal to the line joining the two points where d_{ij} is the distance between them and K_j is the strength of the j th vortex. Therefor the x component of this velocity is

$$-\frac{K_j(y_i-y_j)}{2\pi d_{ij}^2} \qquad \text{and the y component is} \quad \frac{K_j(x_i-x_j)}{2\pi d_{ij}^2}$$

The system of equations to be solved is then:

$$\frac{dx_i}{dt} = -\frac{1}{2\pi}\sum_{\substack{j=1\\ j\neq i}}^{n}\frac{K_j(y_i-y_j)}{d_{ij}^2}, \qquad \frac{dy_i}{dt} = \frac{1}{2\pi}\sum_{\substack{j=1\\ j\neq i}}^{n}\frac{K_j(x_i-x_j)}{d_{ij}^2}$$

since each vortex makes no contribution to its own velocity.

To gauge the accuracy of the method it was tested with two vortices whose strengths were in the ratio 3 to 2. The time steps were chosen such as to make the value

$$R = \frac{\text{time step}}{\text{orbital period}}$$

range from $\frac{1}{128}$ to $\frac{5}{4}$. No accuracy was expected from the case $R = \frac{5}{4}$ although even then the position of the centroid had not moved after 600 time steps. When R is too large for accuracy the method has the effect of rapidly increasing the separation but keeping the vortical centroid stationary. The orbital period is thus increased which in turn reduces the value of R. The rate of increase of separation steadily decreases and approaches zero asymptotically as t tends to infinity. For the most accurate case when $R \doteqdot \frac{1}{128}$, after 5400 time steps representing about 42 orbits there was a relative error in the separation of the two vortices of 3×10^{-7} with an angular error of 4 degrees.

The method was then applied to a system of 41 point vortices spread over a distance of 20 units of length initially. They were equally spaced and their strengths corresponded to what would have been in successive runs elliptic, cosine curve and gable wing loadings character-

ised by the sketches in Fig. 17.

In each case the constants A,B,C were chosen so that the criterion for accuracy would be satisfied.

In the elliptic case $|x| \leq \frac{200}{21}$ to avoid the singularity at $|x|=10$. For this case which is the most commonly considered by investigators in this field, the roll up at the tips was tighter than for a parabolic loading and after only a few time steps the spiral pattern at the centre of each roll up at the ends became progressively less well defined until it was impossible to discern it at all.

The evolution of the trace which moved under the effect of the cosine curve loading was dominated by the positions of maximum vorticity at $x=\pm 5$. The general development was similar to that shown in Appendix B, Plot Set 5 except in that case the H method was used. The double spiral patterns gradually diffused into a jumble as further time steps were plotted.

The gable pattern development was similar to that of two lines of constant but opposite vorticity initially arranged end to end (see Appendix B, Plot Set 4). The centre point, which had zero vorticity and would have been a point of discontinuity in the continuous representation became isolated from the others and descended at a rate noticeably faster than the centre of vorticity of

each of the two centra rotating curves.

Vorticity Distribution.

Elliptic:

$$K(x)= \frac{Ax}{\sqrt{(1-x^2/100)}}$$

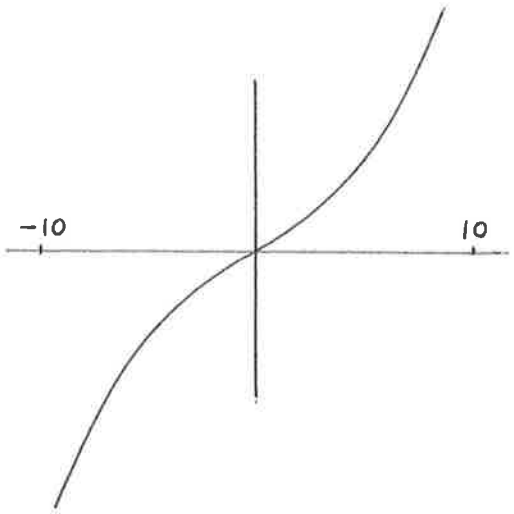

Cosine:

$$K(x)= B\sin(\frac{\pi x}{10})$$

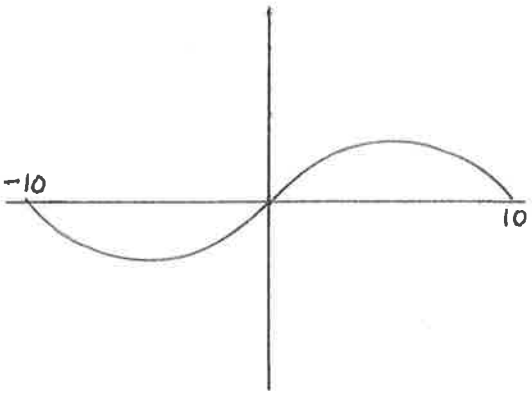

Gable:

$$K(x)=\begin{cases} C & x>0 \\ 0 & x=0 \\ -C & x<0 \end{cases}$$

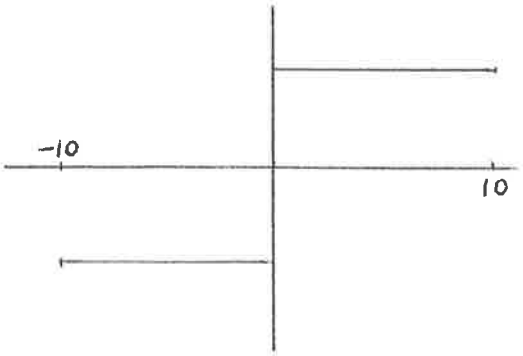

Figure 17

CHAPTER XI

THE CURRENT STUDY PART 3.

In an attempt to suppress the chaotic behaviour of the interior vortices in a rolling up spiral the method of Moore, described earlier, was used with a system of 81 vortices with strengths arranged to correspond to an elliptically loaded wing. The equation

$$K(x) = \frac{Ax}{\sqrt{1-\frac{x^2}{100}}} \qquad |x| \leq \frac{400}{41}$$

governed the strength of each vortex where x is the distance from the midwing position. The constant A was chosen so that $\sum_{i=41}^{81} K_i = 1$.

Each vortex was combined with the tip vortex at their vortical centroid when an amalgamation occurred and this was done sequentially from the tip inwards according to their initial arrangement. At any stage only the positions of those standing first, second and third in line for the next amalgamation were used to decide if it should take place. Thus there was nothing to prevent erratic behaviour of any of the other vortices. Moore claimed that if the criterion for amalgamation was that the angle subtended at the second in succession for combination with those already combined, by the first and the third was less than 90° then chaos would be suppressed. The angle actually measured in the present

program (Appendix C) was the exterior angle formed at the third vortex by the lines joining it to the second and fourth (Fig. 18).

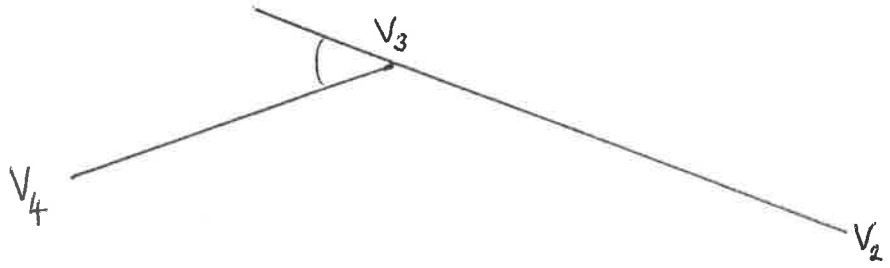

Fig. 18

The criterion for amalgamation was satisfied if this angle was between 90^{o} and 270^{o}. No amalgamation was effected when it was greater than 270^{o}.

Using this criterion, computer runs were made choosing time steps so that the ratio of time step to orbital period of the two outermost vortices was 0.09, 0.19, 0.28, and 0.56. Of course the presence of the other vortices in the system would retard the orbiting rate of the two strongest vortices. These ratios were the result of taking, in the units of time used for giving the vortex strengths, time steps of 1,2,3 and 6 units. For future convenience the units of length and time will be taken as centimetres and seconds.

In each run ten plots were made at intervals of 60 seconds. This meant that in the first run there were six times as many time steps as in the last. When the time step was 1 second, after 180 seconds, seven

amalgamations had occurred (at each tip) without removing all the apparent random placement of the vortices in the tip neighbourhood. However the outside turn was not noticeably affected by this. After 300 seconds twelve amalgamations had taken place leaving a smooth spiral pattern consisting of a central vortex surrounded by a little more than one complete turn of the spiral. In the remaining 300 seconds no further amalgamations had taken place and the spiral shape was defined only by the outside turn which had steadily drawn in more of the vortices originally towards the centre of the wing.

When the program was rerun with time steps of six seconds only six amalgamations had occurred after 180 seconds but all except the points towards the centre of the spirals at each end were in substantially the same position as when the time step was one second. This correspondence continued between the two runs until the final plot in each case at 600 seconds. In the $\Delta t=6$ case fourteen amalgamations had occurred compared with twelve in the case $\Delta t=1$. The nineteenth vortex points in from the tip at each end occupied almost the same positions after 600 seconds for both runs and so did all those originally between them. After this time there was more noticeable irregularity in the $\Delta t=1$ case than for the $\Delta t=6$ case due to the two fewer amalgamations which had taken place.

The two intermediate runs i.e. those in which $\Delta t=2$ and $\Delta t=3$ respectively showed a marked similarity at corresponding elapsed times except for some of the interior vortex points in the $\Delta t=3$ case which were often irregularly placed up until the plot at 420 seconds. Thereafter the amalgamation process was able to suppress chaos satisfactorily.

A further run of ten plots was made with $\Delta t=12$ again plotting at intervals of 60 seconds. Here amalgamation occurred only six times, all in the first 300 seconds. Although the general form of the vortex system showed a marked resemblance at each plot to the corresponding plots for the case $\Delta t=1$ at no stage was there anything less than chaos within the outer turn of each spiral. Even then nearly all pairs of corresponding points on the outer turns at each stage for the two runs $\Delta t=1$ and $\Delta t=12$ did not differ in position by more than one centimetre. A noteworthy exception to this was the aberrant behaviour in the $\Delta t=12$ case of the 25th and 26th vortices in from each tip. These two approached each other more closely than other neighbouring pairs in their vicinity had done in any earlier runs, and remained close from 240 seconds to 600 seconds orbiting each other rapidly.

Of all the runs made only in the $\Delta t=2$ case was chaotic behaviour suppressed at every plot. At every stage for all the runs the horizontal distance of the vortical centroid from the midwing for each semiwing was steady at 7.45 cms while it descended at exactly the same rate for all the runs, about 0.015 cm/sec. Some of the plots of these runs are shown in Appendix B, Plot Set 3.

The general conclusion seems to be that provided amalgamations occur often enough then chaotic behaviour is adequately suppressed. There appears to be no sure criterion for predicting when amalgamations will take place although they can be made to occur more often by increasing the size of the critical angle formed by the three vortices on which the process depends. In all the above runs this was 90^{o}. It should be noted that the amalgamation technique does not produce more smooth turns of the spiral shape. When it works it merely removes the internal irregularity. When it does not work it leaves an apparently random arrangement of vortices within the outside turn. The outer turn is likely to be adversely affected by the irregularity within it. In all the runs there was never more than $1\frac{3}{4}$ turns of a spiral defined by regularly spaced, initially adjacent vortex points, the turns being considered to start at the point where the tangent is first vertical when moving

outwards from the point originally at the midwing position. Neither is the amalgamation process as described by Moore applicable to sheet strength distributions producing roll up which does not begin at the tips; like for example the cosine curve loading discussed earlier.

Table 1 gives the values of the error monitoring function, E, whose invariance is proved in Appendix I. T is the total elapsed time in seconds at each plot; Y is the vertical distance below the initial position of the vortical centroid of each semiwing given in centimetres; A is the total number of amalgamations preceeding each plot; and E is the so called Kirchhoff-Routh path function for all the vortex points:

$$E = \sum_{i=1}^{80} \sum_{j=i+1}^{81} \tfrac{1}{2} K_i K_j \ln\left[(x_i - x_j)^2 + (y_i - y_j)^2\right]$$

(see Appendix A).

It is noted that Y was independent of the time step used and was the same for corresponding plots in all runs.

E is not invariant during amalgamations.

Table 1.

		$\Delta t = 1$		$\Delta t = 2$	
T	Y	A	E	A	E
60	.67	5	-2.01	5	-2.02
120	1.31	5	-2.01	8	-2.00
180	1.94	7	-2.04	9	-2.01
240	2.56	11	-2.04	11	-2.04
300	3.17	12	-2.05	12	-2.05
360	3.80	12	-2.05	13	-2.08
420	4.42	12	-2.05	14	-2.10
480	5.04	12	-2.05	15	-2.12
540	5.67	12	-2.05	16	-2.15
600	6.30	12	-2.05	16	-2.15

	$\Delta t = 3$		$\Delta t = 6$		$\Delta t = 12$	
T	A	E	A	E	A	E
60	3	-2.05	4	-2.02	4	-1.99
120	3	-2.05	5	-2.01	4	-1.99
180	6	-2.06	6	-2.02	5	-1.98
240	10	-2.02	11	-2.04	6	-1.99
300	10	-2.02	12	-2.06	6	-1.99
360	10	-2.02	13	-2.07	6	-1.99
420	11	-2.05	14	-2.10	6	-1.99
480	15	-2.13	14	-2.10	6	-1.99
540	16	-2.15	14	-2.10	6	-1.98
600	16	-2.15	14	-2.10	6	-1.98

CHAPTER XII

THE CURRENT STUDY PART 4.

Modification of Parabolic Loading.

When the Runge-Kutta method was used to plot the simulated motion of vortex points the early irregularity which quickly developed into chaos was always a feature of the roll up process. The H method however and the Euler first order method which uses the formulae

$$\Delta x_i = -\frac{\Delta t}{2\pi} \sum_j \frac{K_j (y_i - y_j)}{d_{ij}^2}, \qquad \Delta y_i = \frac{\Delta t}{2\pi} \sum_j \frac{K_j (x_i - x_j)}{d_{ij}^2}$$

both seemed to contain some sort of chaos suppressing ingredient especially in the case when the vortex strengths corresponded to a parabolically loaded wing. That these two methods are less accurate was emphasised by the changing values of the Kirchhoff-Routh path function which is an invariant of the motion. Because the less accurate H method produced results which better resembled at least qualitatively, the analytical solution, modifications were made to it to simulate the deflection of flaps or some other device which produced more lift over only a section of the wing.

Neglecting fusilage effects, a flap over the central third of the wing was simulated by doubling the strengths of the vortices at the sixteenth positions in from each end of the initial array of 41 vortex points whose strengths

otherwise corresponded to a parabolically loaded wing (Fig. 19). The vortices of doubled strengths represented the additional shed vorticity at the points of discontinuity in the wing loading. In the early stages the motion of the vortices was not noticeably different except for the disturbing behaviour of the two vortices whose strengths had been changed, and the pair each side of these. There were thus two symmetrically placed regions of disturbance each involving five vortices. As the roll-up proceeded the disturbances were drawn into the main spiral shape at each end upsetting the regularity found in the unmodified case.

The reverse situation where the central flap produces less lift was simulated by reversing the sign of the same two vortices (Fig. 20). The original absolute value of the modified vortices was very nearly $1 cm^2 sec^{-1}$ so that changing their sign represented a change of twice the magnitude as doubling them had done. The effect was similar except that the disturbance was greater and involved about seven vortices each side of the midwing point. For this modification the vortex points whose strengths had been changed became progressively more isolated as time went on. An explanation for this is that the immediate neighbours each side of a vortex which has opposite circulation to those in its vicinity, are in two velocity fields which at that point act in the same direction. In the figure 21, B moves down much faster

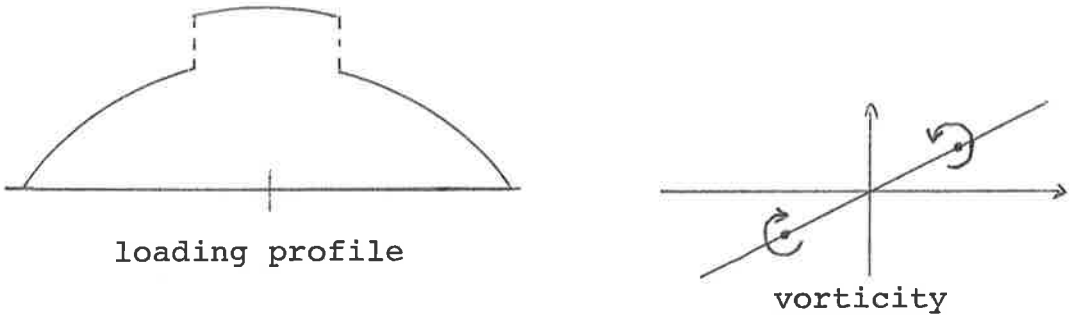

Figure 19

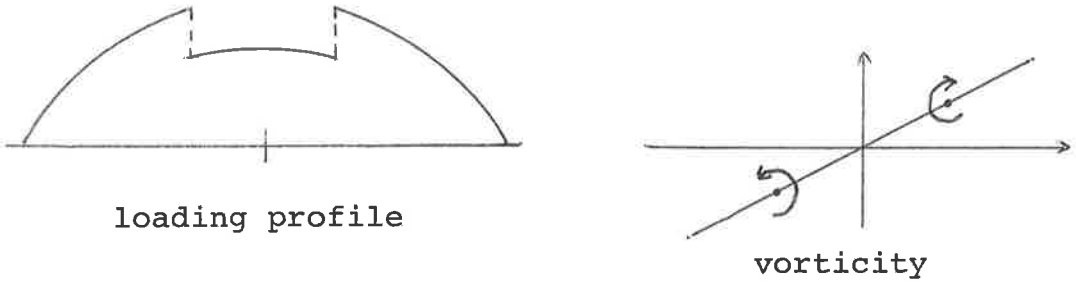

Figure 20

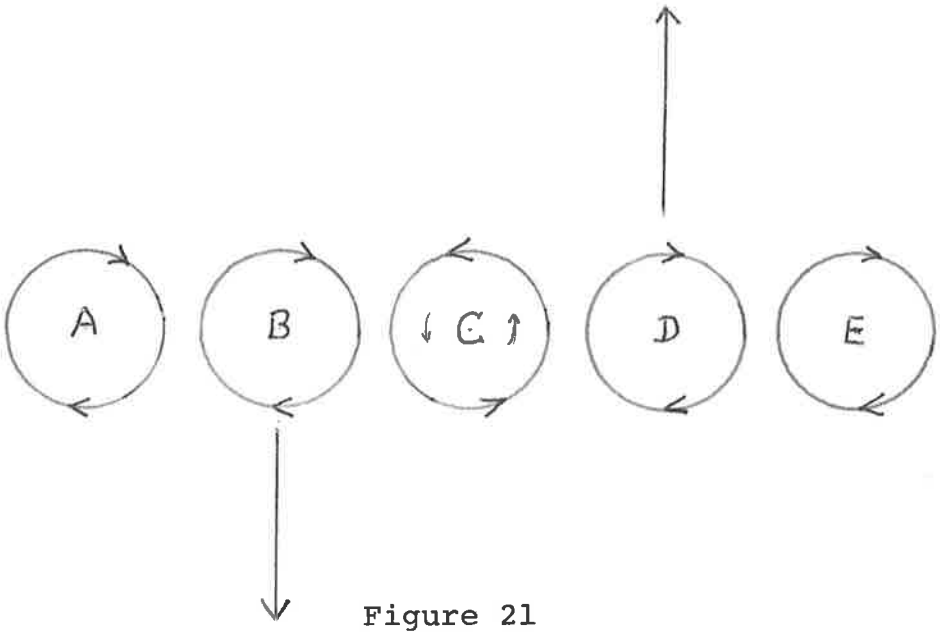

Figure 21

due to the opposite circulation round C than it would otherwise while D moves up for a similar reason. C itself is subject to the stabilizing influence of being between two vortices with much the same circulation. Given that all vortices in that neighbourhood have circulations with comparable absolute values then B and D will move along lines which are almost straight and at right angles to the line initially joining ABCDE. The influence of C on A and E together with other adjacent vortices to these will cause A and E to move in directions roughly parallel (at least to begin with) to those of B and D. Thus the vortex of opposite circulation to its neighbours will become isolated if they are originally in a line and there are enough neighbours to produce the effect. If B, C and D were the only vortices present then B and D would simply orbit the almost stationary C, anticlockwise in this case.

Accuracy of numerical integration methods.

A comparison was made of the relative accuracies of the three numerical integration methods used in plotting the positions of vortex points. Discretization of the vortex sheet behind a parabolically loaded wing was simulated with 41 vortex points initially arranged at half centimetre intervals along the x axis. Their circulation strengths increased in steps of $\pi/50$ $cm^2 sec^{-1}$ from $-2\pi/5$ at x=-10 to $2\pi/5$ at x=10. The three methods

compared have all been described earlier and are designated as the Euler method (first order), the H method (evidently slightly better than first order) and the Runge-Kutta method (fourth order).

Ten plots were made at five second intervals and the values of

$$Y = \frac{\sum_{i=21}^{41} y_i K_i}{\sum_{i=21}^{41} K_i}$$, the y component of the vortical centroid of the right hand half of the array,

$$E = \sum_{i=1}^{40} \sum_{j=i+1}^{41} K_i K_j \ln d_{ij}$$, and

$$V = \sum_{i=21}^{41} K_i \left[(x_i - X)^2 + (y_i - Y)^2 \right]$$, the vortical dispersion about the centroid of the right hand half of the array, were calculated at each plot. (x_i, y_i) is the position of the vortex with circulation K_i and d_{ij} is the distance between (x_i, y_i) and (x_j, y_j). (X, Y) is the position of the vortical centroid of the half of the array in the region $x>0$. E is an invariant of the motion. For both the Euler and H methods roll up was smooth and the ellipticity noted by Moore became apparent at the later stages. The Runge-Kutta method produced increasing chaos almost from the first plot. For all methods X was nearly constant at 6.83 cm. The

values of Y, E and V are given in Table 2 below. It appears that the H method as judged by the variations in E is only slightly better than the Euler method. The Runge-Kutta method is a clear winner in this contest.

Table 2.

	Euler			H			Runge-Kutta		
Secs.	Y	E	V	Y	E	V	Y	E	V
0	0	-320	77	0	-320	77	0	-320	77
5	- .82	-295	98	-.81	-299	93	- .81	-314	85
10	-1.58	-275	121	-1.55	-280	114	-1.57	-312	94
15	-2.30	-261	137	-2.28	-267	128	-2.30	-311	99
20	-3.01	-252	147	-3.00	-258	137	-3.03	-310	100
25	-3.74	-244	153	-3.72	-250	143	-3.76	-310	100
30	-4.47	-238	158	-4.46	-244	148	-4.50	-309	98
35	-5.20	-233	163	-5.19	-239	151	-5.25	-308	97
40	-5.94	-228	167	-5.94	-235	155	-6.00	-308	95
45	-6.68	-225	171	-6.68	-231	159	-6.75	-308	94
50	-7.42	-221	176	-7.42	-228	163	-7.51	-307	91

CHAPTER XIII

CONCLUSION

The description in earlier chapters of some of the models constructed to account for vortex sheet roll-up demonstrates that while much excellent work has been done there is still a long way to go before a complete understanding of the phenomenon is reached. Progress along these lines is likely to go hand in hand with the study of turbulence which it may be fairly said is still in its infancy. Both these research areas are hindered by a difficulty which is at the heart of all real fluid dynamics: the non linearity of the governing equations. Experimental confirmation of analytical results is also hindered by the inability of wind tunnels to produce laminar flow unaffected by the walls, and the even greater difficulty of measuring the flow behind wings in actual flight.

The usefulness of a numerical method to solve any problem where the variables are essentially continuous lies in the ability of its parameters to be varied in order to produce a closer approximation to the continuous situation being investigated. In almost all cases, provided the price in computer time can be paid, there is no lower limit to the difference between the exact solution and that obtained by starting with a discrete

set of values taken from a continuous curve. That the approximation of vorticity continuously distributed along a line by a series of vortex points is an exception to this general rule is strongly suggested by the foregoing computer study. To replace what is really a shear surface by a set of discrete vortices is valid in macrocosm only and ceases to hold in the nearer neighbourhood of each point, as for example, when we wish to examine the inner turns of a rolled up vortex sheet.

Mathematical analysis and experimental observation agree qualitatively and to some extent quantitatively on the vortex sheet roll-up mechanism but nearly all numerical studies have had to contend with the phenomenon of chaos described above. The method of Moore for suppressing this chaos is useful in preserving the shape of the outer turn of the forming spiral by contracting all the internal chaotic vorticity to a single vortex point but this partly defeats the purpose of the investigation which is to examine the whole spiral and not just its outer turns.

The particular case of the vortex strengths chosen to correspond to a parabolically loaded wing and plotted using a less accurate method of numerical integration would seem to be significant. Chaotic behaviour did not appear after an elapsed time far in excess of that for which chaos was already rampant using the Runge-Kutta

method. It might not be too optimistic to expect to find combinations of time step, loading and integration method which by virtue of its good behaviour would allow the effect of small modifications to wing loading to be followed undisturbed by the presence of unruly vortices.

APPENDIX A

The motion of the vortices at the points (x_j, y_j) with circulations K_j, j=1, 2, -----, n is governed by the system

$$\frac{dx_j}{dt} = -\frac{1}{2\pi}\sum_r \frac{K_r(y_j-y_r)}{d_{jr}^2}$$

$$\frac{dy_j}{dt} = \frac{1}{2\pi}\sum_r \frac{K_r(x_j-x_r)}{d_{jr}^2}, \quad r \neq j$$

where d_{jr} is the distance between (x_j, y_j) and (x_r, y_r). Using the complex variable $z_j = x_j + iy_j$ the system can be written

$$\frac{d\bar{z}_j}{dt} = \frac{1}{2\pi i}\sum_r \frac{K_r}{z_j - z_r}, \quad r \neq j$$

Integrals of this system provide some of the invariants of the motion (Sedov).

Multiply by K_j and sum over j.

$$\therefore \quad \Sigma K_j \frac{d\bar{z}_j}{dt} = \frac{1}{2\pi i}\sum_j \sum_r \frac{K_j K_r}{z_j - z_r}$$

$= 0$ since the terms occur in equal but opposite pairs.

$\therefore$ $\Sigma K_j x_j$ and $\Sigma K_j y_j$ are both constant.

Now multiply the complex system by $K_j z_j$ and sum over j.

$$\therefore \Sigma K_j z_j \dot{\bar{z}}_j = \frac{1}{2\pi i}\Sigma\Sigma \frac{K_j z_j K_r}{z_j - z_r}$$

$$= -\frac{1}{2\pi i}\Sigma\Sigma \frac{K_j K_r z_r}{z_j - z_r}$$

by interchanging the dummy suffixes.

$$\therefore 2\Sigma K_j z_j \dot{\bar{z}}_j = \frac{1}{2\pi i}\Sigma\Sigma K_j K_r \text{ by addition.}$$

$\therefore \Sigma K_j z_j \dot{\bar{z}}_j$ is a pure imaginary constant, where the dot denotes the time derivative.

The real part of $z_j \dot{\bar{z}}_j$ is

$$\tfrac{1}{2}(z_j \dot{\bar{z}}_j + \bar{z}_j \dot{z}_j) = \tfrac{1}{2}\frac{d}{dt}(z_j \bar{z}_j)$$

$$\therefore \frac{d}{dt} \Sigma K_j z_j \bar{z}_j = 0$$

i.e. $\Sigma K_j z_j \bar{z}_j$ is constant.

The imaginary part of $z_j \dot{\bar{z}}_j$ is $\dot{x}_j y_j - x_j \dot{y}_j$

$\therefore \Sigma K_j (\dot{x}_j y_j - x_j \dot{y}_j) = -\frac{1}{4\pi}\Sigma\Sigma K_j K_r$ which is also constant. The two expressions $\Sigma K_j z_j \bar{z}_j = \Sigma K_j (x_j^2 + y_j^2)$ and $\Sigma K_j (\dot{x}_j y_j - x_j \dot{y}_j)$ are the vorticity analogues of moment of inertia and angular momentum respectively.

Now write $\psi_j = -\frac{1}{2\pi}\sum_r K_r \ln|z_j - z_r|$

then $\frac{\partial \psi_j}{\partial x_j} = -\frac{1}{2\pi}\sum_r K_r \frac{x_j - x_r}{|z_j - z_r|} = -\frac{dy_j}{dt}$

and $\frac{\partial \psi_j}{\partial y_j} = -\frac{1}{2\pi}\sum_r K_r \frac{y_j - y_r}{|z_j - z_r|} = \frac{dx_j}{dt}$

Multiply by K_j and sum over j:

$$\frac{\partial}{\partial x_j} \Sigma K_j \psi_j = -\frac{d}{dt} \Sigma K_j y_j = 0$$

$$\frac{\partial}{\partial y_j} \Sigma K_j \psi_j = \frac{d}{dt} \Sigma K_j x_j = 0$$

$\therefore \Sigma K_j \psi_j$ is constant

i.e. $\Sigma\Sigma K_j K_r \ln|z_j - z_r|$ is constant, often referred to as the Kirchhoff-Routh path function.

If $\Sigma K_j \neq 0$ then

$\bar{x} = \frac{\Sigma K_j x_j}{\Sigma K_j}$ and $\bar{y} = \frac{\Sigma K_j y_j}{\Sigma K_j}$ are invariant quantities.

The vortical dispersion

$V = \Sigma K_j \left[(x_j - \bar{x})^2 + (y_j - \bar{y})^2 \right]$ can be rewritten as

$\Sigma K_j (x_j^2 + y_j^2) - \Sigma (\bar{x}^2 + \bar{y}^2) \Sigma K_j$ which is constant by the above.

APPENDIX B

PLOT SET 1

The following five frames are plots of positions taken up by 41 vortex points initially equally spaced along a line interval of length 20 cm, the ends of which are marked by asterisks. Their strengths increase linearly from $-2\Pi/5$ cm^2 sec^{-1} at the left hand end to $2\Pi/5$ cm^2 sec^{-1} at the right hand end. This corresponds to the vortex sheet discretization of a parabolically loaded wing. The plotting symbols are letters of the alphabet used in order from each end towards the centre. The plots were made at 10 second intervals using a time step of one second with the H numerical integration method.

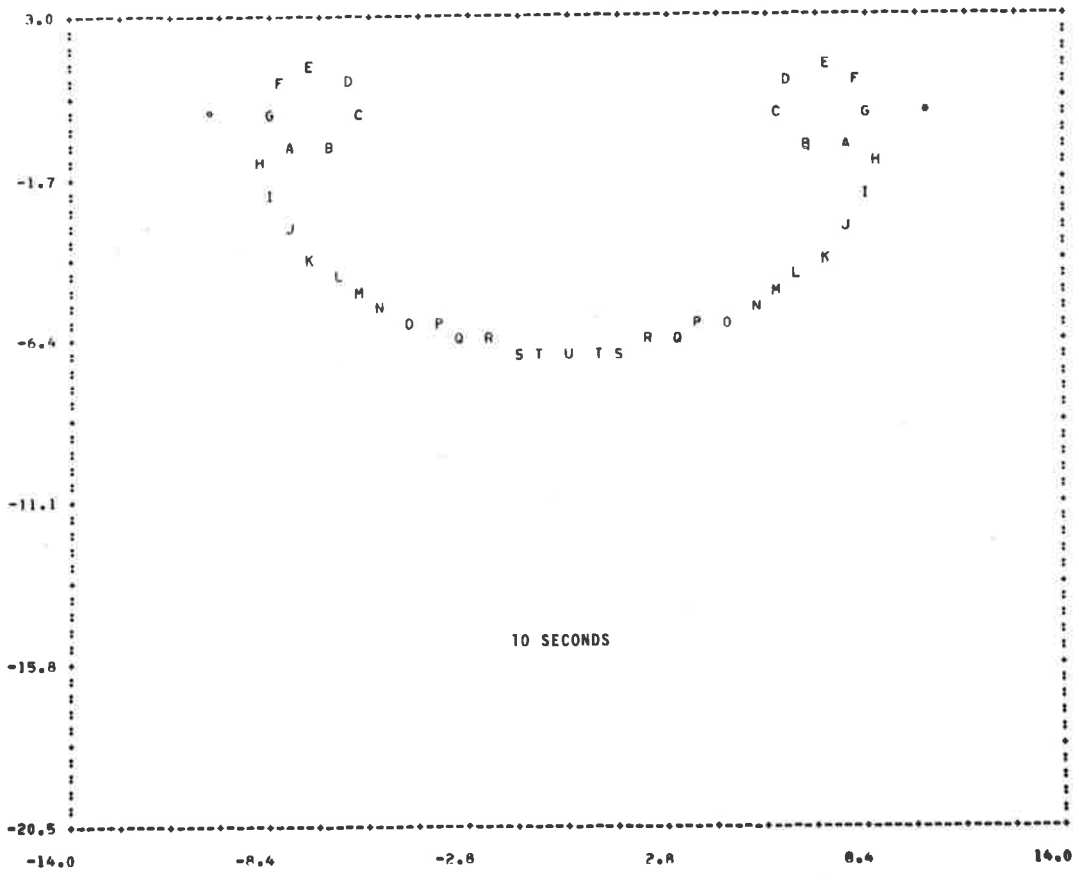

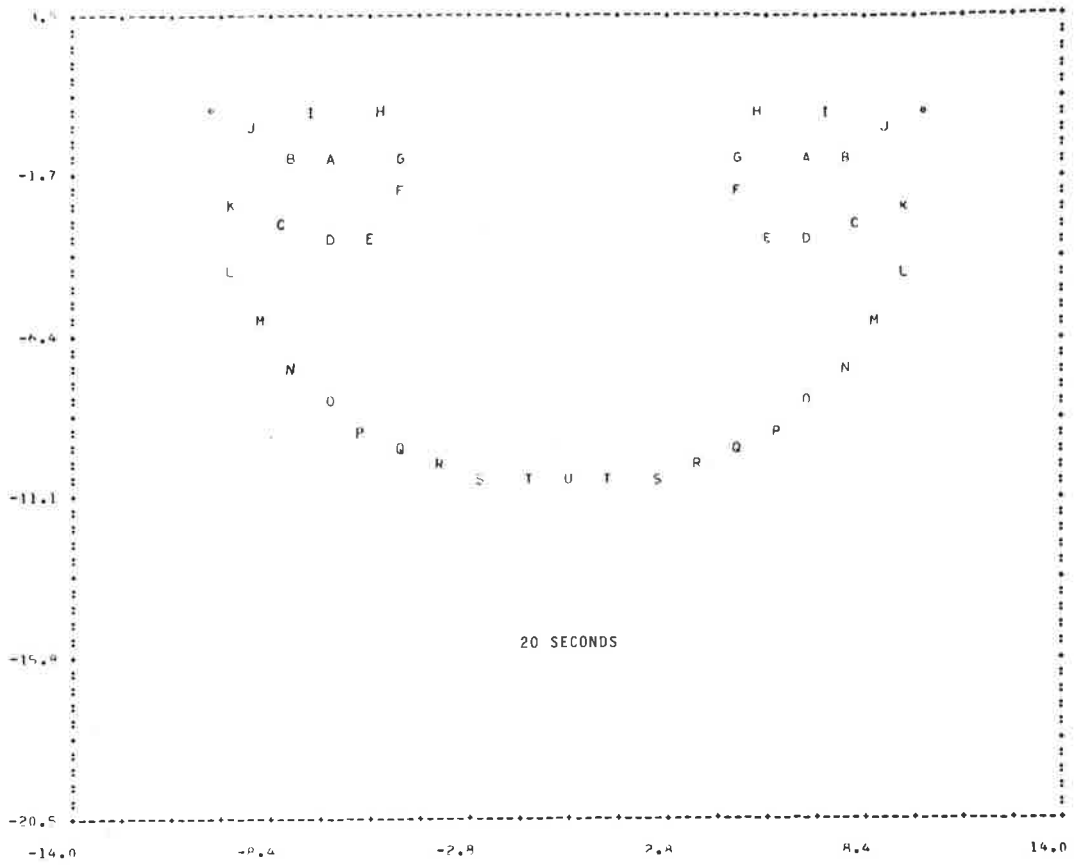
-1.7
-6.4
-11.1
-15.8
-20.5
-14.0
-8.4
-2.8
2.8
8.4
14.0
20 SECONDS

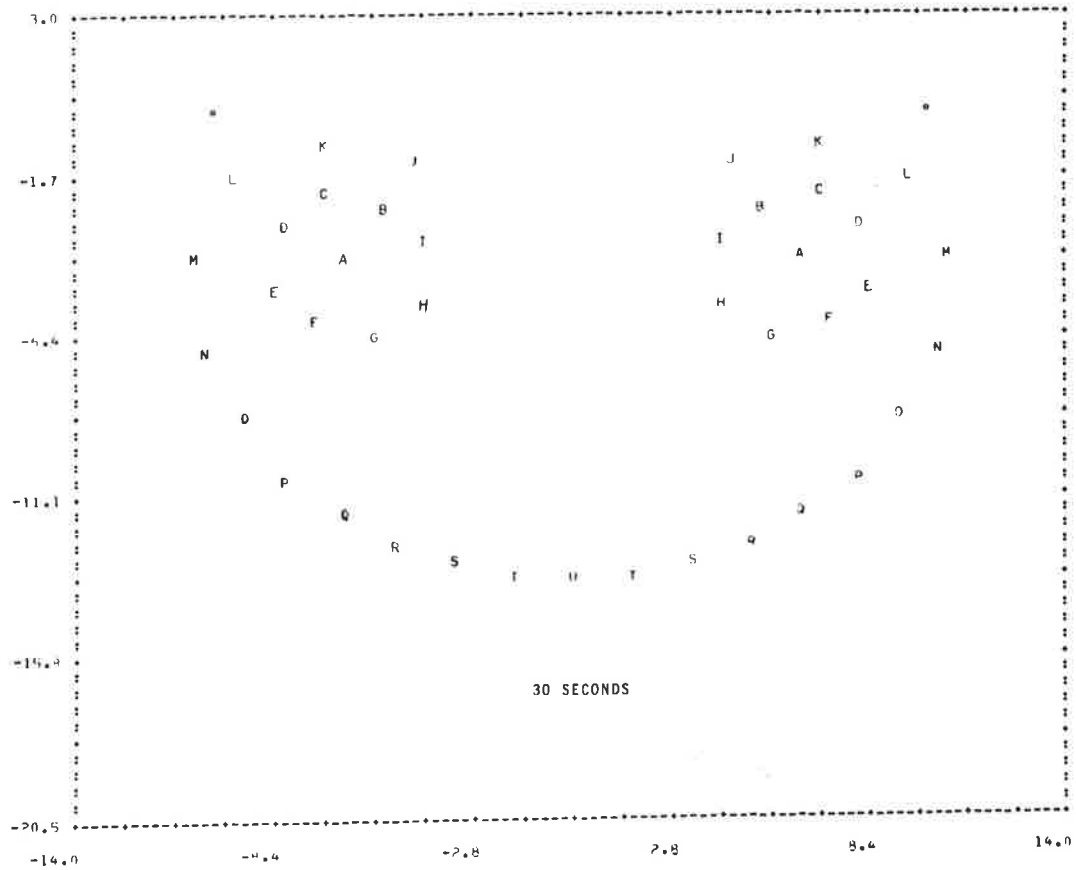
3.0
-1.7
-6.4
-11.1
-15.8
-20.5
-14.0
-8.4
-2.8
2.8
8.4
14.0
30 SECONDS

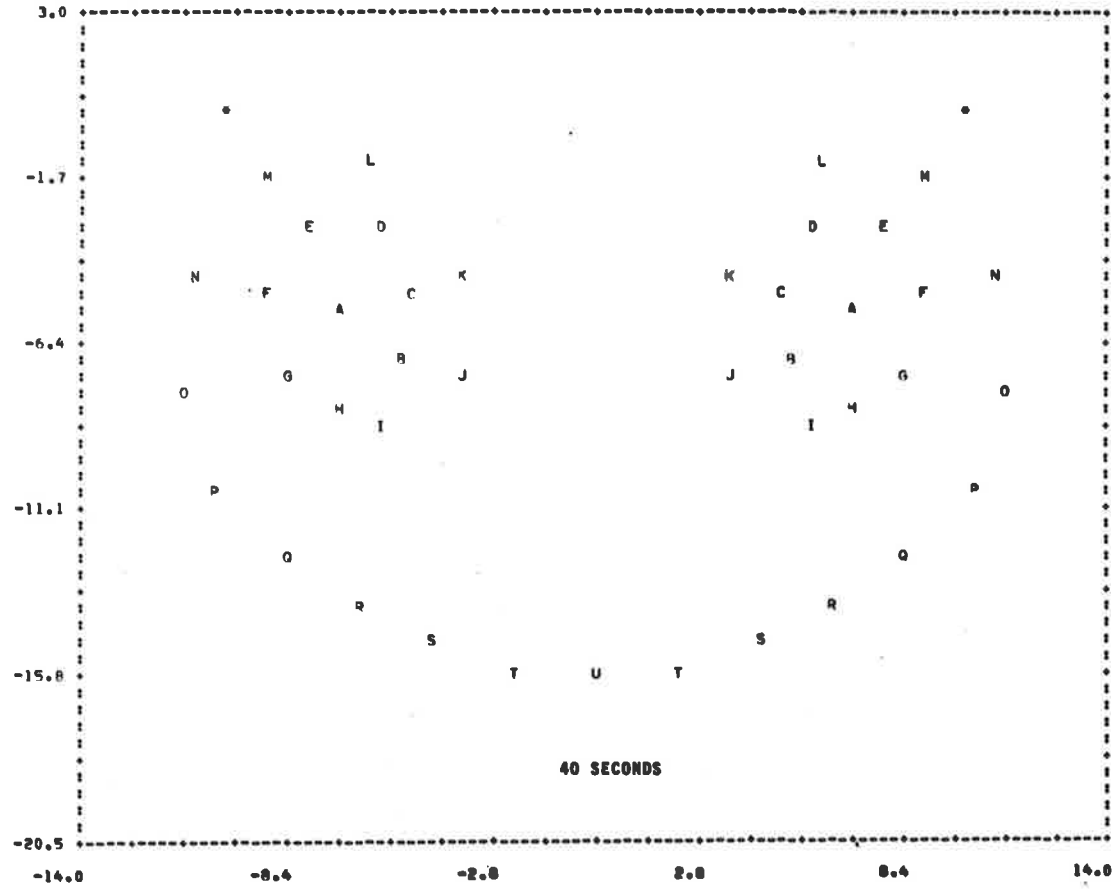
3.0
-1.7
-6.4
-11.1
-15.8
-20.5
-14.0
-8.4
-2.8
2.8
8.4
14.0
40 SECONDS

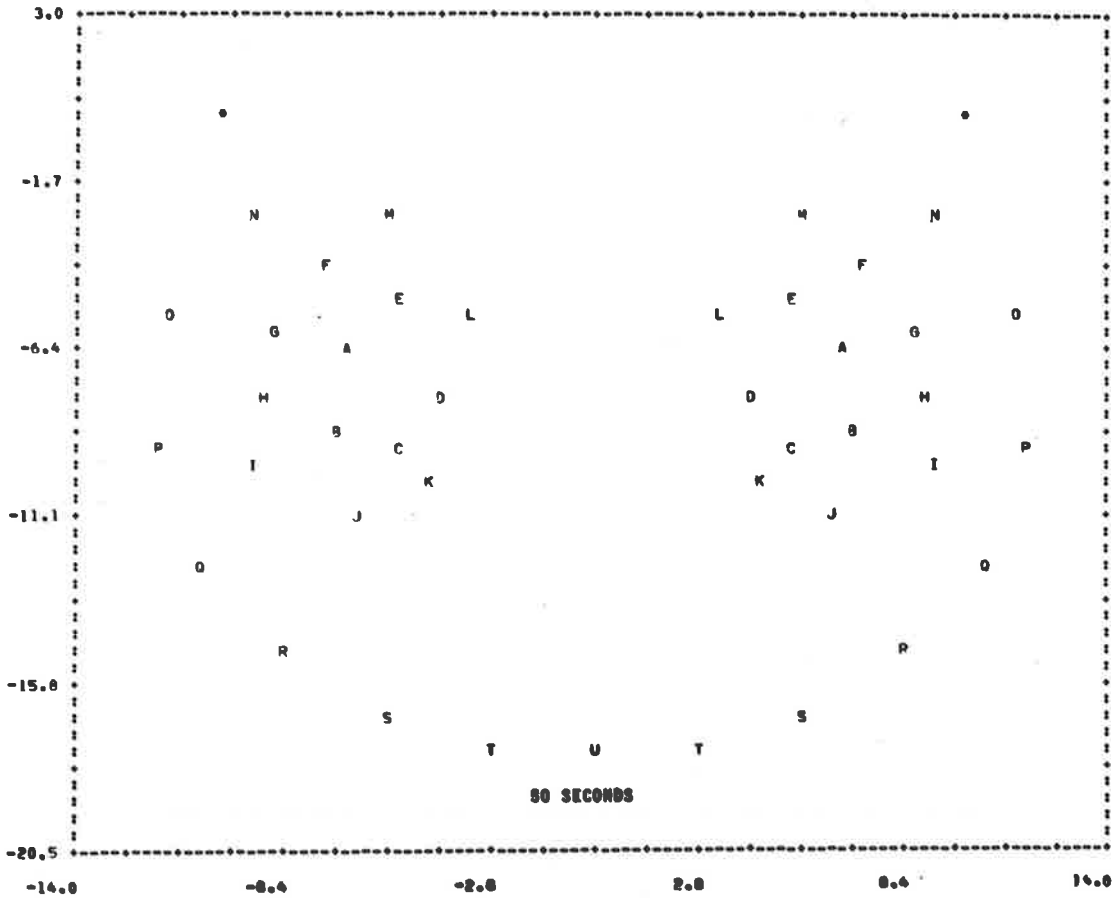
3.0
-1.7
-6.4
-11.1
-15.8
-20.5
-14.0
-8.4
-2.8
2.8
8.4
14.0
80 SECONDS

PLOT SET 2

The following page shows two plots, each at 50 seconds, of the vortex array described in Plot Set 1 using the Euler first order method and the Runge-Kutta fourth order method instead of the H method, all other parameters being the same.

In the first order plot, apart from the positions of I and J, the spirals are well defined and compare fairly closely with the previous 50 second plot using the H method. The interior of the spirals in the Runge-Kutta plot are clearly chaotic.

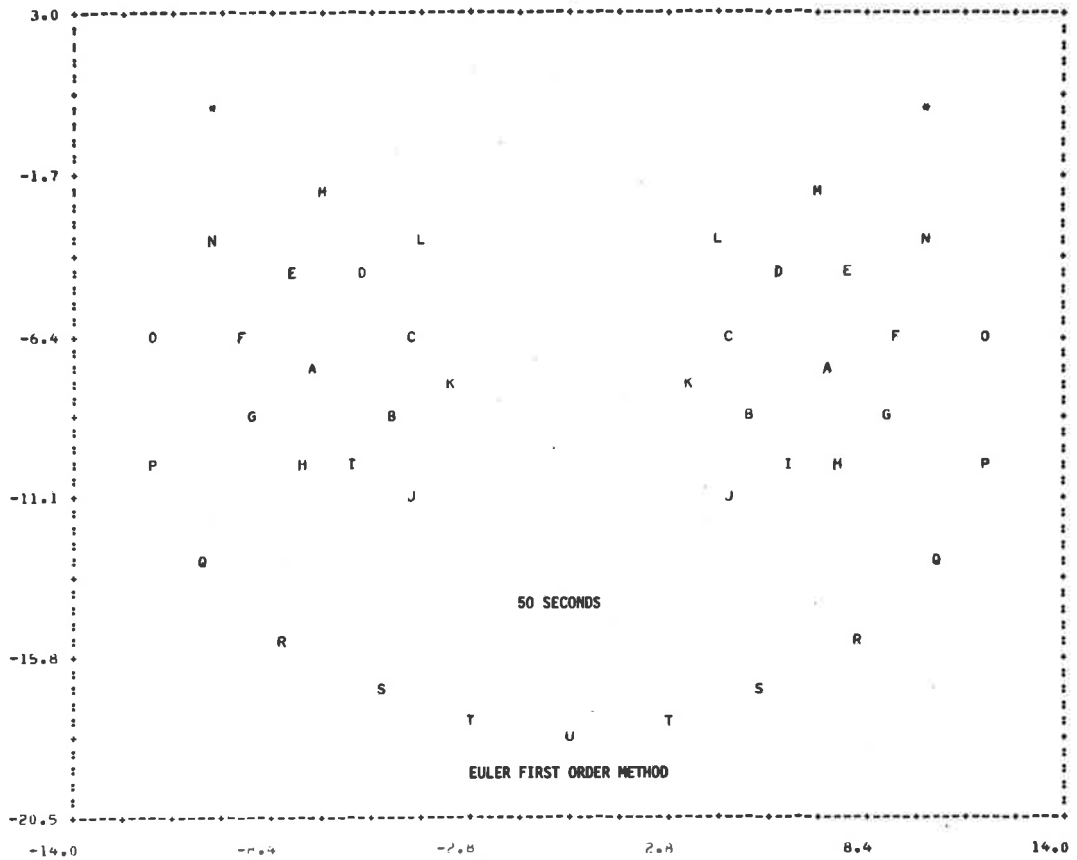
3.0
-1.7
-6.4
-11.1
-15.8
-20.5
-14.0
-8.4
-2.8
2.8
8.4
14.0
50 SECONDS
EULER FIRST ORDER METHOD

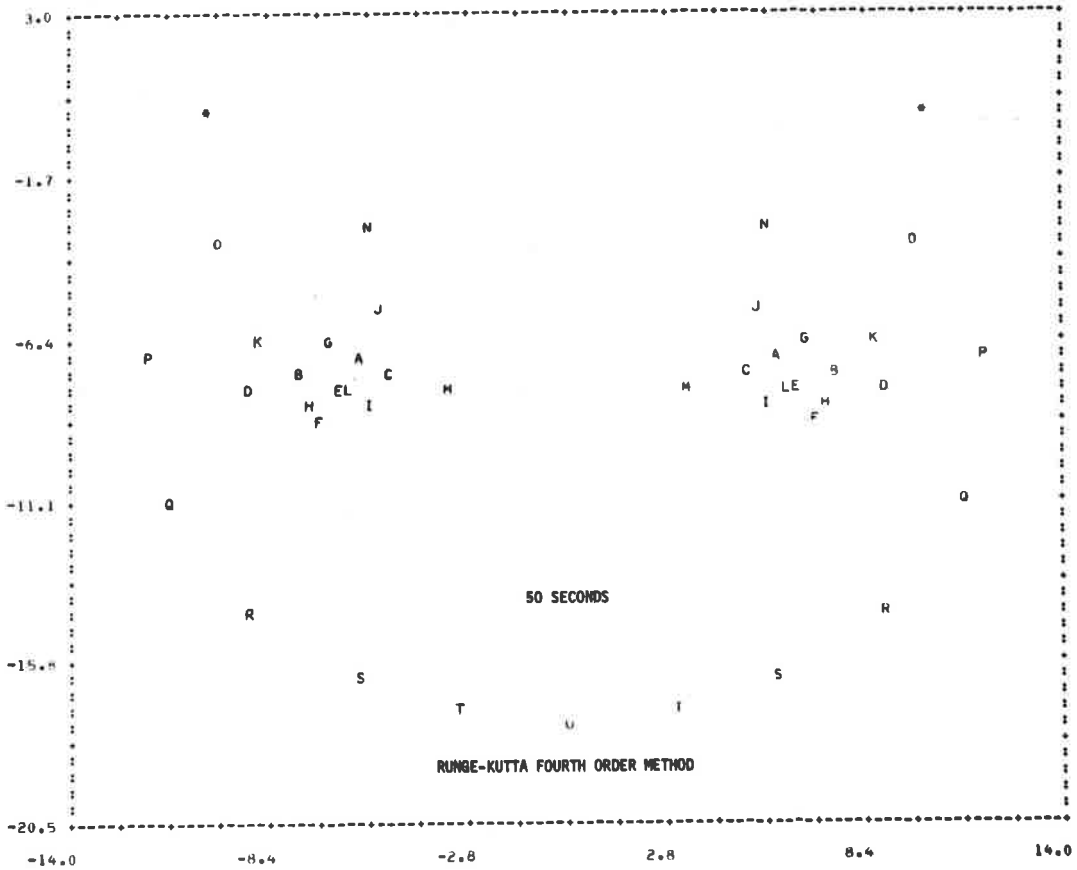
3.0
-1.7
-6.4
-11.1
-15.8
-20.5
-14.0
-8.4
-2.8
2.8
8.4
14.0
50 SECONDS
RUNGE-KUTTA FOURTH ORDER METHOD

PLOT SET 3

The following five pages show the effect of time step size on the plots described in Chapter XI using Moore's amalgamation method to suppress chaos. Plots at total elapsed times of 180 and 600 seconds are shown on each page, with time steps of 1, 2, 3, 6 and 12 seconds shown on different pages. The plotting symbols are, beginning from each end, the numerals from 1 to 9, all the letters of the alphabet in order, and plus signs between the two z's to bring the total number up to 81. Where more than one symbol is calculated to occupy the same character position, as at the centre of each spiral after amalgamations have occurred, then the symbol printed is the right most in the original array. Thus at the centre of the left hand spiral the symbol of the last vortex to amalgamate appears while the symbol 1 always appears at the centre of the right hand spiral.

The two points (±10, 0) on the line between which all the vortices were initially placed are marked by asterisks.

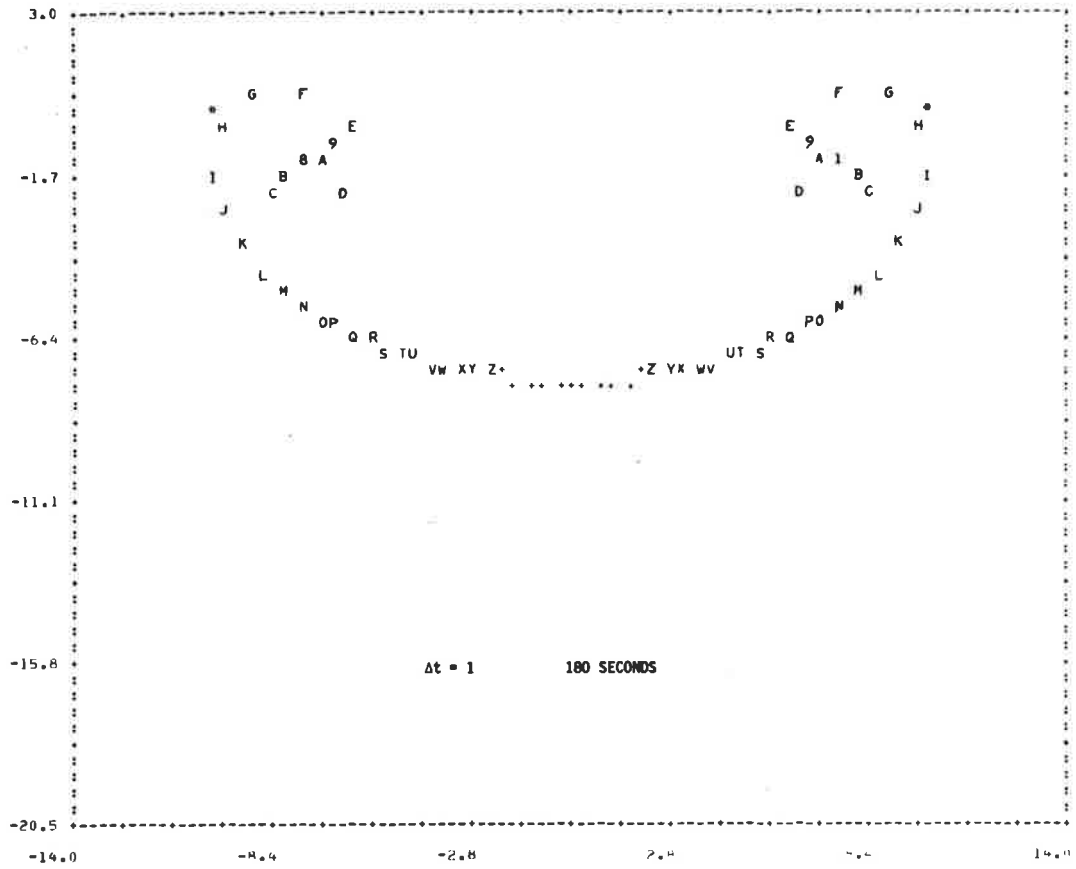
3.0
-1.7
-6.4
-11.1
-15.8
-20.5
-14.0
Δt = 1
180 SECONDS

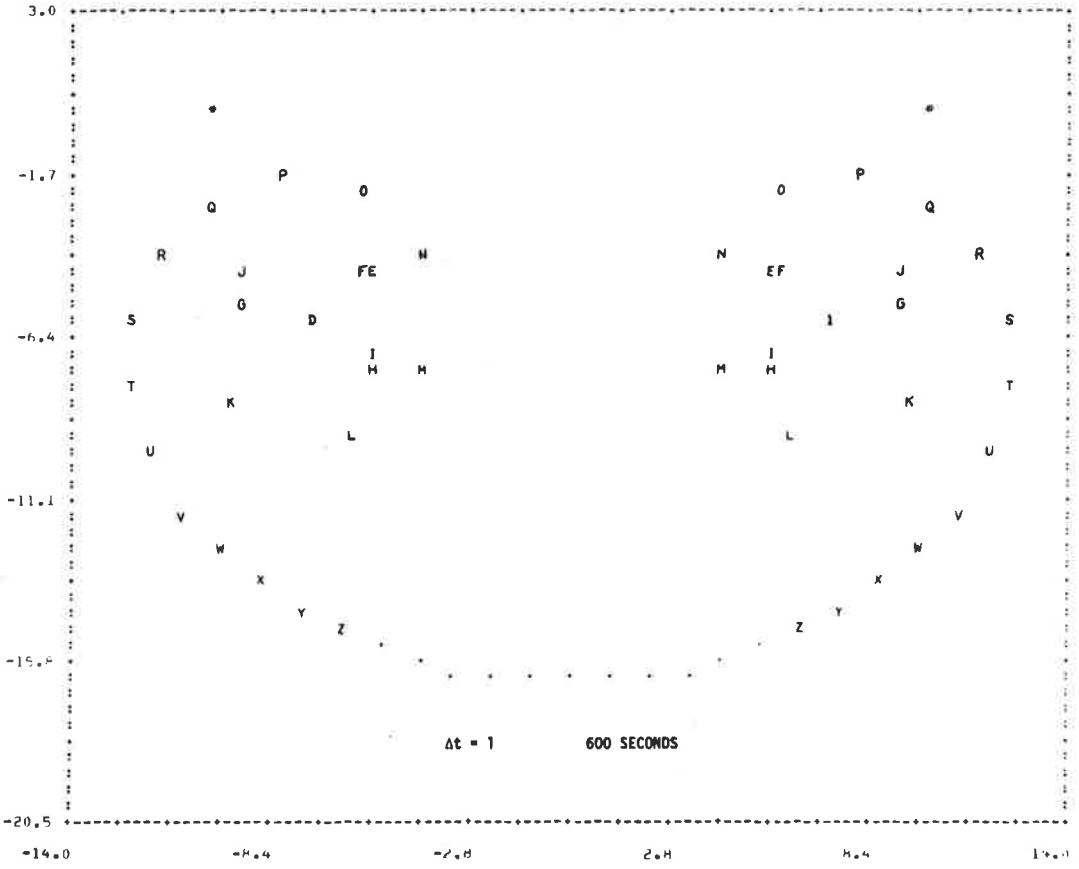
3.0
-1.7
-6.4
-11.1
-20.5
-14.0
Δt = 1
600 SECONDS

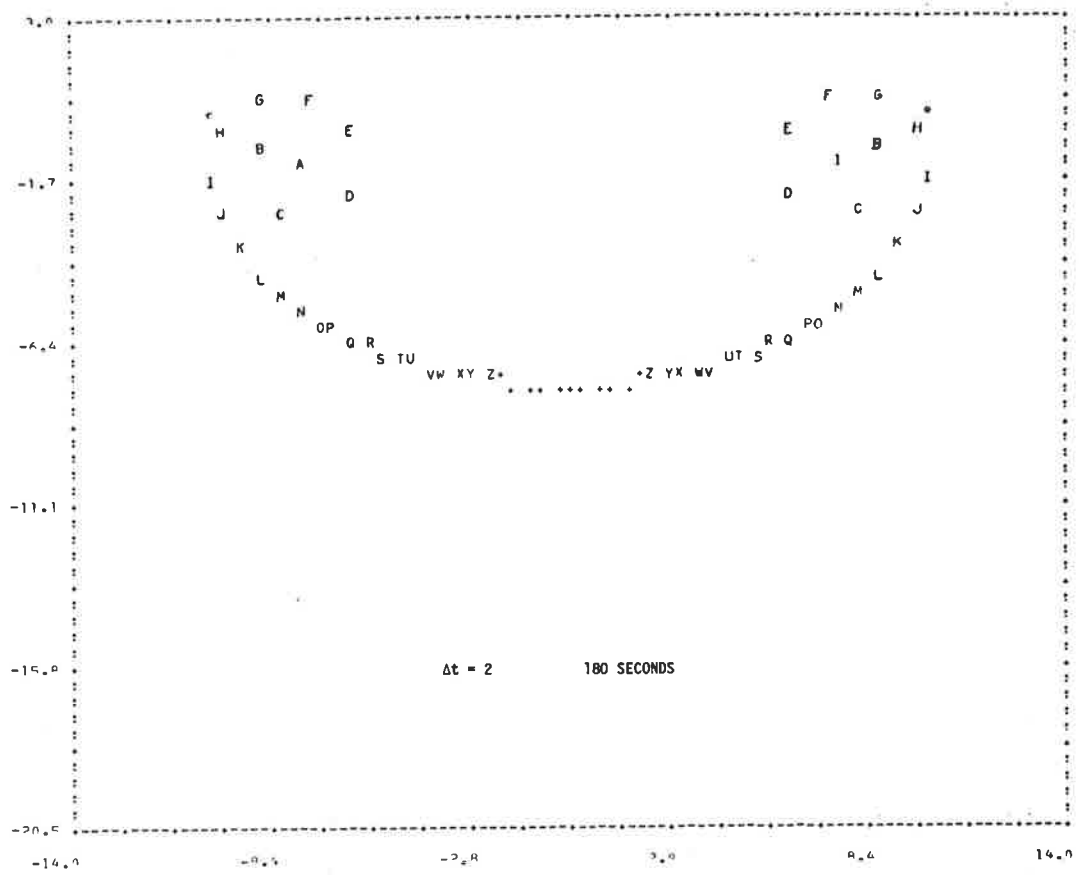
Δt = 2
180 SECONDS

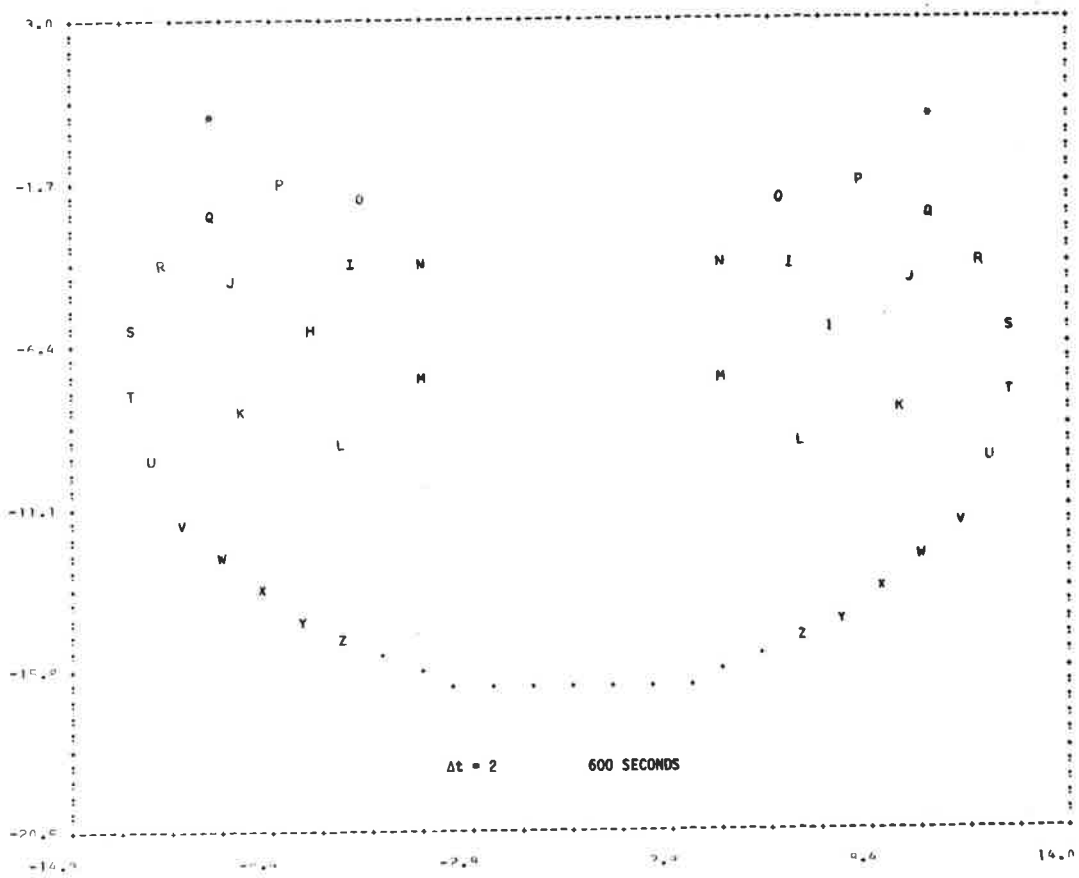
Δt = 2
600 SECONDS

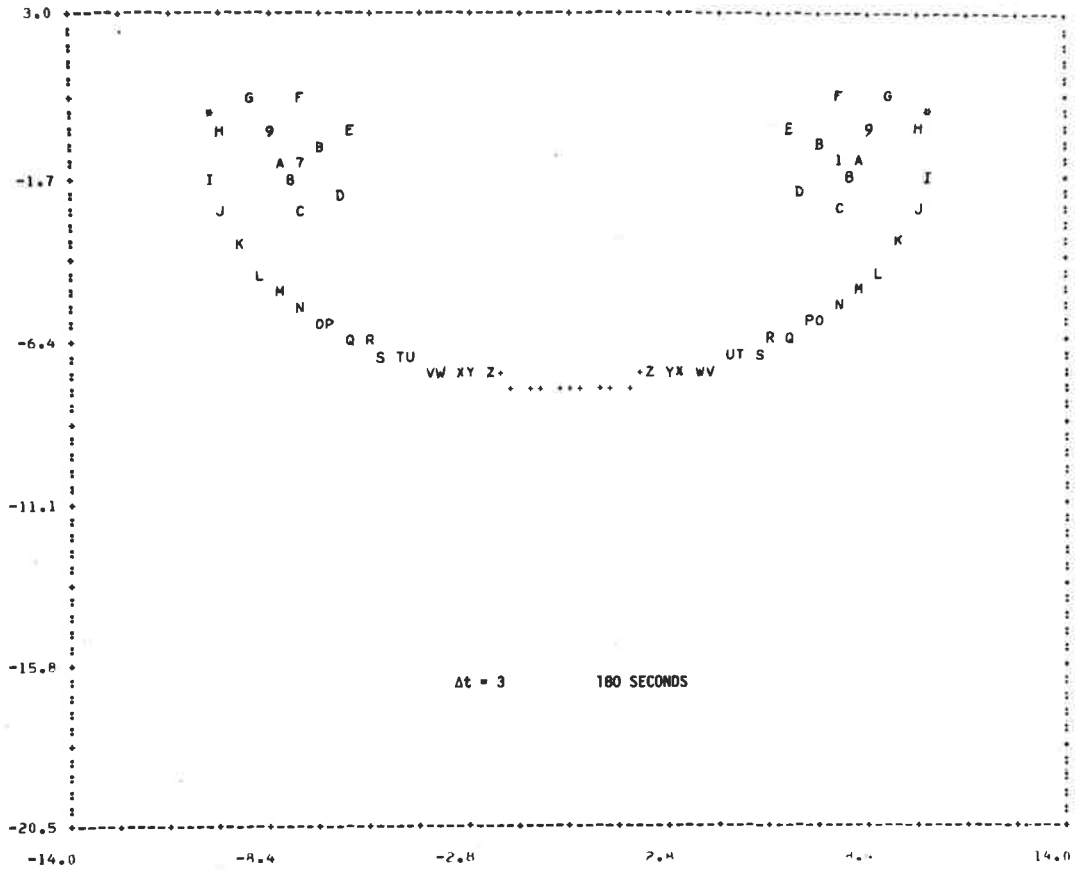
3.0
-1.7
-6.4
-11.1
-15.8
-20.5
-14.0
-8.4
-2.8
2.8
14.0
Δt = 3
180 SECONDS

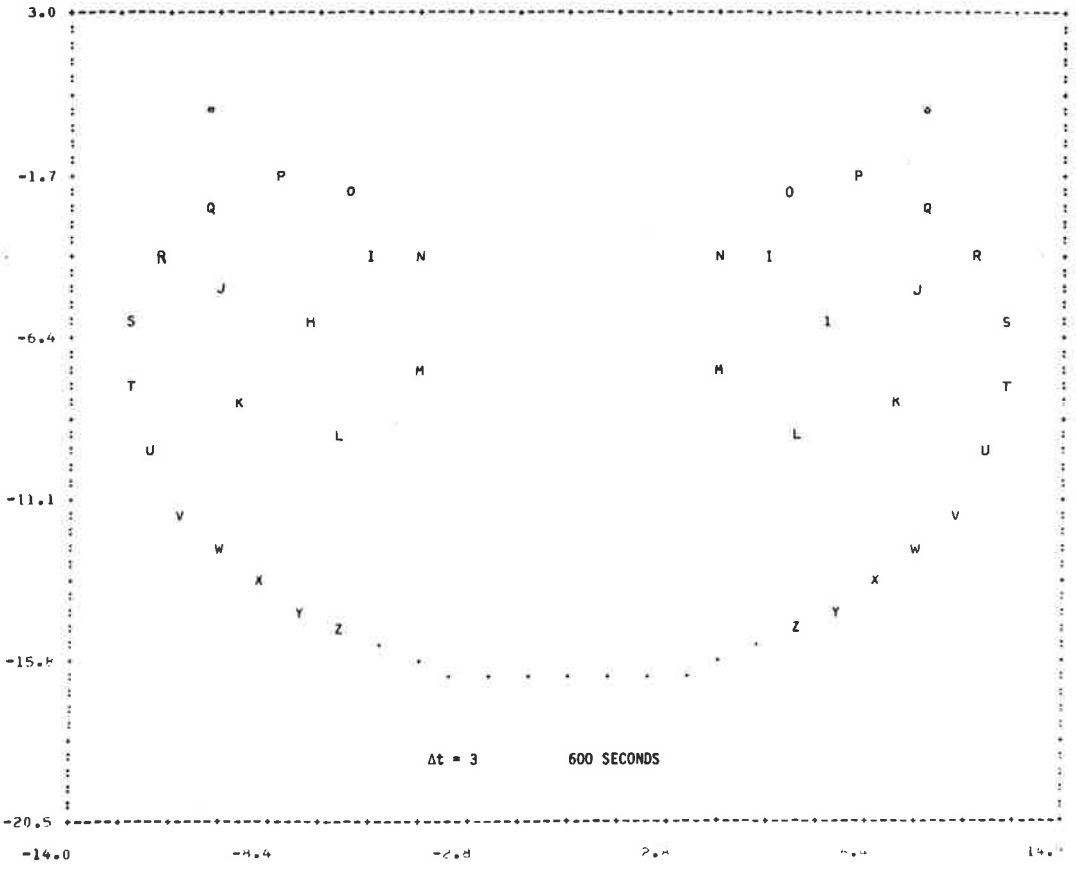
3.0
-1.7
-6.4
-11.1
-15.8
-20.5
-14.0
-8.4
-2.8
2.8
14.0
Δt = 3
600 SECONDS

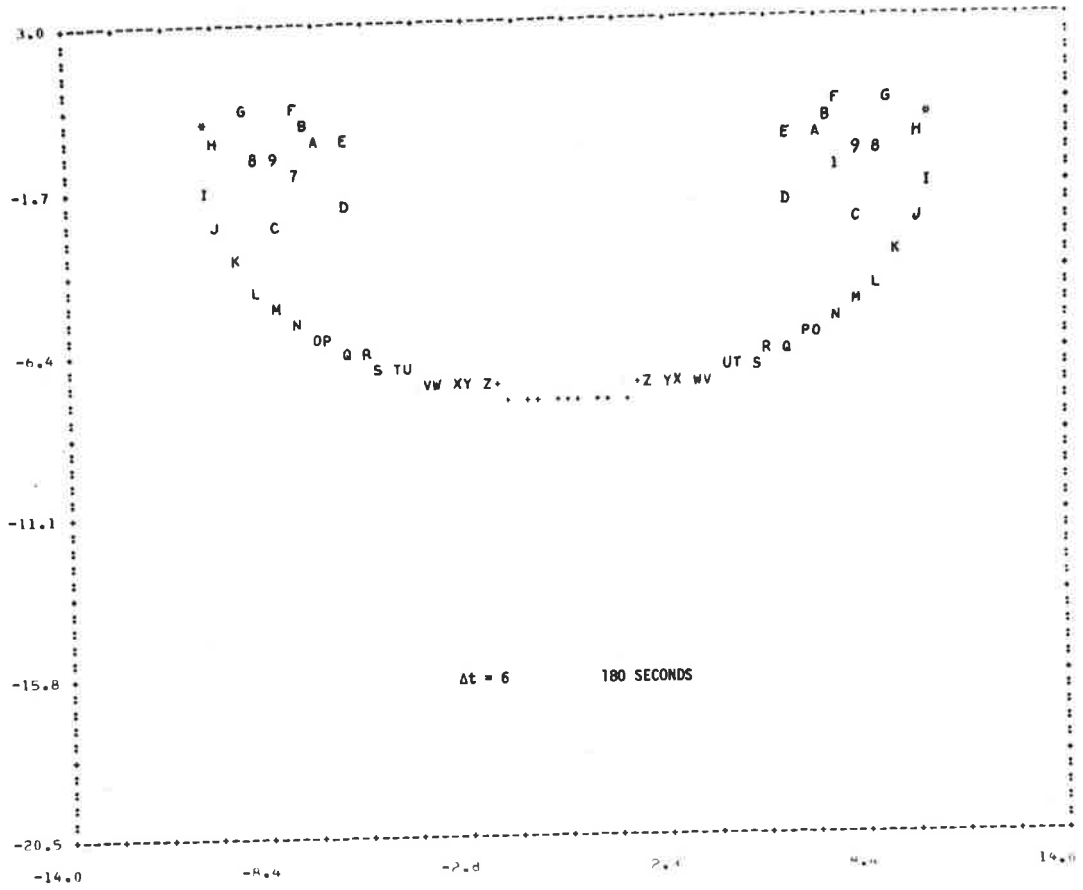
3.0
-1.7
-6.4
-11.1
-15.8
-20.5
-14.0
Δt = 6
180 SECONDS

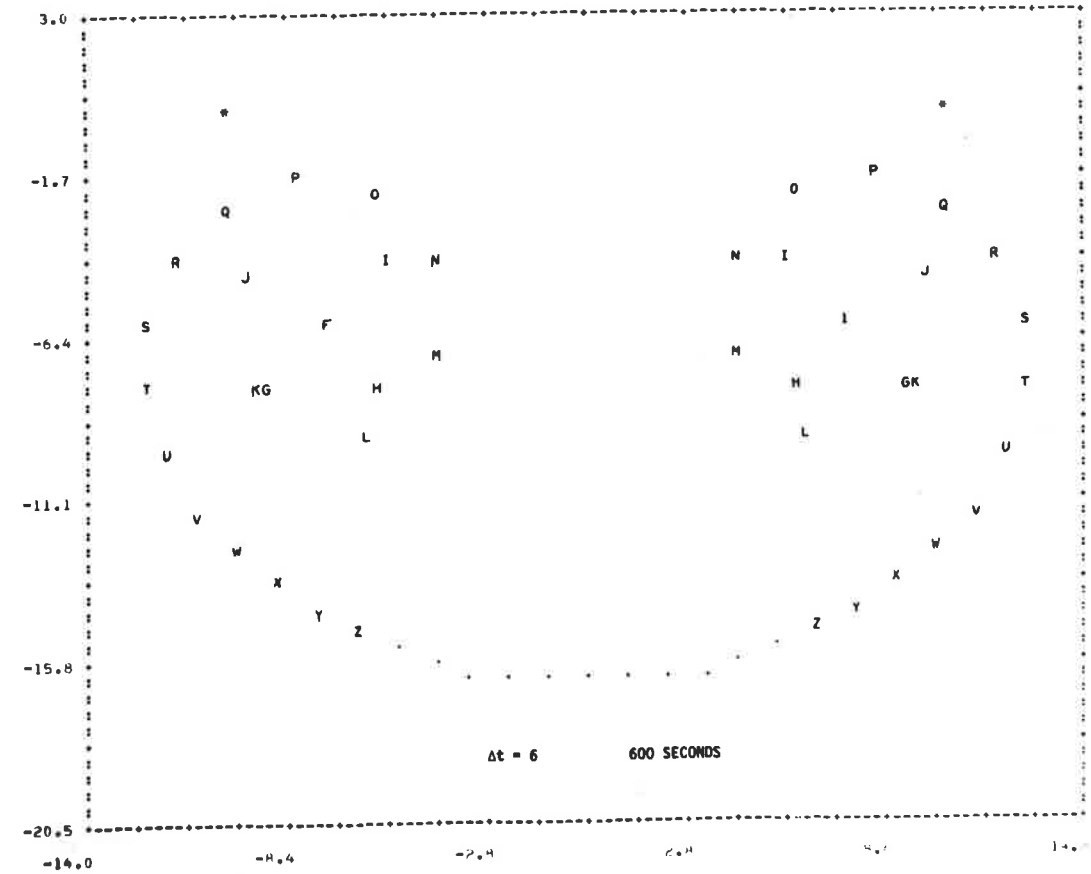
3.0
-1.7
-6.4
-11.1
-15.8
-20.5
-14.0
Δt = 6
600 SECONDS

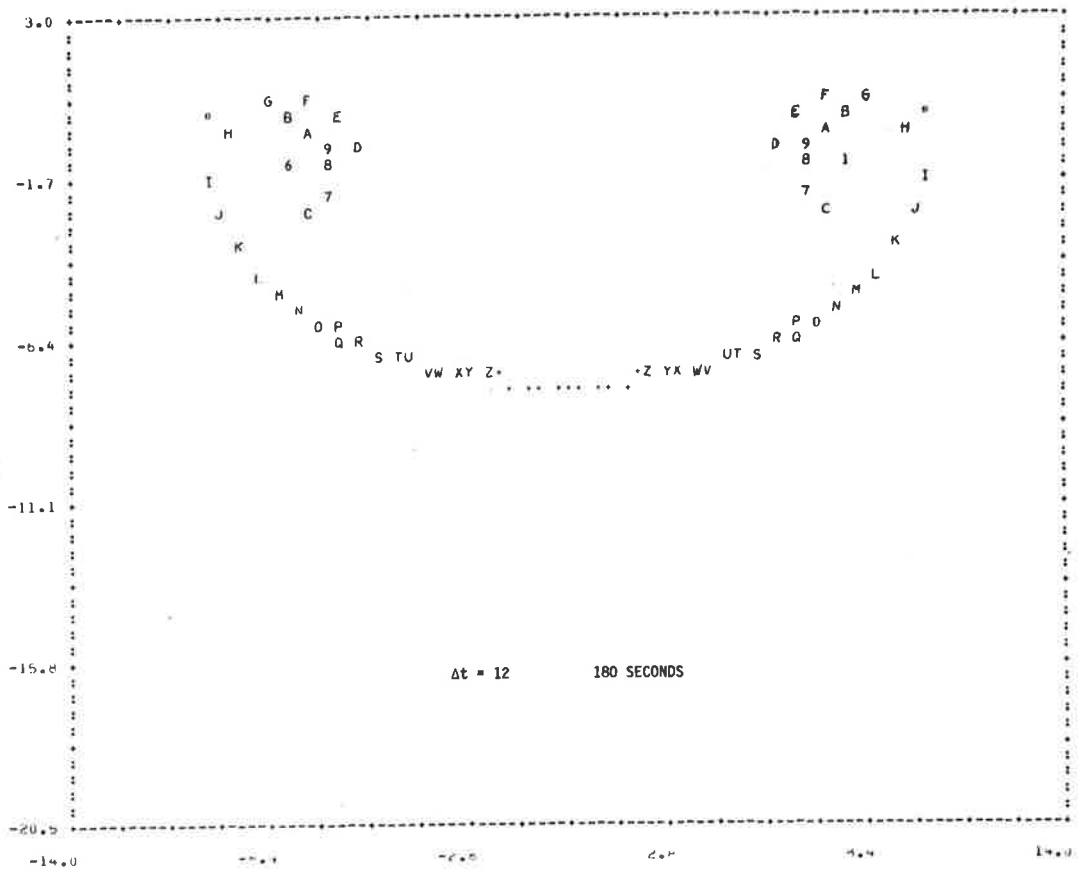
3.0
-1.7
-6.4
-11.1
-15.8
-20.5
-14.0
Δt = 12
180 SECONDS

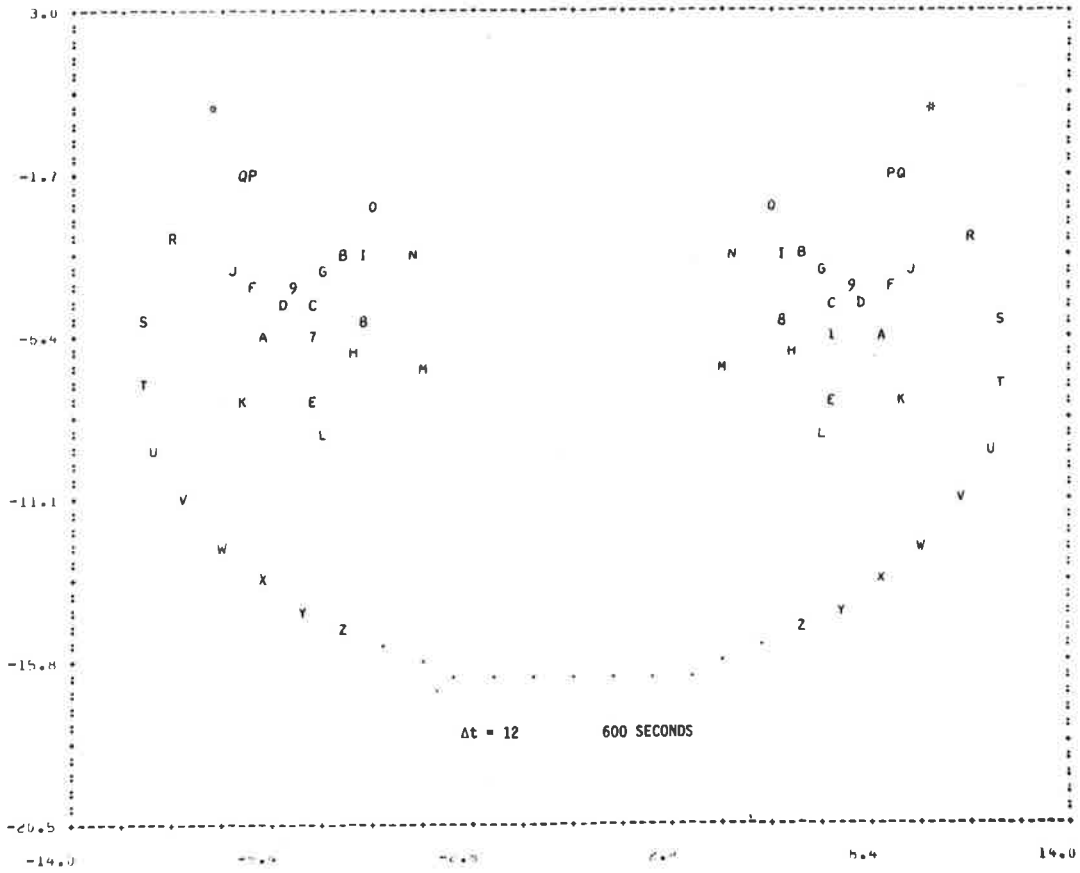
3.0
-1.7
-6.4
-11.1
-15.8
-20.5
-14.0
14.0
Δt = 12
600 SECONDS

Plot Set 4.

These three frames show the development at 5, 15 and 25 seconds of the vortex array corresponding to the gable wing loading described in Chapter X. The 41 vortices are identified by letters as in earlier plots. Those initially to the left of the midwing had strength $-\Pi/5$ and those to the right $\Pi/5$ cm^2 sec^{-1}, while the centre point, U, had zero vorticity. The H method of numerical integration was used.

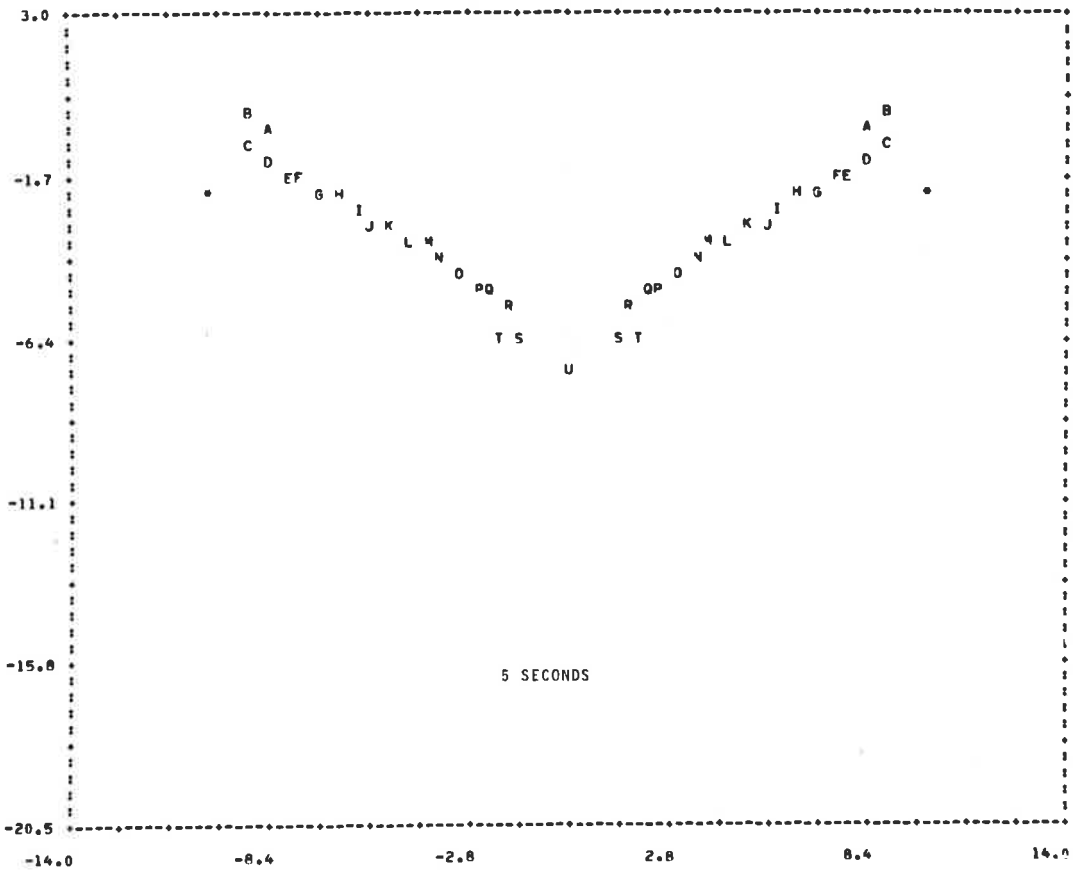

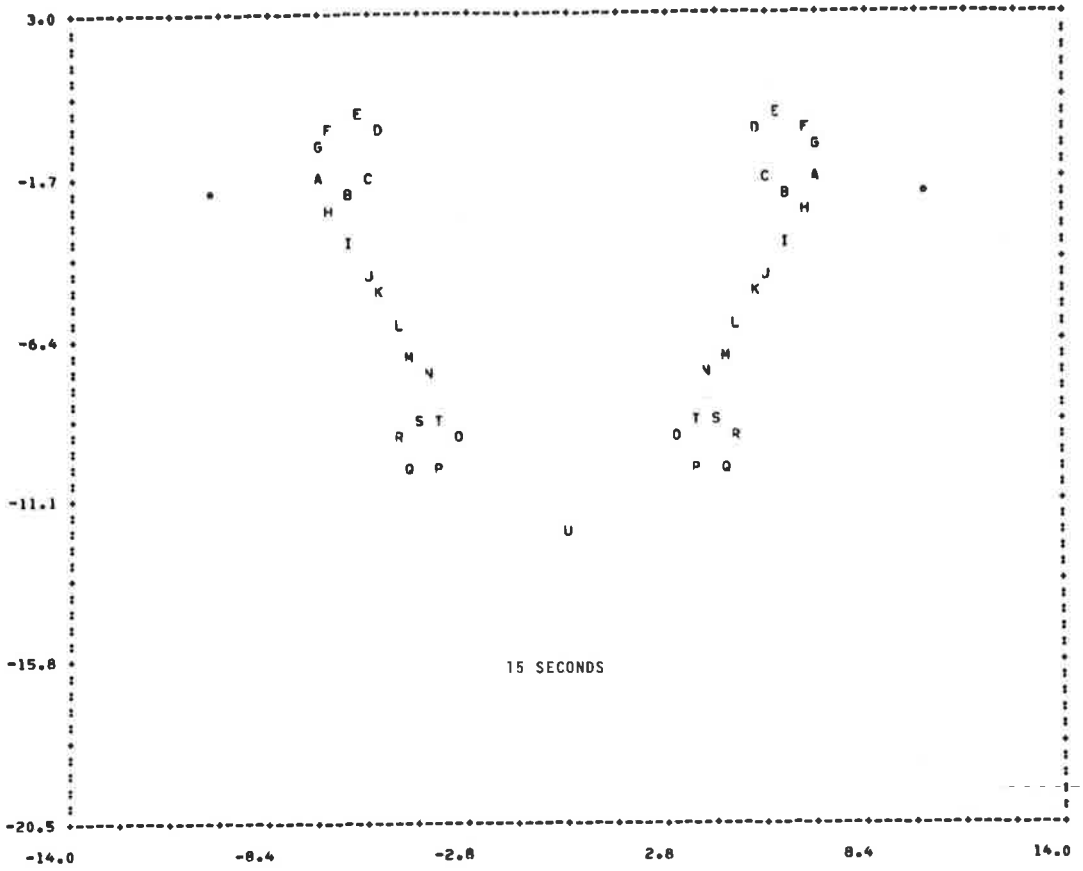
3.0
-1.7
-6.4
-11.1
-15.8
-20.5
-14.0
-8.4
-2.8
2.8
8.4
14.0
15 SECONDS

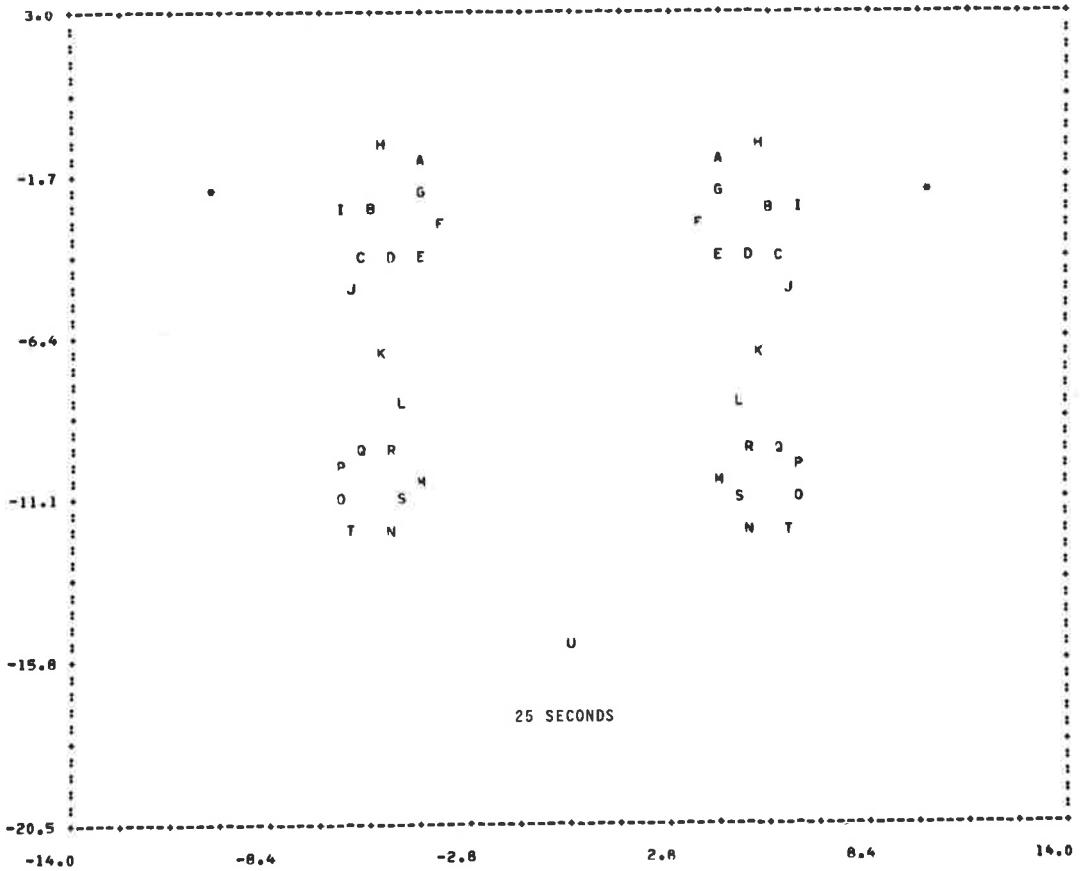
3.0
-1.7
-6.4
-11.1
-15.8
-20.5
-14.0
-8.4
-2.8
2.8
8.4
14.0
25 SECONDS

Plot Set 5.

These three frames show the development at 5, 15 and 25 seconds of the vortex array corresponding to the cosine curve wing loading described in Chapter X. The initial arrangement was as in Plot Set 4 except that the circulation strength of each vortex was given by

$$K = \frac{\Pi}{10} \text{ SIN } \frac{\Pi x}{10}$$ where x is the initial (directed) distance from the midwing. The H method of numerical integration was used.

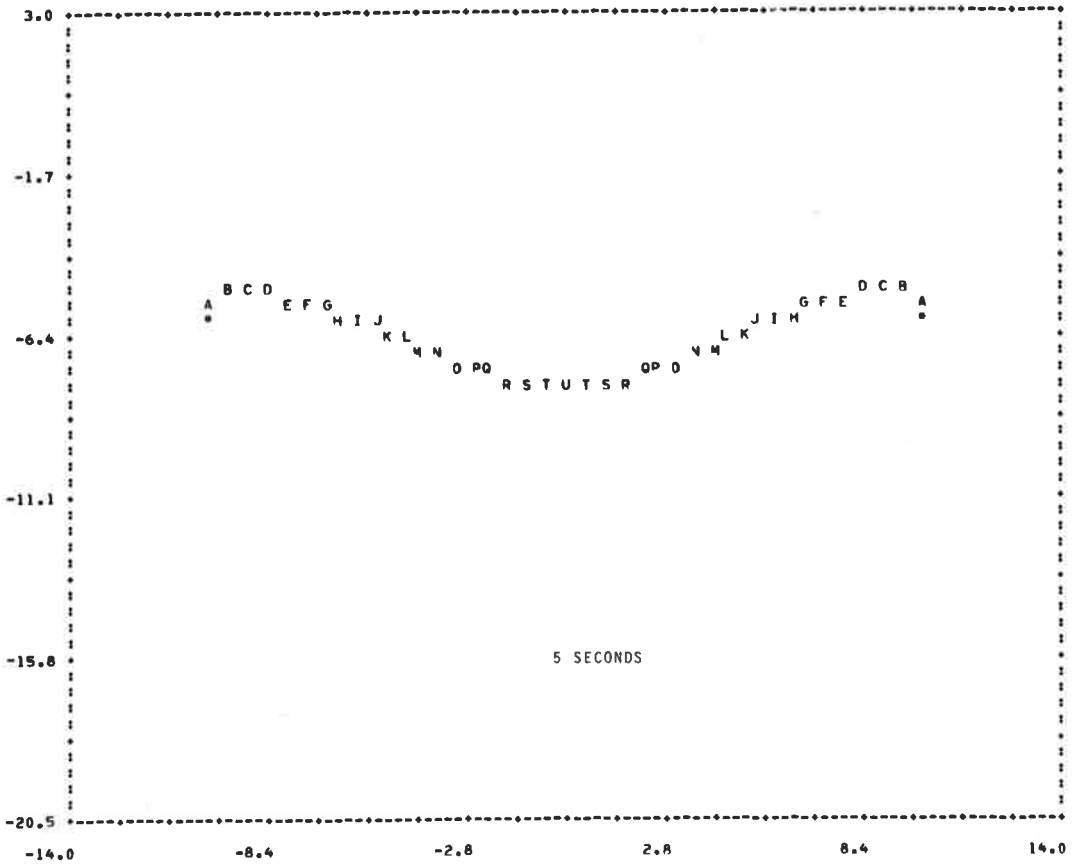

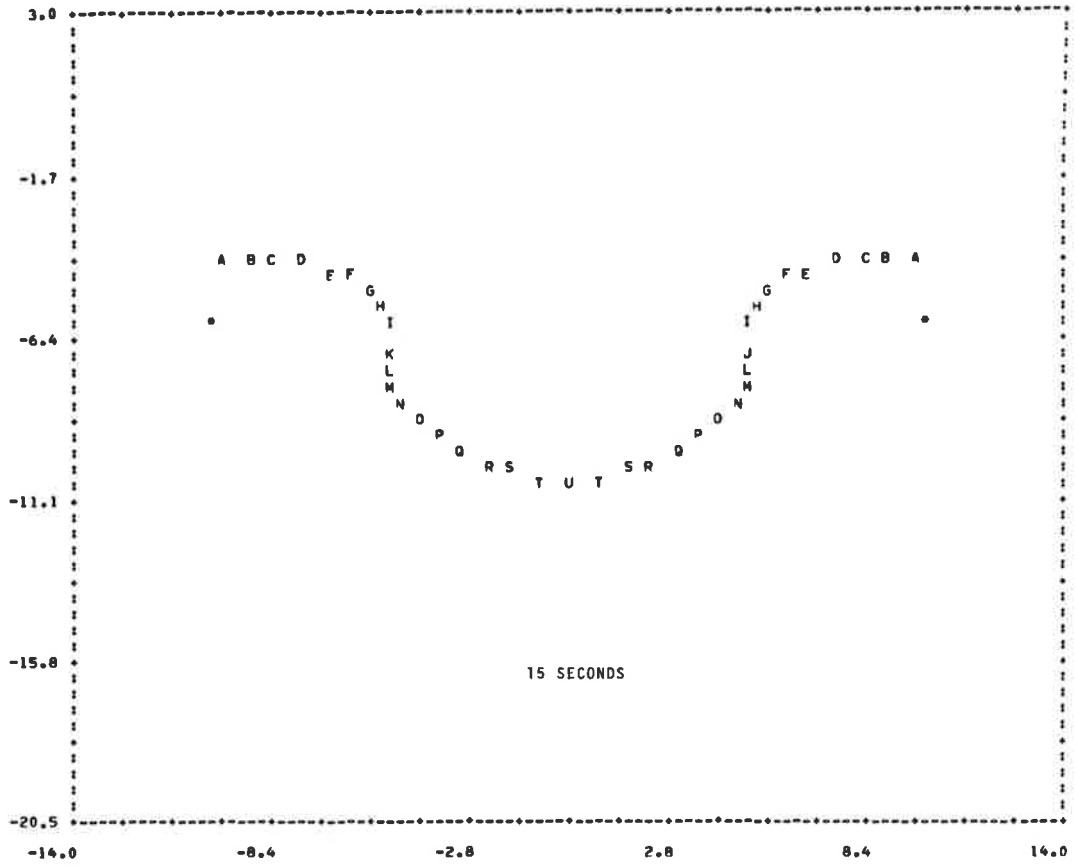
3.0
-1.7
-6.4
-11.1
-15.8
-20.5
-14.0
-8.4
-2.8
2.8
8.4
14.0
15 SECONDS

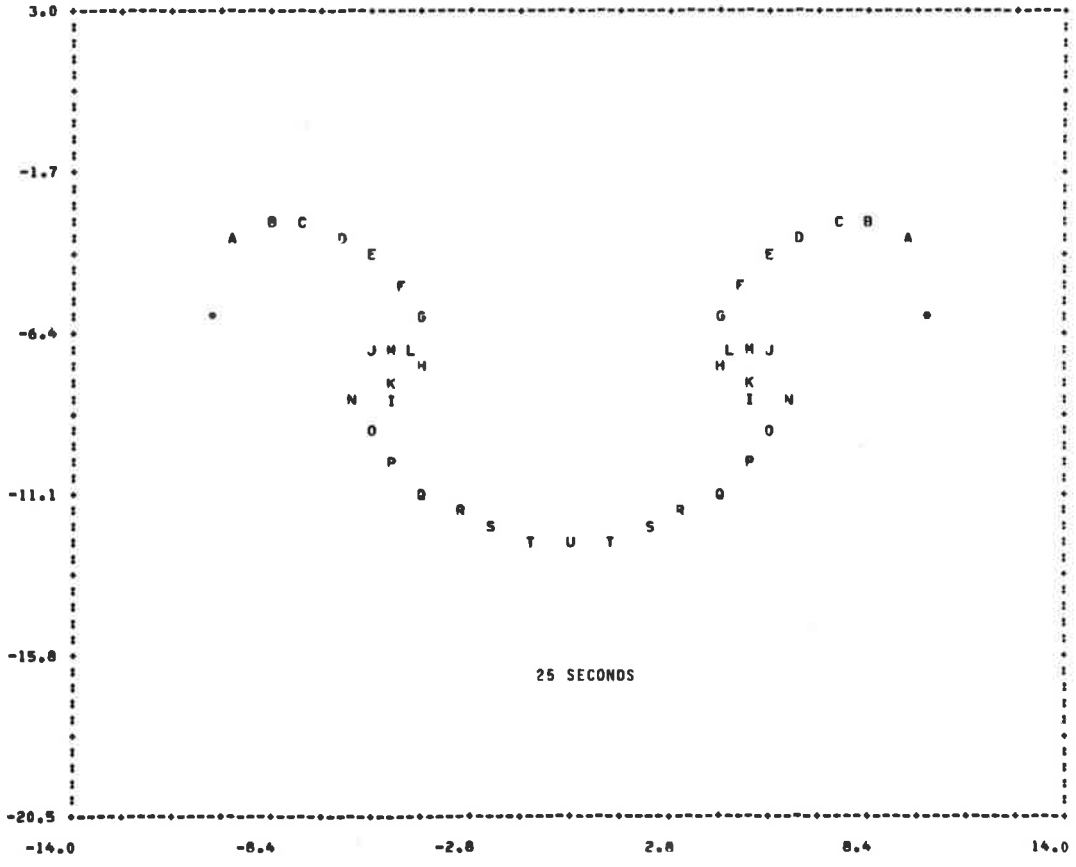
3.0
-1.7
-6.4
-11.1
-15.8
-20.5
-14.0
-8.4
-2.8
2.8
8.4
14.0
25 SECONDS

APPENDIX C

The following are the essential parts of the FORTRAN IV programs used to calculate the positions of a vortex array at various time intervals.

The H Method

The real arrays K(41), P(2, 41) and N(2, 41) were dimensioned to hold the vortex strengths, their position coordinates at the beginning of a time step and those at the end of the same time step respectively. PI2 held the constant 2π. With the values in K, P and the time step T, assigned, the procedure was as follows.

```
      DO 80 J=1, 41
      X = Y = 0
      DO 60 I=1, 41
      IF (I.EQ.J)  GO TO 60
      Z1 = P(1, J)-P(1, I)
      Z2 = P(2, J)-P(2, I)
      D = SQRT(Z1*Z1+Z2*Z2)
      TH = ACOS(Z1/D)
      IF(Z2.LT.O.) GO TO 30
      TH = TH+K(I)*T/(D*D)/PI2
      GO TO 50
30    TH = PI2-TH+K(I)*T/(D*D)/PI2
50    R = P(1,I)+D*COS(TH)
      S = P(2,I)+D*SIN(TH)
```

```
      X = X+R-P(1,J)
      Y = Y+S-P(2,J)
60    CONTINUE
      N(1,J) = P(1,J)+X
80    N(2,J) = P(2,J)+Y
```

The Euler First Order Method

This procedure uses the same variable names as with the H method in conjunction with the system of equations quoted at the beginning of Chaper XII.

```
      DO = 80 J=1, 41
      X = Y = O.
      DO 60 I=1, 41
      IF (I.EQ.J) GO TO 60
      Z1 = P(1,J)-P(1,I)
      Z2 = P(2,J)-P(2,I)
      D2 = Z1*Z1+Z2*Z2
      X = X-K(I)*(P(2,J)-P(2,I))/D2
      Y = Y+K(I)*(P(1,J)-P(1,I))/D2
60    CONTINUE
      N(1,J) = P(1,J)+X
80    N(2,J) = P(2,J)+Y
```

The Runge-Kutta Method with amalgamation as described in Chapters X and XI.

N was the initial number of distinct vortex points. X,Y,X1,Y1 were one dimensional arrays containing N values each. The values of the k_{ij} (see Chapter X) were stored in the array RK(4,2,N). At any stage of the run JK was one more than the number of amalgamations which had already taken place.

```
      M = N+1-JK
      DO 20 J=JK,M
      CALL RKXY(X,Y,J,M.F1,F2,JK)
      RK(1,1,J) = T*F1
20    RK(1,2,J) = T*F2
      R = 2.
      DO 40 I=1,3
      IF(I.EQ.3) R=1
      DO 30 JA=JK,M
      X1(JA) = S(JA)+RK(I,1,JA)/R
30    Y1(JA) = Y(JA)+RK(I,2,JA)/R
      DO 40 J=JK,M
      CALL RKXY(X1,Y1,J,M,F1,F2,JK)
      RK(I+1,1,J) = T*F1
40    RK(I+1,2,J) = T*F2
      DO 70 JB=JK,M
      P = 2.*(RK(2,1,JB)+RK(3,1,JB))
      Q = 2.*(RK(2,2,JB)+RK(3,2,JB))
      X(JB) = X(JB)+(RK(1,1,JB)+P+RK(4,1,JB))/6.
```

```
70    Y(JB) = Y(JB)+(RK(1,2,JB)+Q+RK(4,2,JB))/6.
      A1 = X(JK+3)-X(JK+2)
      B1 = X(JK+2)-X(JK+1)
      A2 = Y(JK+3)-Y(JK+2)
      B2 = Y(JK+2)-Y(JK+1)
      TN = (A1*B1+A2*B2)/SQRT((A1*A1+A2*A2)*(B1*B1+B2*B2))
      IF(ACOS(TN).GT.PI2/4.) CALL AMALG(X,Y,JK)
      MALG = JK-1
      IF(JK.EQ.1) GO TO 72
      DO 71 ID=1, MALG
      X(ID) = X(JK)
      Y(ID) = Y(JK)
      X(N+1-ID) = X(N+1-JK)
71    Y(N+1-ID) = Y(N+1-JK)
72    CONTINUE
. . . . . .
      SUBROUTINE RKXY(XS,YS,JS,NS,FX,FY,JKS)
      FX = FY = 0
      DO 500 L=JKS,NS
      IF(L.EQ.JS) GO TO 500
      C = XS(JS)-XS(L)
      D = YS(JS)-YS(L)
      G = D*D+C*C
      FX = FX-VS(L)*D/(G*PI2)
      FY = FY+VS(L)*C/(G*PI2)
500   CONTINUE              (VS is vortex strength)
. . . . . .
```

```
      SUBROUTINE AMALG(X,Y,L)
C     THIS AMALGAMATES THE (L+1)TH VORTEX WITH
C     THOSE ALREADY AT THE CENTRE
      VT = VS(L+1)+VS(L)
      X(L+1) = (VS(L+1)*X(L+1)+VS(L)*X(L))/VT
      Y(L+1) = (VS(L+1)*Y(L+1)+VS(L)*Y(L))/VT
      VS(L+1) = VT
      VT = VS(N-L)+VS(N+1-L)
      X(N-L) = (VS(N-L)*X(N-L)+VS(N+1-L)*X(N+1-L))/VT
      Y(N-L) = (VS(N-L)*Y(N-L)+VS(N+1-L)*Y(N+1-L))/VT
      VS(N-L) = VT
      L = L+1
. . . . . .
```

The code given in this appendix has omitted many statements which are not essential to the logic but would be necessary for the programs to be effectively run on a computer.

BIBLIOGRAPHY

Batchelor, 1964, Axial flow in trailing vortices. Journal of Fluid Mechanics, Vol 20, part 4. 645-658.

Betz, A, 1932, Verhalten von Wirbelsystemen. Z. agnew. Math. Mech 12, 164. English translation N.A.C.A. Technical Memo no. 713.

Brown, C.E, 1973, Aerodynamics of Wake Vortices, American Institute of Aeronautics and Astronautics Journal, Vol 11, no 4, 521-526.

Brown, C.E, and Kirkman K, 1974, Simulation of Wake Vortices descending in a Stably Statified Atmosphere. U.S. Department of Transportation Report no. FAA-Rd-74-116.

Hackett, J.E, and Evans, M.R, 1971, Vortex Wakes behind High-Lift Wings. Journal of Aircraft, Vol 8, no 5, 334-340.

Jordan, P.F, 1973, Structure of Betz Vortex Cores, Engineering note, Journal of Aircraft, Vol 10, no 11, 691-693.

Lamb, H, Hydrodynamics, Dover, Sixth Edition

McCormick, Tangler & Sherrieb, 1968, Structure of Trailing Vortices, Journal of Aircraft, May-June, 260-267.

Moore and Saffman, 1973, Axial Flow in Laminar Trailing Vortices, Proceedings of the Royal Society, London, A333, 491-508.

Moore, D.W, 1974, A Numerical Study of the Roll up of a Finite Vortex Sheet, Journal of Fluid Mechanics, Vol 63, part 2, 225-235.

Newman, B.G, 1959, Flow in a Viscous Trailing Vortex, Aeronautical Quarterly, Vol 10, 149-162.

Rossow, V.J, 1973, On the Inviscid Rolled-Up Structure of Lift-Generated Vortices, Journal of Aircraft, Vol 10, no 11, 647-650.

Rossow, V.J, 1975, Theoretical Study of Lift-Generated Vortex Wakes Designed to Avoid Rollup, American Institute of Aeronautics and Astronautics Journal, Vol 13, no 4, 476-484.

Sedov, L.I, A Course in Continuum Mechanics, Vol 3, Wolters-Noorhoff

Sprieter & Sacks, 1951, The Rolling up of the Trailing Vortex Sheet and its Effect on the downwash behind Wings, Journal of the Aeronautical Sciences 18: 21-32

Widnall, S.E, 1975, The Structure and Dynamics of Vortex Filaments, Annual Review of Fluid Mechanics (Pub. Annual Review Inc.) Vol 7, 141-165.